FRACTURE TOUGHNESS EVALUATION BY R-CURVE METHODS

STP 527

75TH ASTM ANNIVERSARY

AMERICAN SOCIETY FOR TESTING AND MATERIALS

FRACTURE TOUGHNESS EVALUATION BY R-CURVE METHODS

A symposium
sponsored by
Committee E-24 on
Fracture Testing of Metals
AMERICAN SOCIETY FOR
TESTING AND MATERIALS

ASTM SPECIAL TECHNICAL PUBLICATION 527
D. E. McCabe, symposium chairman

List price $9.75
04-527000-30

AMERICAN SOCIETY FOR TESTING AND MATERIALS
1916 Race Street, Philadelphia, Pa. 19103

Library of Congress Catalog Card Number 72-97867

NOTE

The Society is not responsible, as a body,
for the statements and opinions
advanced in this publication.

Printed in Tallahassee, Fla.
April 1973

Foreword

This publication is a collection of papers presented at a technical symposium on R-curves held during the regular Committee E-24 meetings in the Fall of 1971. It represents an early effort by a Subcommittee 1 task group to organize the present state of R-curve technology in preparation for a renewed attempt to apply the method to plane-stress fracture toughness evaluation. The symposium was sponsored by Committee E-24 on Fracture Testing of Metals, American Society for Testing and Materials. D. E. McCabe, Armco Steel Corp., presided as symposium chairman.

Related ASTM Publications

Fracture Toughness, STP 514 (1972), $18.75, 04-514000-30

Review of Developments in Plane Strain Fracture Toughness Testing, STP 463 (1970), $18.25, 04-463000-30

Electron Fractography, STP 436 (1968), $11.00, 04-436000-30

Contents

Introduction

The R-curve approach has a basis in fracture mechanics and, when coupled with new hypotheses pertaining to R-curve characteristics, can be used for instability condition predictions. To be sure, some of the hypotheses can be reasonably challenged, and the need for some additional fundamental studies is apparent. It is intended, therefore, that the contents of this publication will serve to stimulate new involvement in R-curve research work. In particular, help is needed in extending the method to lower strength, high toughness materials, and examples are needed to demonstrate the predictive capabilities of the method.

In reading these papers, it will be apparent that a variety of specimen types and test techniques are available to draw upon, all arriving at a common method of data presentation: toughness development as a function of crack extension. The introductory paper reviews the development of R-curve technology from the early and somewhat misleading model of 1954 to the present model which is believed to be suitable for making instability predictions. Other authors present methods of test, and, in some cases, the fundamental concepts of R-curve technology are presented, tested, and evaluated.

An interesting feature of R-curve concepts is that they contradict the widely held belief that a singular K_c-value can be used to define instability conditions in all types and sizes of sheet specimens. Conversely, it recognizes the role that specimen configuration and dimensions play in controlling the instability event. Early efforts of the Special Committee on Fracture Testing of High Strength Materials, now ASTM Committee E-24 on Fracture Testing of Metals, were aimed at the determination of a K_c-value. Although R-curve principles were fairly well established at that time, the R-curve approach was not accepted generally as a useful tool for materials evaluation. Several laboratories carried out expensive programs in wide panel testing, attempting to arrive at the rather elusive constant K_c-value. An apparently constant value was oftentimes obtained with panels up to 48 in. wide, but experimental difficulties in defining the instability event eroded confidence. Because of these problems and the urgency of fracture toughness evaluation of thicker materials, Committee E-24 turned its attention to the plane strain, K_{Ic}, analysis, which was believed to be more manageable. Here, determinations are made under conditions where little to no stable crack growth is present. Also nearly constant K_{Ic}-values could be determined using relatively compact specimens. This change in emphasis proved productive, and a standard practice, E 399, Test for Plane-Strain Fracture Toughness of Metallic Materials, has resulted. However, many commercial materials in the typical thicknesses provided are not amenable to K_{Ic} analysis. Interest, therefore, is returning to the plane-stress fracture problem.

A recommended standard, E 338, Test for Sharp-Notch Tension Testing of High-Strength Sheet Materials, has been available from E-24 activities for sheet toughness testing using standard size center cracked and edge notched specimens. The notch strength is determined. Interest in such an approach has been sustained, and further developments can be expected. However, the results of this type of procedure offer little prospect of component failure prediction capability. Its primary usefulness is in ranking of materials according to toughness. In application, the need for judgment based on built-up experience is not eliminated. On the other hand, R-curve technology utilizes fracture mechanics concepts and hence offers the prospect of critical fracture stress and flaw size determinations for untested configurations. Presently, the surface has just been scratched on applications for R-curves, and the need for new and original work is great. Low-strength high-toughness materials provide the more challenging testing problems. New ideas will have to be introduced in order to extend the present concepts developed from testing high-strength sheet materials to the common grades of structural plate materials.

D. E. McCabe

Senior research metallurgist,
Research and Technology, Armco
Steel Corp., Middletown, Ohio
45042; symposium chairman.

R. H. Heyer[1]

Crack Growth Resistance Curves (R-Curves) - Literature Review

REFERENCE: Heyer, R. H., "**Crack Growth Resistance Curves (R-Curves)–Literature Review**," *Fracture Toughness Evaluation by R-Curve Methods, ASTM STP 527*, American Society for Testing and Materials, 1973, pp. 3-16.

ABSTRACT: The development of the concept of crack-growth resistance as a means of characterizing fracture toughness is reviewed. While the first model was proposed in 1954, major developments, experimental determinations, and applications of R-curves date from 1960.

KEY WORDS: crack propagation, fracture toughness, fracture strength, fracture tests, aluminum alloys, transition temperature, documents

Slow crack growth is a minor consideration in the fracture of high-strength, relatively frangible materials under conditions of plane-strain. The E 399 Test for Plane-Strain Fracture Toughness of Metallic Materials evaluates the stress intensity factor for crack extension, and when plasticity and slow crack growth begin to obscure the start of crack extension, the test results are procedurally invalid. On the other hand, Creager and Liu [*1*][2] state: "It is well known that the fracture process of a cracked thin metal sheet is not usually comprised of a single sudden explosive-type change from initial crack length to total failure . . . as the load increases considerable slow stable crack growth takes place prior to catastrophic failure . . . the amount of slow stable tear is highly dependent on the structural configuration . . . the configuration and the applied loads combine to determine the stress intensity factor, which indicates the magnitude of the stresses around the plastic zone at the crack tip. Krafft et al [*2*] postulated that for a given material and thickness there is a unique relationship between the amount a crack grows and the applied stress intensity factor . . . they called this a crack growth resistance curve (R-curve)."

Development of Crack Growth Resistance

Fracture energy and fracture appearance transition temperatures have been the most generally accepted criteria of toughness of nonfrangible materials. A fracture mechanics approach to crack growth resistance development has been known since 1954, and is now becoming recognized as a basis for useful test

[1] Principal research associate, Research Center, Armco Steel Corp., Middletown, Ohio 45042.

[2] The italic numbers in brackets refer to the list of references appended to this paper.

methods applicable to the less brittle materials. The procedure involves measurements of the resistance to crack growth in terms of the stress intensity factor, K, or the strain energy release rate, G. In this review highlights of the literature on this subject will be presented.

Major Developments

The concept was introduced by Irwin and Kies in 1954 [*3*], using the energy approach, and concluding, "that the strain energy release rate and the fracturing work rate must be equal at onset of instability, and that they are unlikely to differ widely in magnitude as fracturing continues" (in reference to a central crack in a flat plate). The fracturing resistance at that time was represented as decreasing with crack extension, reaching a steady state. This concept was further developed by Boyd [*4*] as applied to fracturing of remotely loaded wide plates.

The Krafft et al paper of 1961 [*2*], presents this 1954 concept in Fig. 1*a*, and the 1959 Irwin concept in Fig. 1*b*. The latter was introduced in the Special ASTM Committee report of January 1960 [*5*]. The rising crack growth resistance or R-curve of Fig. 1*b* results from growth of the plastic zone as the crack extends from a sharp defect, notch, or fatigue crack. Krafft et al attributed the early rise of the curve to the transition from flat to shear or slant fracture. This has proved to be a minor effect for sheet thickness specimens. In Fig. 1*b* crack instability for remote-loaded specimens, G_c, is represented as the tangency of the R-curve and the G-curve, where G is taken as the crack driving force, with dimensions in.-lb/in.^{2}, a_0 is the initial crack length (half crack length of a center cracked specimen), and W is the specimen width.

Since the G-curve is geometry dependent, the point of tangency, G_c, is geometry dependent; for example, G_c increases with increase in specimen width

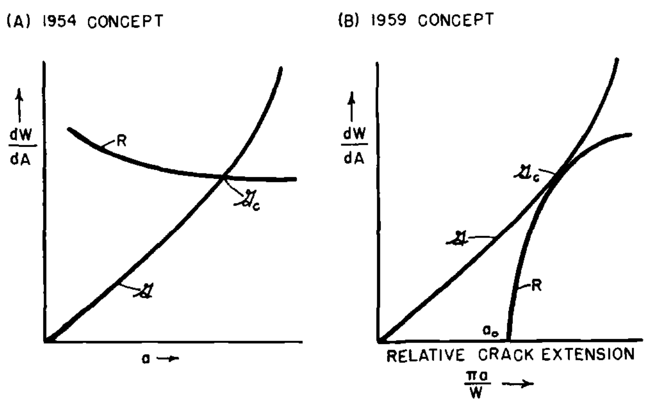

FIG. 1—*Early versus current concepts of fracture instability (in center-cracked remote-loaded panel) showing how crack growth resistance* R *is now believed to increase with crack length rather than remain constant or decrease as previously supposed [2].*

for remote-loaded specimens. (Note: Originally "R-curves" were developed in terms of G, with units of in.-lb/in.^{2}, or lb/in. Later, K, with units of ksi-in.$^{1/2}$, was often used. Recently, the terms G_R and K_R have been introduced by Clausing and Irwin, and these terms appear to have merit in that the resistance curve of the material can be distinguished from the stress intensity curve of the specimen, and from the onset of instability; for example, K_R, K, K_c, or G_R, G, G_c, respectively.)

The more detailed illustration from the 1960 Committee Report, Fig. 2, shows the R-curve represented empirically as a parabola, intersecting the abscissa at a distance C from the initial relative crack length $\pi a_0/W$, where C is related empirically to the shear lip fraction. This model used with certain graphical procedures yielded G_c or K_c-values for center-cracked specimens without resort to the ink-staining methods then in use for determining the crack length at onset of instability.

The Krafft et al paper featured an R-curve, Fig. 3, which was a composite of results from several independent investigations of 7075-T6 aluminum alloy, in specimen widths from 1.5 to 42 in., thickness 1/8 in. The abscissa was absolute crack extension, Δa, rather than relative, or a/W extension. This implies that the R-curve is independent of initial crack length. Recently, Walker has proposed an alternate concept, R-slope, in which there is dependency of the R-curve upon initial crack length and upon specimen geometry; this is the subject of a presented paper at the 8 Oct. 1970 meeting of ASTM Committee E-24.

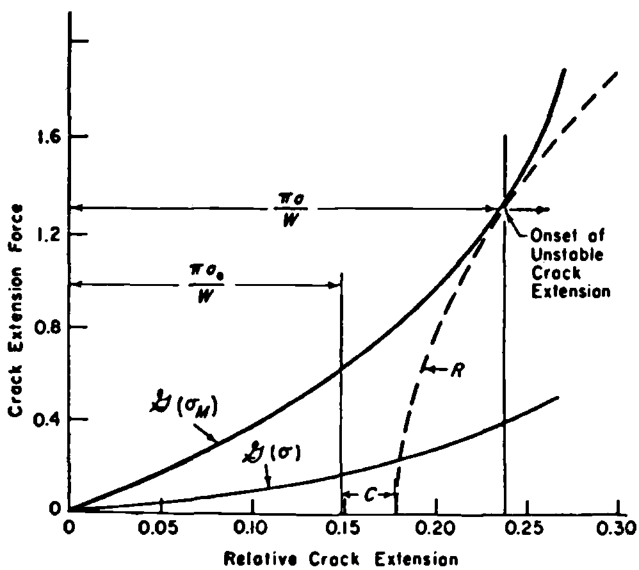

FIG. 2—*Steps leading to unbalance of crack extension force over resistance to crack extension and, thus, to crack growth instability (remote-loaded specimen) [5].*

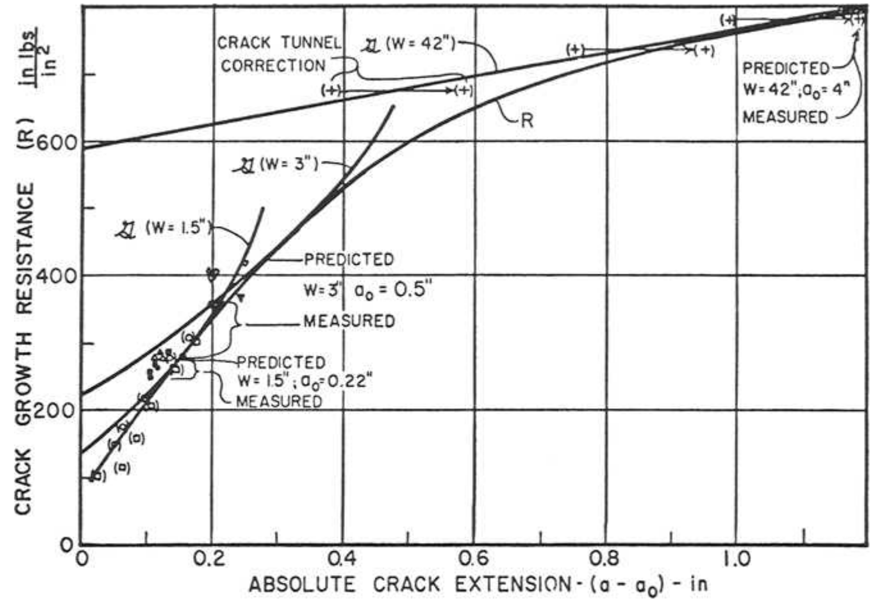

FIG. 3—*Crack growth resistance* R *increases as a function of absolute extension from the initiating flaw* (a - a_0) *independent of its size or that of the total plate width as based on* (1) *critical σ and ink stain* a *measurements for specimen widths:* ● *1.5 in.;* ■ *2.0 in.;* △ *3.0 in.;* ▽ *6.0 in.;* ◇ *9.0 in.; by Smith,* (2) *continuous σ and* a *measurement with compliance gage for width* o □ *3.0 in. by Boyle, and* (3) *visual tracking of surface crack plus allowance for tunneling of crack tip for width +42 in. by Smith and Bird. Typical crack extension force* (G) *curves show predictions of instability point. Bracketed points are in stable range of crack growth, others are "critical" values (remote-loaded specimens) [2].*

Broek's extensive center cracked tension panel tests on 2024-T3 and 7075-T6 sheets, reported in a series of papers in 1965-1966, showed that within his limits of accuracy, a 2 to 1 change in initial crack length tended to confirm Krafft's hypothesis [*6*]. However, when panel width was varied from 150 to 600 mm, with 8 to 1 change in initial crack length, the scatter in the R-curves was such that no conclusion was drawn upon the validity of the Krafft hypothesis [*7*].

In tests at Armco Research using wedge-opening load (WOL) type crack-line-wedge-loaded (CLWL) specimens with 2 to 1 change in initial crack length, essentially coincident R-curves have been obtained [*8*].

Experimental Determinations

In ASTM STP 381 [*9*], Srawley and Brown discuss R-curve characteristics, including the effects of specimen geometry on G_c instability. One example, Fig. 4, shows the effect of initial crack length in a wide plate of a material which exhibits a pop-in followed by gradual crack extension with rising load. The short crack remote-loaded specimen fails by pop-in and a low G_{Ic} crack extension force, at the point of tangency of the G- and R-curves. The Brown and Srawley illustrations assume that the R-curve is independent of specimen geometry, and

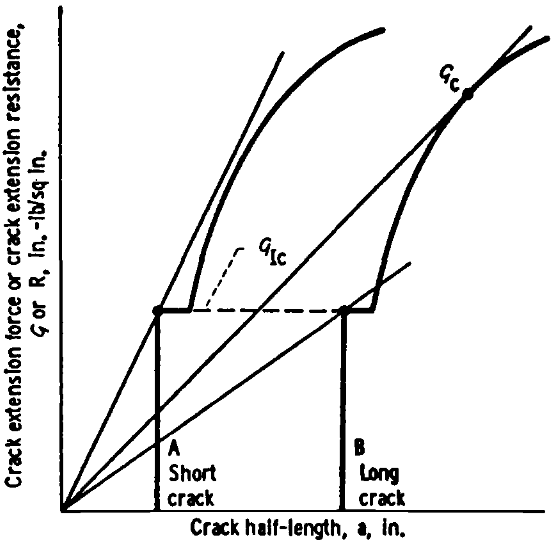

(a) Short crack, specimen breaks at load corresponding to G_{Ic}.
(b) Long crack, ultimate load is considerably higher than that corresponding to G_{Ic}.

FIG. 4—*Instability behavior of remote-loaded wide plate specimens having different crack lengths [9].*

that the change in crack driving force curves with geometry account for the variations in G_c or K_c.

In 1968 Clausing [*10*] explored the characteristics of several specimen types from the standpoint of crack stability. His analysis yielded the dimensionless parameters f_2 and f_3. (f_2 is a function of specimen geometry, and f_3 is a function of the compliance of the specimen and loading system as well as the geometry). Crack stability increases as f_2-f_3 decreases to negative values. In Fig. 5, single-edge-cracked plate, center-cracked plate, and double cantilever beam (DCB) specimens are compared on this basis. Other variables are relative crack length, a/W; L/W or W/H ratios; and system compliance, where 600 is high compliance "typical of a rather flexible grip system in a tension testing machine;" and 1.5 is "typical of very stiff loading systems, such as a bolt that directly opens the crack."

In Fig. 5*a* it is evident that the center-cracked plate at a high level of (f_2-f_3) has a low level of crack stability, that is, at the onset of instability the crack will accelerate rapidly and sever the specimen. This specimen is relatively insensitive to compliance and the $L/2W$ ratio. On the other hand, Clausing showed that the DCB type specimens, Fig. 5*b*, tested in stiff, low compliance systems have high crack stability, so that it is difficult to run the crack to complete separation.

Clausing concluded, "The experimental determination of the complete G_R-curve for a material is much more informative than one value of G_c. After the G_R-curve is determined, G_c can be calculated for any experimental

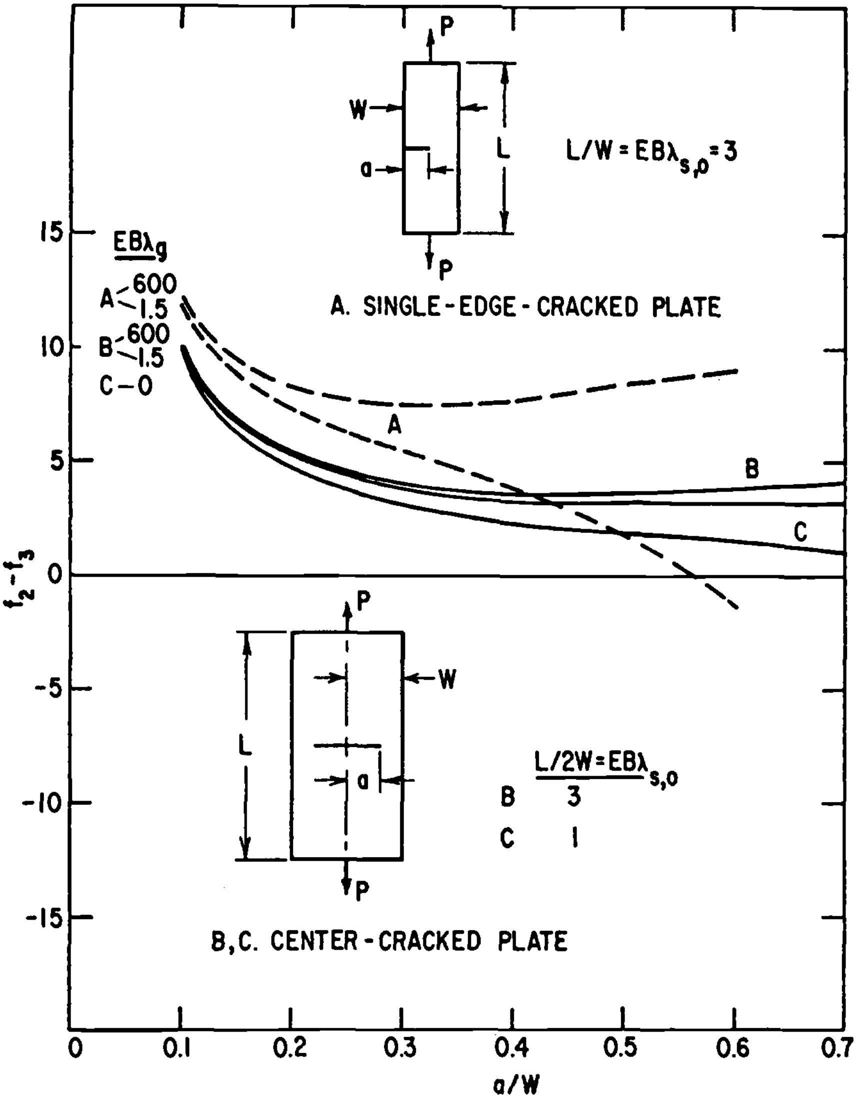

FIG. 5a–*Stability parameter for tension specimens [9].*

configuration by using the analysis presented in this paper. The complete G_R-curve can be determined in one stable specimen by measuring load and crack length as the crack propagates."

Heyer and McCabe [*11*] use a crack-line-wedge-loaded specimen (CLWL) having the proportions ($H/W = 0.486$) of the Westinghouse WOL specimen, see Fig. 6. Specimens having compact proportions ($H/W = 0.6$) have been used for crack opening displacement (COD) determinations in the plastic range, as reported in this technical session. Both are displacement controlled DCB type

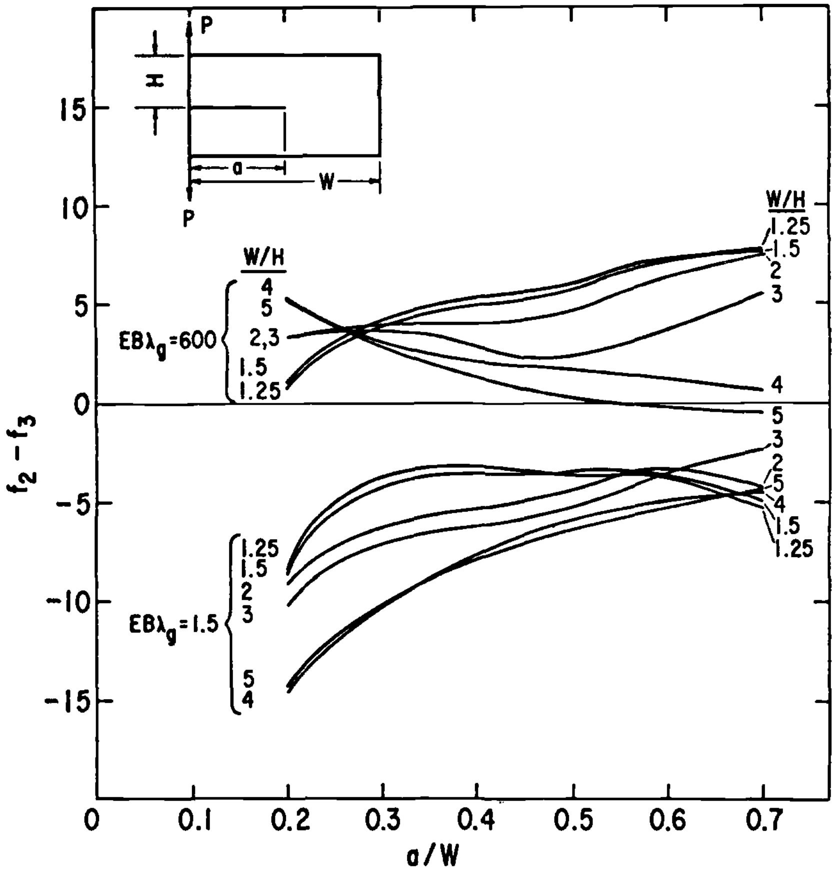

FIG. 5*b*–*Stability parameter for straight DCB specimens [9].*

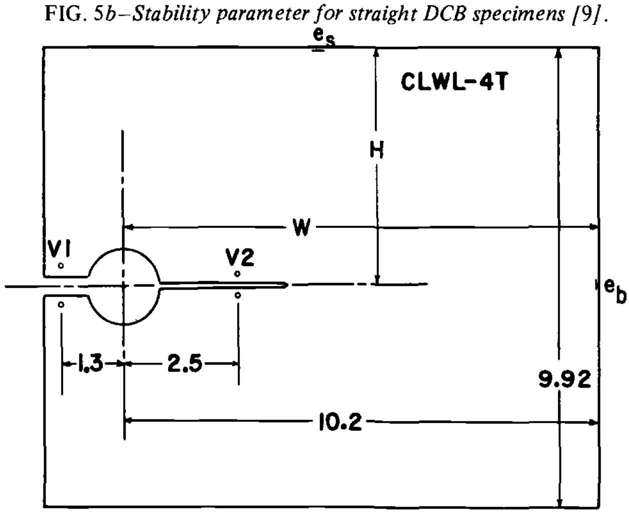

FIG. 6–*Double compliance CLWL-4T specimen,* H/W = *0.486 [11].*

specimens with high crack stability. Displacement is measured by transducers at positions *V*1 and *V*2. The wedge loading fixtures, shown in Fig. 7, provide displacement control and a very stiff loading system as in Fig. 5*b* bottom, whereas the tension loading system of Fig. 8 more nearly conforms to the conditions in Fig. 5*b* top.

The influence of these loading systems on crack stability is shown in Fig. 9, where the solid lines with negative slope represent the K or crack driving force curves at three levels of displacement corresponding to three stages of wedge loading [*8*]. At each intersection with the R-curve, the crack arrests at the indicated value of relative crack length a/w. At no time does the crack become unstable. The corresponding K-curves for tension loading are the dash lines, with positive slope, at two levels of loading. At load $P = 6.05$ kips, the point of tangency with the R-curve defines the load and crack length at the onset of instable fracture, K_c. An example of K_R-curves obtained by the two loading systems is shown in Fig. 10, where the curve for tension-loading terminates at X, the K_c instability point.

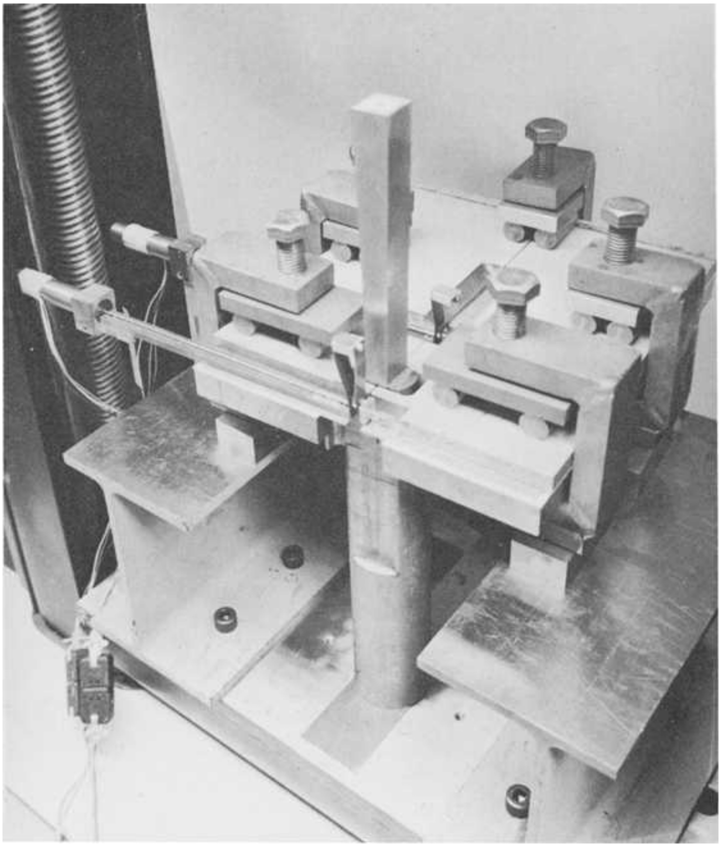

FIG. 7—*Wedge loading of CLWL-4T sheet specimen, horizontally mounted transducers.*

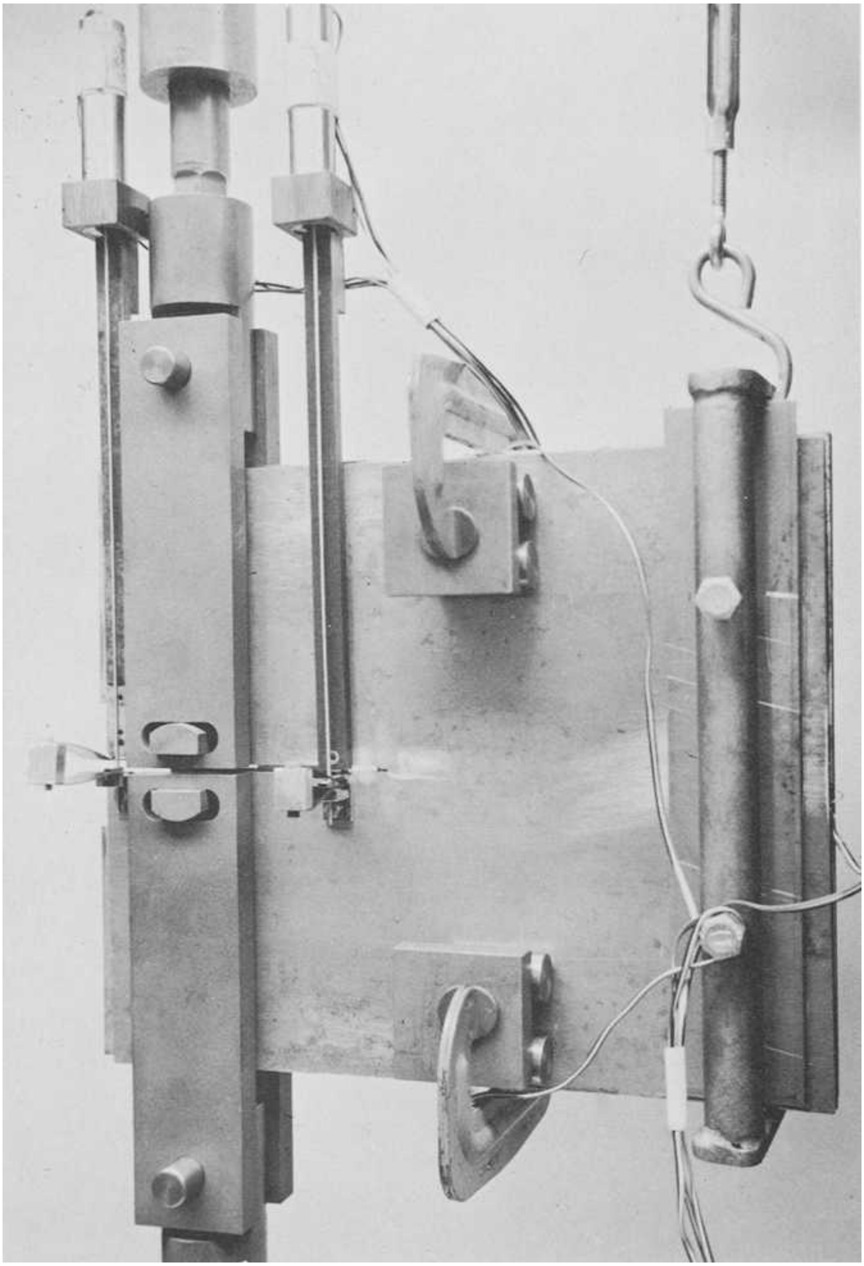

FIG. 8–*Tension loading of CLWL-4T plate specimen.*

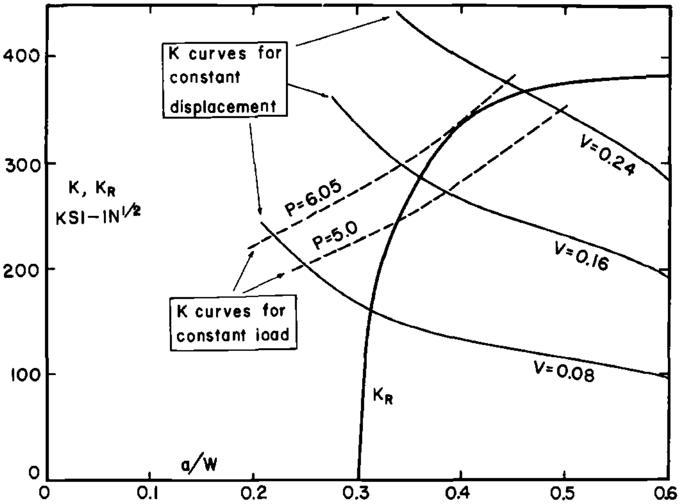

FIG. 9—*R-curve with displacement and load control crack driving force curves for CLWL-4T specimen of PH14-8Mo, SRH950, vacuum melt [8].*

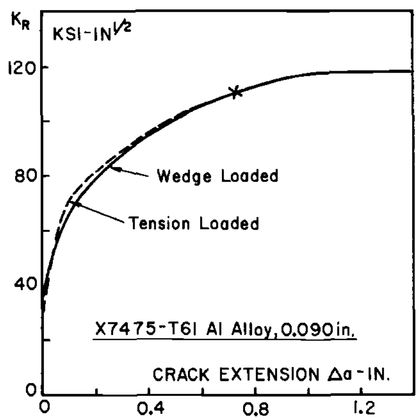

FIG. 10—*R-curves for wedge and tension loading of a high-strength aluminum alloy.*

Applications of R-Curves

Crack growth resistance curves and K_c determinations for center-cracked tension specimens have been made by several investigators. Boyle [*12*] established the compliance technique whereby the effective crack length is obtained without plastic zone correction. Carman et al [*13*] used this technique on 4-in.-wide aluminum alloy panels, and they used high speed movies to observe crack length in 20-in.-wide panels. Lauta and Steigerwald [*14*] determined the K_R-curve for a 4340 steel using Boyle's technique. Forman [*15*] used visual observation of crack length for determining K_R-curves for steel and aluminum panels up to 24 in. wide.

Rooke and Bradshaw [*16*] found that Z (thickness) strains in the plastic zone were approximately equal to Y (tension directed) strains. They surveyed Y strains throughout the plastic zone, using scribed grid lines, and determined the work of plastic deformation, which was taken equal to R, the resistance to crack growth. The R-curves thus generated were roughly equivalent to G_R-curves calculated by fracture mechanics methods.

Carman and Irwin [*17*] have recently used contraction measurements in the plastic zone as a means of determining K_R-curves. The assumption is made that the Z (thickness) strain is approximately equal to the Y (tension direction) strain in center-cracked tension loaded panels. The maximum $Z = Y$ strain is taken to be a measure of cracking-opening displacement, which is related to G or K. Hence, a sequence of maximum thickness strains defines a K_R-curve which is approximately equal to the corresponding curve from displacement measurements.

Pellini and Judy [*18*] and Goode and Judy [*19*] at The Naval Research

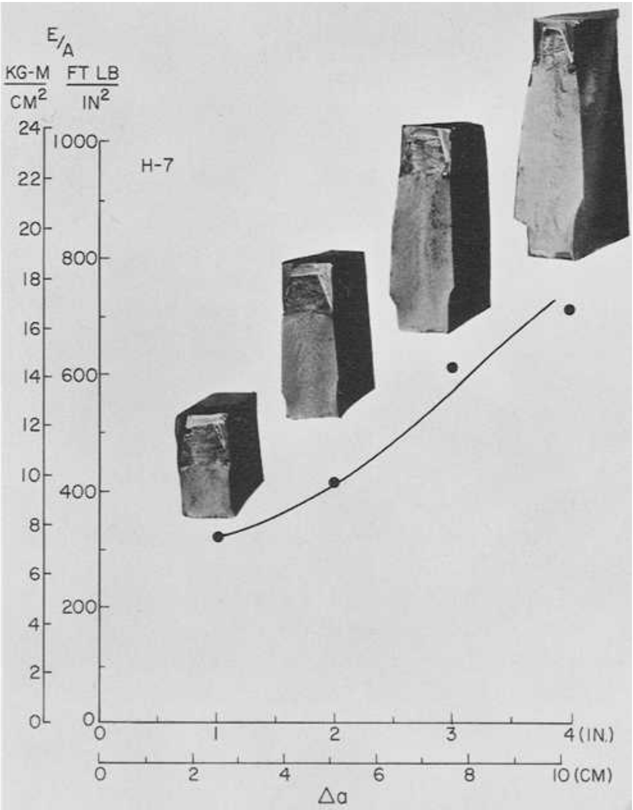

FIG. 11—*R-curve features and transition from plane strain to plain stress fracture with fracture extension for a high-toughness alloy [19].*

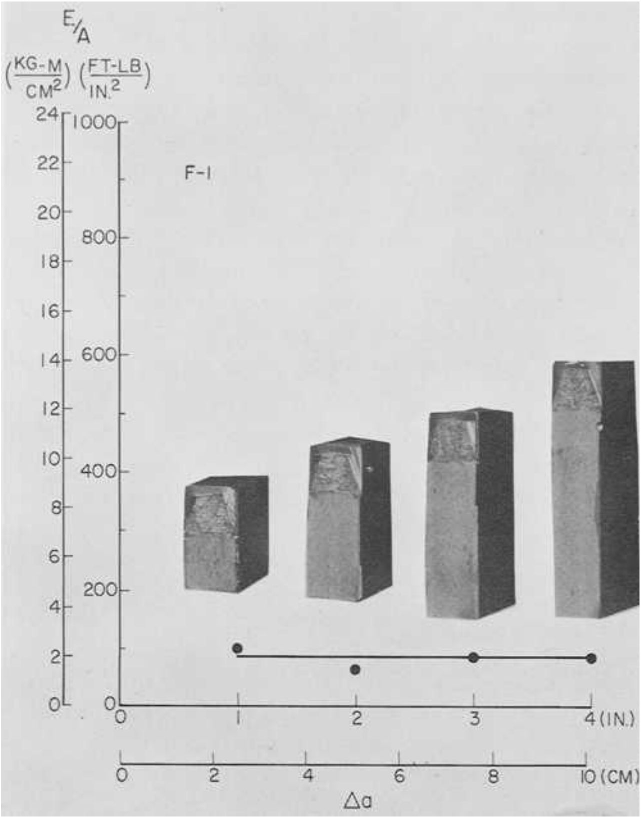

FIG. 12—*R-curve features and fracture appearance for a frangible alloy (Note the flat R-curve and lack of a transition from flat plane strain fracture with increased* Δa *which is typical for brittle material) [19].*

Laboratory (NRL) use energy data from dynamic tear tests to develop fracture extension resistance (R-curve) features, as in Fig. 11 and 12. Dynamic tear energies are determined for specimens of varying W, providing different crack extensions, Δa. Energy/fracture area, E/A, of tough materials increases with W, due to increase in slant (plane-stress) fracture area as W is increased, Fig. 11 [*19*]. Brittle materials which maintain a flat fracture at all specimen widths show no rise in the E/A-Δa curve, Fig. 12.

Jones and Brown [*20*] have converted K_{IC} load displacement test records to K-Δa (R-curves) as in Fig. 13. This example demonstrates that at two percent crack extension Δa increases with the initial crack length. The intersections of the vertical lines with the crack growth resistance curve give the K_Q values, which increase with crack length (and W). Other features of K_{IC} tests are interpreted using R-curves.

Creager and Liu [*1*] analyzed the stress intensity patterns of strap reinforced

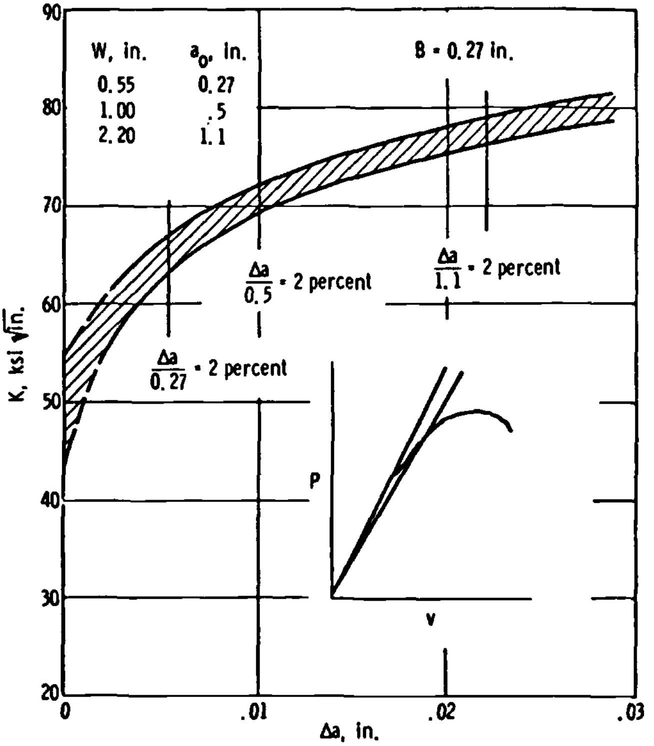

FIG. 13—*Crack growth resistance curve for 4340 steel tempered 750 F, 1 h as determined using 0.27-in.-thick bend specimens (σ_{ys}) = 213 ksi [20].*

2024-T3 aluminum alloy panels, 48 in. wide by 83 in. long, with seven stiffeners at 6-in. spacing. A 12-in.-long center slot, with fatigue-cracked tips was used. The failure loads, using four different strap materials, were predicted within 10 percent from the R-curve for 2024-T3 which we had reported using the CLWL specimen, with W = 10.2 in. [8]. These Lockheed tests are of interest because the stiffened panels are probably the most complicated structure for which such predictions have been attempted.

Summary

Crack growth resistance curves have been found to be useful for characterizing fracture toughness over a wide range of material properties and specimen thickness. They are likely to become most useful for tougher materials exhibiting mixed mode or full slant fracture surfaces.

References

[*1*] Creager, M. and Liu, A.F., "The Effect of Reinforcements on the Slow Stable Tear and Catastrophic Failure of Thin Metal Sheet," American Institute of Aeronautics and Astronautics, Paper No. 71-113, Jan. 1971.

[*2*] Krafft, J.M., Sullivan, A.M., and Boyle, R.W. in *Proceedings*, Crack Propagation Symposium, College of Aeronautics, Vol. 1, Cranfield, England, 1961, pp. 8-26.

[*3*] Irwin, G.R. and Kies, J.A., *Welding Research Supplement*, Vol. 19, April 1954, pp. 193-198.

[*4*] Boyd, G.M. in *Transactions*, Institute of Naval Architects, Vol. 99, 1957, pp. 349-358.

[*5*] ASTM Special Committee on Fracture Testing of High-Strength Materials, *ASTM Bulletin*, Jan. 1960, pp. 29-40.

[*6*] Broek, D., "The Residual Strength of Aluminum Alloy Sheet Specimens Containing Fatigue Cracks or Saw Cuts," NLR-TR M2143, National Space Laboratory, Amsterdam, March 1966.

[*7*] Broek, D., "The Effect of Finite Specimen Width on the Residual Strength of Light Alloy Sheet," NLR-TR M2152, National Space Laboratory, Amsterdam, Sept. 1965.

[*8*] Heyer, R.H. and McCabe, D.E., "Plane-Stress Fracture Toughness Testing Using a Crack-Line-Loaded Specimen," Third National Symposium on Fracture Mechanics, Lehigh University, August 1969, to be published in *Engineering Fracture Mechanics.*

[*9*] Srawley, J.E. and Brown, W.F., Jr., in *Fracture Toughness Testing and Its Applications, ASTM STP 381,* American Society for Testing and Materials, 1965, pp. 133-198.

[*10*] Clausing, D.P., *International Journal of Fracture Mechanics,* Vol. 5, Sept. 1969, pp. 211-227.

[*11*] Heyer, R.H. and McCabe, D.E., "Crack Growth Resistance in Plane-Stress Fracture Testing," Fourth National Symposium on Fracture Mechanics, Carnegie-Mellon Institute, Aug. 1960, to be published in *Engineering Fracture Mechanics.*

[*12*] Boyle, R.W. in *Materials Research and Standards,* Vol. 2, 1962, pp. 646-651.

[*13*] Carman, C.M., Armiento, D.F., and Markus, H. in *Proceedings,* First International Conference on Fracture, Sendai, Japan, 1965, Vol. 2, pp. 995-1038.

[*14*] Lauta, F.J. and Steigerwald, E.A., "Influence of Work Hardening Coefficient on Crack Propagation in High-Strength Steels," Technical Report AFML-TR-65-31, Air Force Materials Laboratory, May 1965.

[*15*] Forman, R.G., "Experimental Program to Determine Effect of Crack Buckling and Specimen Dimensions on Fracture Toughness of Thin Sheet Materials," AFFDL-TR-65-146, Air Force Flight Dynamics Laboratory, Jan. 1966.

[*16*] Rooke, D.P. and Bradshaw, F.J. in *Proceedings*, 2nd International Conference on Fracture, Brighton, England, 1969, pp. 46-57.

[*17*] Carman, C.M. and Irwin, G.R., "Plane Stress Fracture Toughness Testing," unpublished report.

[*18*] Pellini, W.S. and Judy, R.W., Jr., "Significance of Fracture Extension Resistance (R-curve) Factors in Fracture-Safe Design for Nonfrangible Metals," NRL Report 7187, Naval Research Laboratory, 19 Oct. 1970.

[*19*] Goode, R.J. and Judy, R.W., Jr., "Fracture Extension Resistance (R-curve) Features of Nonfrangible Aluminum Alloys," NRL Report 7262, Naval Research Laboratory, 11 June 1971.

[*20*] Jones, M.H. and Brown, W.F., Jr., in *Review of Developments in Plane Strain Fracture Toughness Testing, ASTM STP 463,* American Society for Testing and Materials, 1970, pp. 63-101.

D. E. McCabe[1] and R. H. Heyer[1]

R-Curve Determination Using a Crack-Line-Wedge-Loaded (CLWL) Specimen

REFERENCE: McCabe, D.E. and Heyer, R.H., "**R-Curve Determination Using a Crack-Line-Wedge-Loaded (CLWL) Specimen,**" *Fracture Toughness Evaluation by R-Curve Methods, ASTM STP 527,* American Society for Testing and Materials, 1973, pp. 17-35.

ABSTRACT: A procedure is described for determining crack-growth-resistance curves, R-curves, using crack-line-wedge-loaded (CLWL) specimens. In testing high-strength sheets, a compliance procedure has been used to determine the applied load, and the effective crack length is taken as the visible crack length plus the Irwin plastic zone correction. For lower strength, higher toughness sheets and light plates, the effective crack length is determined by a double compliance technique. For these materials the $r_y = 1/2\pi \times (K/\sigma_{YS})^2$ plastic zone radius was found to overcorrect the crack length.

Currently a plastic hinge model is being investigated as a means of extending R-curve determinations well into the plastic deformation range.

A comparison of R-curves determined by CLWL specimens and by center-cracked tension specimens of high-strength sheets shows quite good agreement. There is little information of this type on the tougher materials. Present work is directed at R-curve determinations on low-alloy, high-toughness light-plate material.

KEY WORDS: crack propagation, fracture toughness, aluminum alloys, structural steels, loads (forces), strains, stresses, stainless steels, measurement, tests, evaluation, fracture strength

The currently favored methods for rating the fracture toughness of structural steels are based on energy and transition temperature measurements, as in the Charpy, NDT, drop weight tear test, and dynamic tear test. It is not likely that these test methods will soon be displaced, for specification purposes, by the more complex and expensive fracture mechanics methods. Nevertheless, there is a need for more basic information on fracture toughness, such that critical load and crack length conditions can be predicted for specific structures and materials. This type of information is available for high-strength, relatively brittle materials for which valid K_{IC}-values can be readily determined. What is needed are comparable methods of determining fracture mechanics K-values for the tougher materials which do not develop plane-strain at the crack front in thicknesses of interest. The plane-strain stress intensity factor K_{IC} is a unique material property, insensitive to geometry within stated limits, whereas K_C is

[1]Senior research metallurgist and principal research associate, respectively, Research and Technology Center, Armco Steel Corp., Middletown, Ohio 45042.

specimen dependent. However, by testing wide center-notched panels in sheet thicknesses an apparent constant value of K_C can be approached. Normally, there is a certain amount of stable crack growth and plastic zone development prior to rapid fracture, and the crack length and stress at instability depend upon the geometry of the part and toughness development of the material. As the crack grows, the resistance to fracture increases due to increased volume of plastically deformed material just ahead of the crack. This increase can be expressed in terms of an R-curve for the material: the relationship between crack growth resistance development, R, and crack extension, Δa. The crack growth resistance may be expressed in the same units as G or the fracture mechanics term K, and recently the designation K_R (ksi-in.$^{1/2}$) has been introduced, as in Fig. 1. Here the R-curve rises sharply from a starting crack length a_0. The same R-curve is obtained from other starting crack lengths within the practical working range of the test specimen. Also shown are crack driving force curves, K-curves, at four levels of applied load, P. These curves are calculated from the K-equation for the appropriate specimen geometry; for example, $K = (P\sqrt{a})/(BW)Y$ for a center notched specimen, where Y is a function of a/W, B is specimen thickness, and W is specimen width. The intercept between the crack driving force curve, K, and the crack growth resistance of the material, K_R, determines the incremental stable crack extension. The point at which the K and K_R-curves are tangent determines the instability conditions for K_C. This K_C is not necessarily descriptive of instability for another specimen or component.

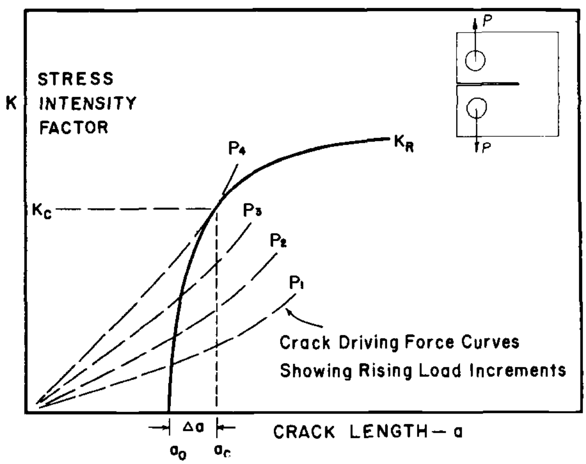

FIG 1—*Crack-growth-resistance curve and crack driving force curves for load controlled test.*

Development of Method

Displacement Control Concept

In the case of tests made by tension loading, with suitable instrumentation for determining the R-curve, the maximum attainable K_R will be K_C, at the tangency point as described in Fig. 1. A crack-line loaded specimen with displacement control rather than load control will have negatively sloped crack driving force as shown in Fig. 2. Because there can be no tangency to the developing crack growth resistance, K_R, the crack tends to remain stable usually up to a plateau level. There are exceptions in the case of very brittle materials where a free running crack may develop even with displacement control. Characteristics of crack-line-loaded and various other specimen types under load and displacement control are treated by Clausing [*1*].[2] The specimen configuration selected for the present work, Fig. 3, has the well-known Westinghouse WOL proportionality, with an H/W ratio of 0.486 [*2*]. Two specimen sizes were chosen, corresponding to the lateral dimensions of the Westinghouse 2T and 4T specimens, but ignoring the thickness specifications. The Westinghouse 2T and 4T convention was retained in the present work, but prefixed with the designation CLWL (crack-line-wedge-loaded).

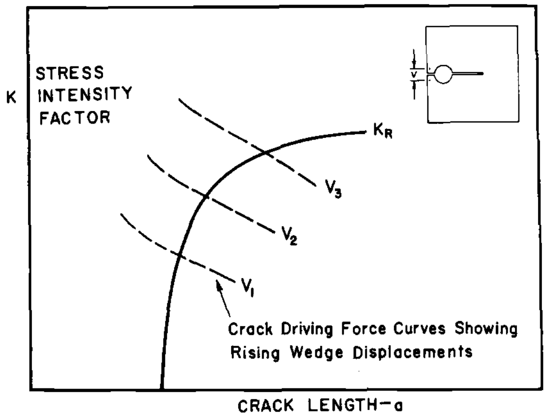

FIG. 2—*Crack-growth-resistance curve and crack driving force curves for load displacement controlled test.*

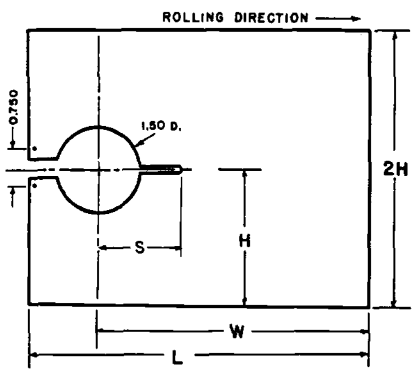

	CLWL-2T	CLWL-4T
H	2.48	4.96
W	5.1	10.2
L	6.46	11.56
S	1.50	3.0

FIG. 3—*Modified WOL-T specimens for single compliance CLWL tests of high strength materials.*

[2]The italic numbers in brackets refer to the list of references appended to this paper.

Single Compliance Technique

Tapered wedge loading is a very effective method of obtaining displacement control of crack-line-loaded specimens. Our first setup showing a CLWL-2T specimen appears in Fig. 4. The wedge load is transmitted through tapered segments which fit within a 1½-in.-diameter hole. Loads are obtained by a compliance procedure based on the relationship

$$\frac{EBV}{P} = f_1\,(a/W) \tag{1}$$

where

E = modulus of elasticity,
B = thickness,
P = load,
a = effective crack length,
W = specimen width, and
V = displacement.

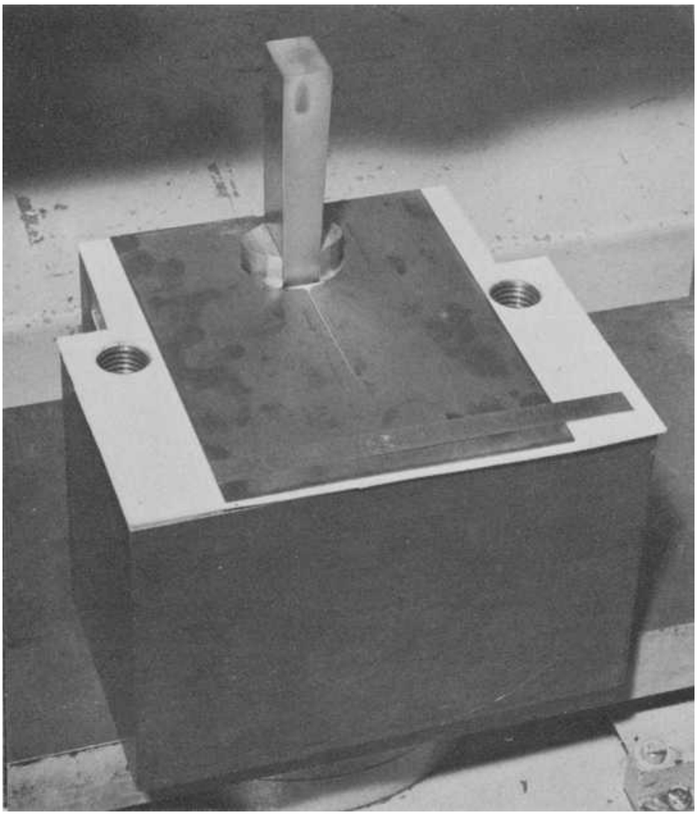

FIG. 4—*Test setup for CLWL-2T test, cover plate removed.*

This relationship may be obtained analytically by a variety of methods, and may be checked experimentally by calibration within the elastic range, using various crack lengths. The displacement measurement points at 0.750 in. gage span are shown in Fig. 3. The experimental calibrations were obtained on sheet thickness specimens, and are shown in Fig. 5 to be in agreement with results of Novak and Rolfe [*3*] who used a standard WOL-1T specimen, 1 in. thick. Brown [*4*] has reported that experimental compliance relationships vary with loading hole and pin arrangements, slot width, and specimen thickness. All of these variables were involved in the data shown in Fig. 5. Individual specimens of the same geometry and loading conditions may have vertically displaced compliance curves, but no change in their shape has been observed.

R-curve development involved incremented crack extension, with stage micrometer readings of the displacement and visible crack length. The effective crack length was then obtained by adding the Irwin plastic zone correction for plane-stress to the measured crack length.

$$\begin{aligned} r_y &= 1/2\pi \times (K/\sigma_{YS})^2 \\ a &= a_m + r_y \end{aligned} \qquad (2)$$

where

r_y = plastic zone correction, in.,
a_m = measured visible crack length, in., and
a = effective crack length, in.

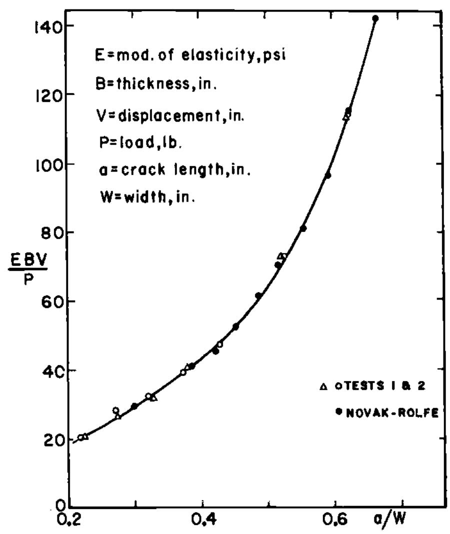

FIG. 5—*Compliance calibration for CLWL specimen,* H/W = *0.486.*

The K-equation for this specimen is

$$K = \frac{P}{B\sqrt{a}} f_2(a/W) \tag{3}$$

From Eqs 1 and 3:

$$K = \frac{EV}{\sqrt{a}} \frac{f_2(a/W)}{f_1(a/W)} \tag{4}$$

Since the crack length, a, includes a correction for plastic zone size which in turn depends upon K, an iterative calculation procedure is required. The form of the K-curves for displacement control was shown in Fig. 2.

Load Prediction from Compliance

In wedge loading the burden of predicting an accurate load, P, using compliance is not in the accuracy of measurement of displacement V, or of a_m, but in the accuracy of the determination of the plastic zone correction, r_y. Load predictions have been in agreement with loads determined directly under tension loading for high-strength stainless steel sheets, but not in the case of 2024-T3 aluminum alloy. For many materials which develop rather large plastic zones, the Irwin plane-stress r_y has been found to overestimate the plastic zone contribution, increasing the effective Δa, and moderately reducing K_R-values of R-curves. Subsequently a double compliance procedure was developed where the effective crack length is determined from the elastic displacement of the specimen. This involved the introduction of a second displacement measurement point along the crack line (see Fig. 6).

In Eq 1 E, B, V, and W are known or measured at any point during the test, while the load, P, and crack length, a, are to be calculated. Measuring V at two separate locations on the specimen, V1 and V2, gives two independent estimates of compliance determined load and effective crack length. The correct P- and a-values may be calculated by an iterative procedure. It soon becomes

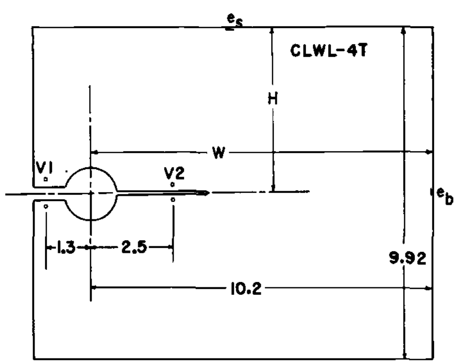

FIG. 6—*Double compliance CLWL-4T test specimen,* H/W = *0.486.*

evident that a more practical way to apply this principle is to determine the ratio of displacements as a function of effective crack length, and obtain crack length directly from:

$$V1/V2 = f_3\ (a/W) \tag{5}$$

The relationship shown in Fig. 7 was obtained under elastic loading conditions as in conventional compliance calibrations.

Test records for development of R-curves now can be obtained by a V1-V2 plot on an X-Y recorder. A typical example is given in Fig. 8.

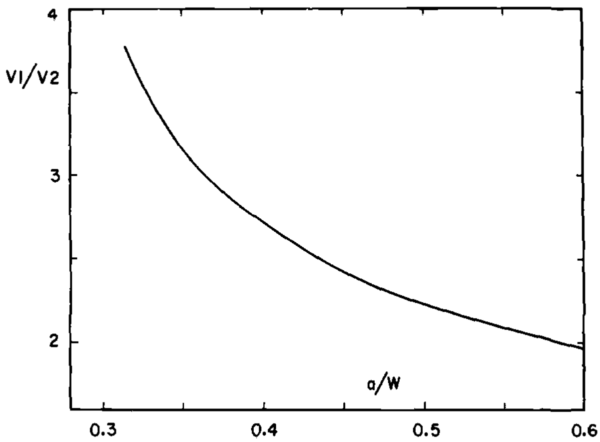

FIG. 7—*V1/V2 displacement ratio versus crack length for CL WL-4T specimens.*

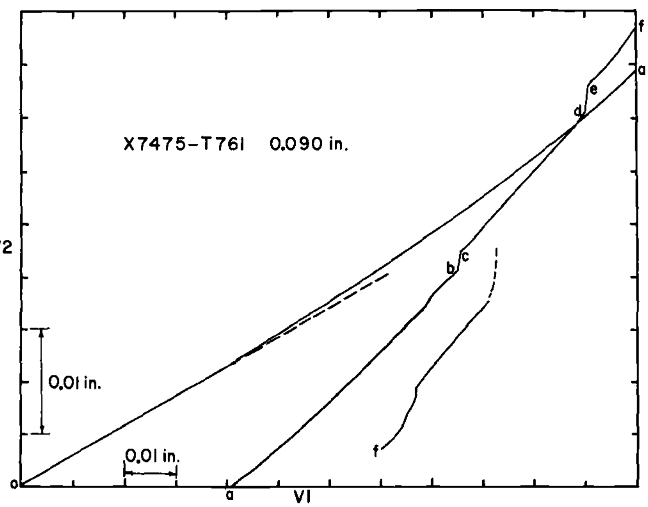

FIG. 8—*V1 and V2 displacements for high-strength aluminum alloy.*

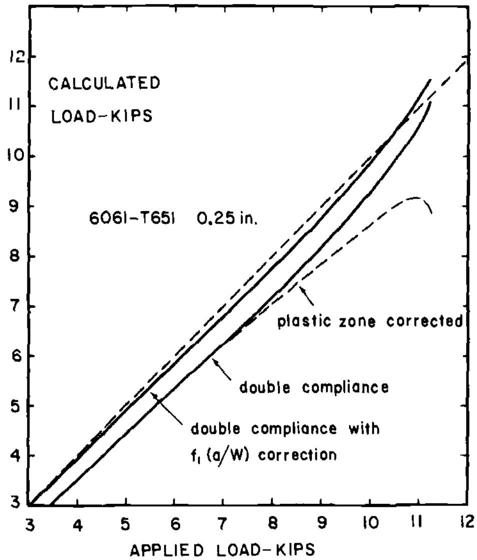

FIG. 9–*Comparison of calculated and applied loads in a load controlled test of a CLWL-4T specimen.*

An example of the improvement in load predictions using this double compliance technique is demonstrated in Fig. 9, bottom curves. The calculated or predicted loads tend to be offset parallel to the measured loads. Accuracy is further improved by a compliance correction procedure to be described later. The Irwin plastic zone corrected crack lengths yield calculated loads which fall away from the measured loads at about 7 kips. The upper curve appearing in this figure refers to an improved compliance correction procedure to be described later.

The influence upon the R-curve of the two methods of determining effective crack length and load is illustrated by an example in Fig. 10. Here the crack extension, m, between the curve labeled "visible crack" and the double compliance R-curve represents the crack extension due to plastic deformation ahead of the measured crack. The corresponding extension $m + n$ is equal to r_y for the same K level. A given datum point P on the double compliance R-curve corresponds to the datum point P on the plastic zone corrected R-curve.

Instrumentation

The early single compliance tests were made by stepwise loading, using a stage micrometer to measure V and a_m at each increment. Our first double compliance tests were instrumented by mounting National Aeronautics and Space Administration (NASA) type clip gages at positions V1 and V2, spanning 0.8 and 0.4 in., respectively. Because of the limited range of linearity of these gages, (nominally 0.070 in.) it was necessary to reset the span every 0.070 in. of

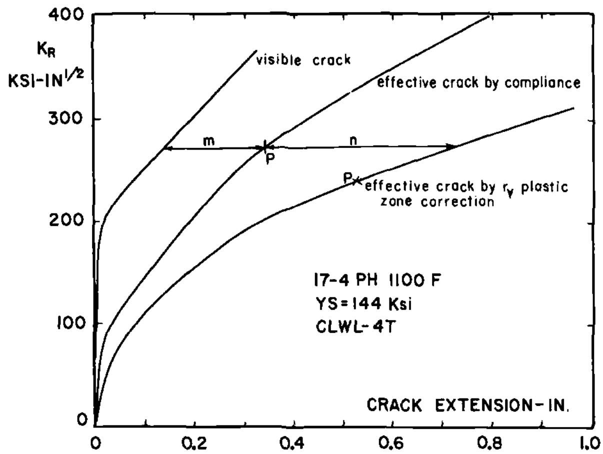

FIG. 10—*Crack-growth-resistance of 17-4PH-1100F sheet, 0.063 in.*

displacement during the test. Stepwise mounts were used for this purpose. The voltage outputs were charted on an X-Y recorder. The clip gages were later replaced by Hewlett-Packard DCDT-7 linear transducers having 0.5 in. linear range. They were mounted vertically as shown in Fig. 11. The direction of motion was changed by passing a thin steel band over a pulley.

This system was found to be difficult to handle because of the inherent problems associated with maintaining high precision with mechanical linkages. It since has been replaced with a horizontally mounted system (see Fig. 12). Extension arms are provided to extend DCDT transducers outside of an environment box presently used in low-temperature work.

Fixturing

The first wedge loading system with the simple wedge and split pin arrangement was used successfully in the development of R-curves on high-strength materials using the Irwin plastic zone corrections to crack length. With the introduction of the double compliance technique, using a calibration curve to determine effective crack length, it became evident that the accuracy of the method was highly sensitive to the mechanics of the loading system. It was determined that the load line was shifting slightly with increased displacement. A remedy was found through the replacement of the split pins with the tapered blocks and circular segments shown in Fig. 13. This system provides for rotation, and the load line is maintained.

In testing sheet materials, the tendency for buckling was restrained using a 1/2-in.-thick holddown plate very lightly loaded. Oiled Teflon sheets were placed between the specimen and plate. A later development for use at cryogenic temperatures where lubricants tend to freeze is shown in Fig. 14. Roller pads are substituted for the Teflon sheets. Gaps in the padding are provided for the

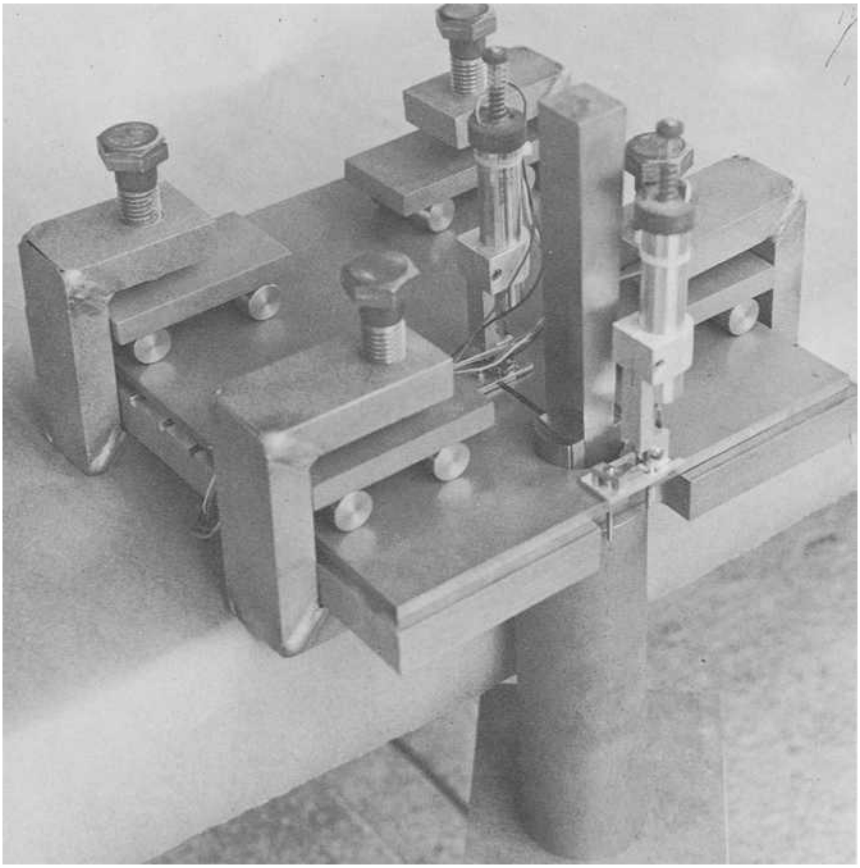

FIG. 11–*CLWL-4T test of light plate, vertically mounted transducers.*

horizontally mounted DCDT displacement gages. A system using ball bearing pads is being presently considered as an alternate.

In testing material of 1/4 in. thickness or more, uniform holddown is not necessary, and roller type holddowns shown in Fig. 12 have been used.

Present Procedures

The double compliance procedure, with transducer measurement of V1 and V2, is used to obtain an X-Y plot during continuous wedge loading. Using a magnification ratio of 100:1 for V1 and 200:1 for V2, it is usually necessary to zero suppress the recorder in midtest, resulting in discontinuous plots, such as Fig. 8. However, digital voltmeters may also receive the V1 and V2 outputs, and the voltage readings can be automatically printed on tape with a printer attachment at suitable time intervals during a test. The test can be then run continuously without pause for reset.

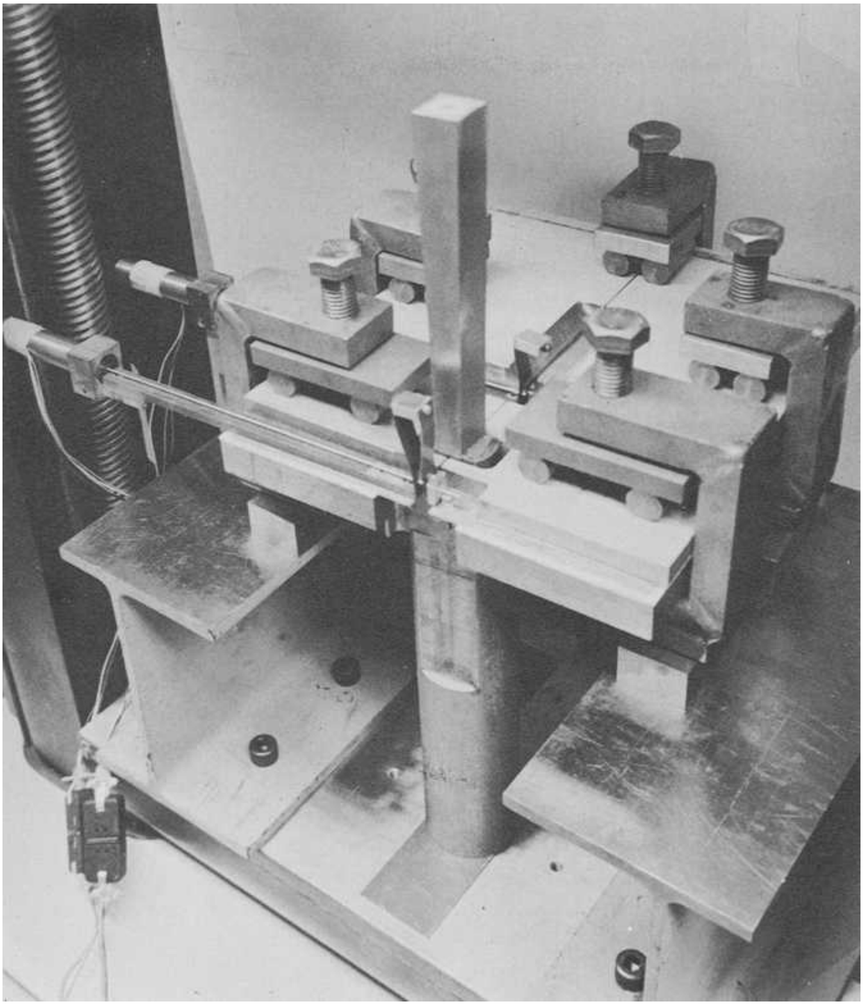

FIG. 12–*Wedge loading of CLWL-4T sheet specimen, horizontally mounted transducers.*

A resistance type strain gage is applied to one edge of the specimen at 0.3 in. ahead of the fatigue crack front, see point e_s in Fig. 6, to refine the measurement technique. In the linear elastic range, the strain gage provides an auxiliary and highly sensitive indication of the initial elastic response of the specimen and, therefore, can be used to correct for start-up lag in the V1 and V2 transducers. In addition, the strain gage output can be used to adjust the level of the compliance curve of Fig. 5 for elastic modulus error, a technique suggested by Boyle [*5*]. The following procedure is used:

In the early portion of the test record, a linear relationship exists between strain at e_s and the V1 and V2 displacements, as illustrated in Fig. 15.

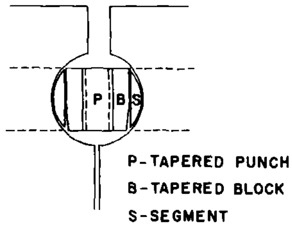

FIG. 13–*Plan view of punch and dies for wedge loading, load line is maintained by rotation.*

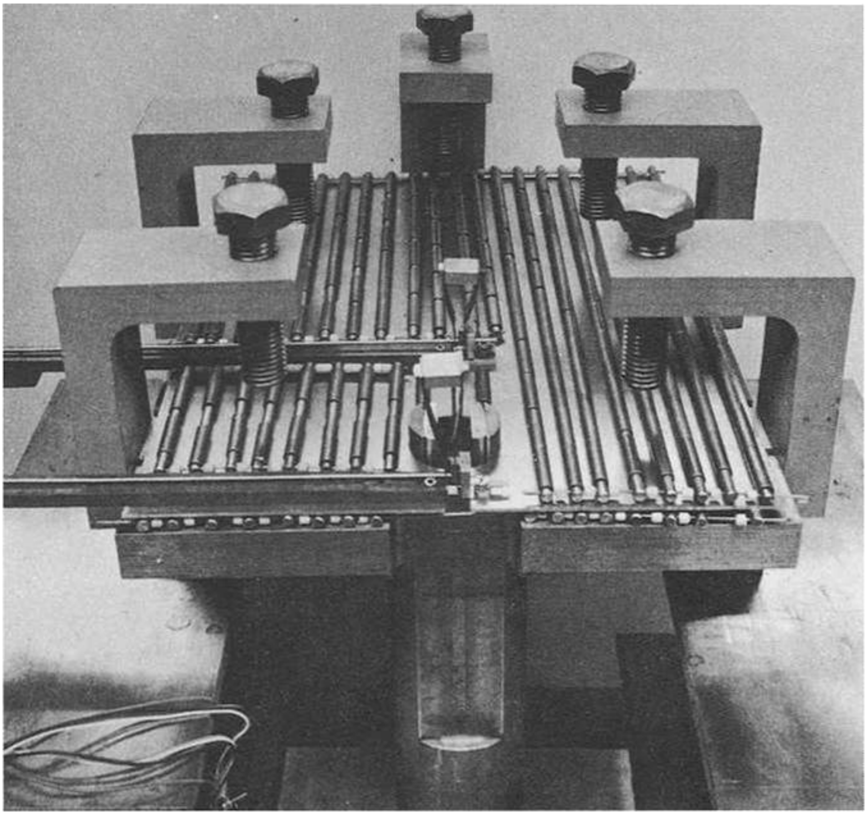

FIG. 14–*Roller pads for reducing frictional constraint. Top holddown plates removed.*

Extrapolation to zero strain provides corrections for startup lag in the displacement gages.

The compliance adjustment to the curve of Fig. 5 is then made by applying the flexural stress equation for a cantilever beam:

$$P = \frac{eE}{a} \times \frac{I}{c} \tag{6}$$

where

P = applied load,
a = initial starting crack length obtained through Eq 5 from the ratio V1/V2,
I = moment of inertia of the specimen arms,
c = half height of specimen arms,
e = strain at strain gage position e_s, and
E = modulus of elasticity.

Substituting for P in Eq 1

$$f_1\ (a/W) = \frac{acBV1}{eI} \tag{7}$$

where

B = thickness and
$V1$ = displacement at a selected strain, e.

In Fig. 15, for example, taking e = 850 μ in./in., $V1/V2$ = 3.52; and from the relationship of Fig. 7 a = 3.264, and from Eq 7 $f_1(a/W)$ = 25.72. The

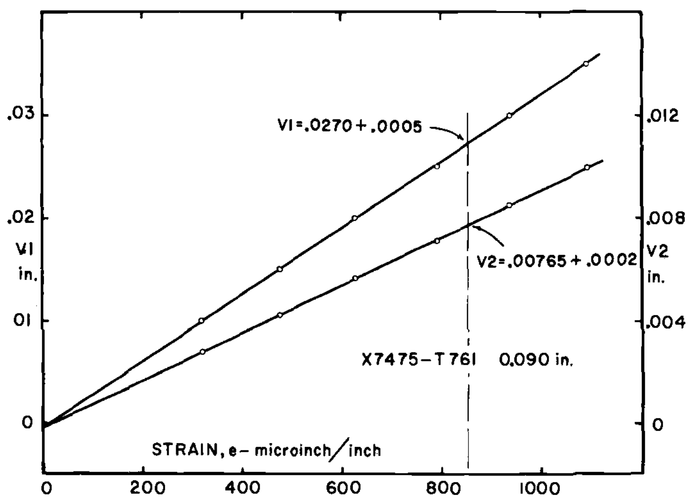

FIG. 15—*Relationship between V1 and V2 and the strain* e_s *(see Fig. 6).*

corresponding value for $a = 3.264$ in Fig. 5 is 26.17. The basic curve is vertically shifted 0.45 units, and load predictions are then made from the adjusted curve. A typical example of the improvement in calculated load is given in Fig. 9.

The material in the preceding example is a high-strength aluminum alloy, Alcoa X7475-T761, 0.090-in.-thick sheet, tested as a CLWL-4T specimen, with $W = 10.2$ in. and $H/W \approx 0.486$. The V1-V2 test record in Fig. 8 shows discontinuities resulting from short bursts of rapid crack extension followed by crack arrest and continued slow growth. The corresponding dips in K_R and P versus a-curves are seen in Fig. 16. This is in contrast to the typically smooth curves which characterize continuous slow crack growth [6].

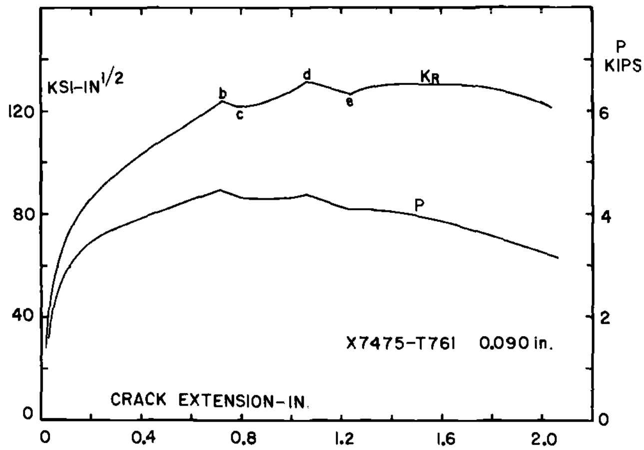

FIG. 16–*K_R and P (load) curves for high strength aluminum alloy (see Fig. 8).*

Specimen Dependence of R-Curves

The concept that R-curves are a material characteristic independent of specimen type, size, or initial crack length (within normal range of application of the specimen) has been tentatively accepted as a working hypothesis. Experimental checks have been made principally by comparison of R-curves developed from center-cracked tension (CCT) specimens and CLWL specimens [7]. Both favorable and marginally unfavorable results have been reported. One means of evaluating the concept is by prediction of K_C-values for center-cracked tension specimens from R-curves determined with CLWL specimens. Results based on center-cracked tension tests made at three laboratories are summarized in Table 1 [7]. These are high-strength materials with relatively small plastic zone sizes; hence, the Irwin plastic zone correction of crack length in the CLWL tests is quite suitable.

R-curves from Armco CCT and CLWL tests of PH14-8Mo SRH1050 stainless steel sheets 0.050 in. thick, 206 ksi yield strength, are shown in Figs. 17 and 18. Fig. 17 makes the comparison on the basis of Irwin r_y plastic zone corrected

TABLE 1–*Comparison of predicted and experimental* K_C*-values for CCT tests.*

Program[c]	Material	Test Direction	B, in.	CCT, $2a_0$,	CCT, W,	Yield Strength, ksi	CCT[a] K_C ksi-in.$^{1/2}$	CLWL[b] K_C ksi-in.$^{1/2}$
I	7075-T6	WR	0.066	3.0	9.0	75.7	62.5	59.1
		RW	0.066	3.0	9.0	75.7	66.5	60.6
II	Ti-6Al-4V	WR	0.050	4.2	12.0	142.4	166.2	162.9
		RW	0.050	4.2	12.0	135.8	135.1	132.7
III	7075-T6	RW	0.0625	2.5	5.0	74.6	62.6	58.4
		WR	0.0625	1.5	5.0	72.8	55.7	51.2
		WR	0.0625	2.5	5.0	72.8	48.5	50.9
		RW	0.0315	1.5	5.0	75.1	65.9	60.4

[a] Experimental values for CCT specimens.

[b] Predicted for CCT specimen from R-curve for CLWL specimen, using plastic zone corrected crack length.

[c] I–CCT tests by Frankford Arsenal, C. M. Carman.
II–CCT tests by The Boeing Co., R. Carter.
III–CCT tests by The Northrop Corp., D. P. Wilhem.

cracks, and Fig. 18 compares compliance corrected cracks. At this strength level there is little difference between the Irwin r_y corrected and the double compliance results. The CCT and CLWL R-curves are in substantial agreement.

Oftentimes CCT and CLWL comparisons were made by different investigators and under noncomparable loading conditions. The CCT tests sometimes were semidynamic, under rising load conditions, where difficulty is associated with determination of instability conditions. On the other hand, the CLWL R-curves

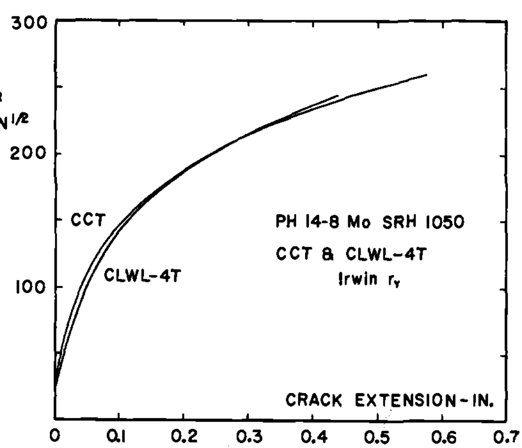

FIG. 17–*R-curves for CCT and CLWL-4T tests of PH14-8Mo,* r_y *corrected crack lengths.*

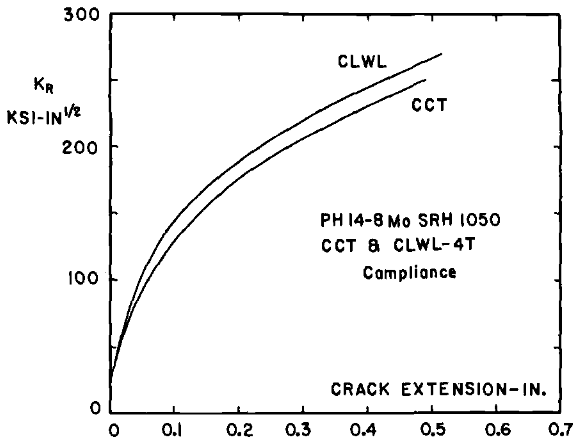

FIG. 18—*R-curves for CCT and CLWL-4T tests of PH14-8Mo, effective crack lengths by double compliance.*

had been determined under conditions where the crack was allowed to completely arrest before measurement. Additional experimental problems associated with the CCT specimen are nonsymmetrical loading in wide panel tests, and appropriate restraint against buckling, which can be particularly critical when compliance techniques are used to determine effective crack length.

Recent Applications

The main thrust of the CLWL work has been to investigate the high-strength materials where full R-curves were well defined and could be developed with moderate size specimens. There is no reason to doubt that toughness development in lower-strength high-toughness materials can be also described in terms of R-curves. The main difference is that the relative proportion of effective crack extension due to plastic zone development as opposed to physical crack extension will be larger. These larger plastic zone effects are not likely to be described accurately by Irwin's r_y relationship, and more reliance will have to be placed on empirical means of determining effective crack length. Additionally, the fundamental problem of embedding these large plastic zones in a predominantly elastic body required that specimen sizes be increased.

The K measuring capacity for specimens of WOL configuration is limited by plasticity at points of maximum compression stress in the specimen arms. This may be estimated using the flexural stress equation for cantilever beam loading of the specimen arms in conjunction with Eq 3 and assuming an a/W ratio of 0.5.

$$K_{cap} = 0.817\, \sigma_{YS} W^{1/2}$$

K_{cap} = desired K capacity,
σ_{YS} = yield strength, and
W = specimen width.

R-curves may be made over a range of temperatures, using an environment chamber for temperature control. At low temperatures, strain sensitive materials may develop instability and rupture even under the rigid displacement control conditions of wedge loading. In wedge loading the rapid drop of load, hence crack driving force, with crack extension will usually arrest crack growth.

Simultaneous to the development of tests on larger specimens to extend the valid R-curve range, we are experimenting with a plastic extension technique suggested by Irwin. When the specimen proportions are changed from $H/W = 0.486$ (WOL) to $H/W = 0.60$ (CTS), a plastic hinge effect will develop with a hinge axis occurring along the crack plane [8]. Under such conditions, crack opening stretch (COS) can be estimated by geometric construction. Based on displacement at location V2, the COS is given by:

$$\text{COS} = 0.45\,(W - a)\,\theta \tag{9}$$

where

$0.45\,(W-a)$ = hinge distance,
θ = $\tan^{-1}\,\Delta V2/[(a - 2.5) + 0.45\,(W - a)]$, and
$\Delta V2$ = displacement at location V2.

Figure 19 shows a typical R-curve development in terms of COS. The effective crack length is determined using the double compliance method. The location for calculating the COS is at the effective crack tip determined by double compliance, which lies within the plastic zone. In the early portion of the R-curve where fracture mechanics K-values are applicable:

$$\text{COS} = \frac{K^2}{E} \Big/ \sigma_{YS} \tag{10}$$

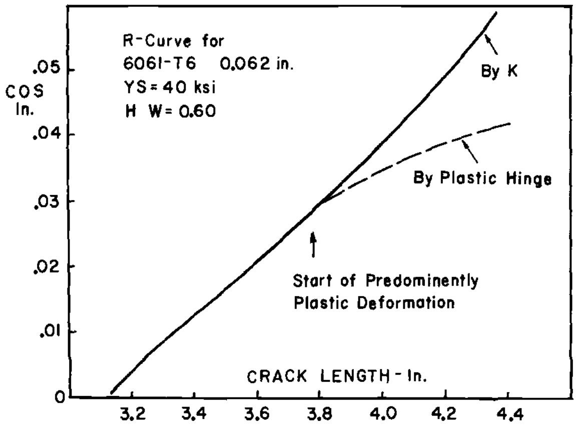

FIG. 19—*Crack-growth-resistance in terms of crack-opening stretch.*

The fracture mechanics and the plastic hinge methods agree reasonably well where the specimen first goes into yielding. The validity of this technique depends on the capability of the double compliance procedure to determine effective crack length when the specimen is displaced according to the plastic hinge model. This will be tested experimentally when equipment becomes available for larger size specimens in which more of the elastic portion of the R-curve can be developed.

Strain Measurements of CLWL Specimens

It has been shown that strain measurement on the edge of the CLWL specimen, position e_s in Fig. 6, gives useful information in the early linear elastic part of the R-curve. The position of the maximum edge strain advances as the crack extends; hence, a series of gages would be required to determine the maximum elastic compressive strain along the specimen edge. However, an approximation may be obtained using a gage position estimated to attain its maximum reading when the specimen edge first deforms plastically. This may be ½ in. or more ahead of the e_s position, depending on the crack growth resistance of the material. Strain at the back edge may be determined continuously with a single strain gage at location e_b in Fig. 6. Using specimens of the compact tension proportions, $H/W = 0.6$, the strain e_b reaches the limit of elasticity before the specimen arms. For $H/W = 0.486$ plastic deformation occurs first at specimen arms, and bending of the specimen arms precludes plasticity at e_b. The e_b strain is approximated by the equation:

$$e_b = \frac{6Pa}{EB(W-a)^2} \tag{11}$$

using the beam flexural stress equation with

$$I = \frac{B(W-a)^3}{12} \qquad C = \frac{W-a}{2} \tag{12}$$

Using P and a determined by the double compliance procedure, comparison may be made to determine directly strains e_b and e_s. Favorable confirmation of the above expressions has been found when the strains e_s and e_b are within the elastic range. This confirms prior observations of other investigators that the stress at the outer edges can be reasonably predicted using simple beam equations.

Summary

This report reviews the development of the Westinghouse WOL type specimen into a method of test for the determination of R-curves on high-strength sheet materials. The method has progressed from a rather simple procedure, adequate only for high-strength low-toughness materials, to a more instrumented version suitable for evaluating tougher materials. Instead of incremented measurement

points, continuous test records are now made, thereby opening possibilities of studying strain rate effects. With the addition of a strain gage to one of the specimen arms, further refinement of measurement precision has been accomplished.

Tests are now being made on strain rate sensitive materials where specimen size has been a limitation. New fixturing has been made for a larger version of the test and for determination of R-curves over a temperature range.

References

[1] Clausing, D. P., *International Journal of Fracture Mechanics*, Vol. 5, 1969, pp. 211-227.

[2] Wessel, E. T., *Engineering Fracture Mechanics*, Vol. 1, 1968, pp. 77-103.

[3] Novak, S. R. and Rolfe, S. T., *Journal of Materials*, Vol. 4, 1969, pp. 701-728.

[4] Brown, W. F., Jr., "Effects of Some Dimensional Variables on Compact Tension Specimens," Note for ASTM E-24 Meeting, American Society for Testing and Materials, 23 Sept. 1969.

[5] Boyle, R. W., *Materials Research and Standards*, Vol. 2, Aug. 1962, pp. 646-651.

[6] Heyer, R. H. and McCabe, D. E., "Plane-Stress Fracture Toughness Testing Using a Crack-Line-Loaded Specimen," to be published in *Engineering Fracture Mechanics*.

[7] Heyer, R. H. and McCabe, D. E., "Crack Growth Resistance in Plane-Stress Fracture Testing," to be published in *Engineering Fracture Mechanics*.

[8] Nichols, R. W. et al, "The Use of Critical Crack Openings Displacement Techniques for the Selection of Fracture Resistant Materials," CODA Panel Report of the Navy Department Advisory Committee on Structural Steels, II W IX-655-69. X-534-69.

E. J. Ripling[1] *and Eliezer Falkenstein*[1]

Measuring K_R-Curves for Thin Sheets

REFERENCES: Ripling, E.J. and Falkenstein, Eliezer, "**Measuring K_R-Curves for Thin Sheets**," *Fracture Toughness Evaluation by R-Curve Methods, ASTM STP 527*, American Society for Testing and Materials, 1973, pp. 36-47.

ABSTRACT: A modification of the tapered double cantilever beam specimen for measuring K_R-curves of thin sheets is described. The modification consists of adhering properly contoured cover plates to the sheet to form a composite zero K-gradient (ZKG) specimen.

This testing procedure has a number of advantages over those presently used for plane stress testing:

1. K is proportional to the applied load and independent of crack length. Consequently, the specimen is stable, allowing for the collection of the complete K_R-curve.
2. The testing procedure is simplified, and the instrumentation required to collect data, even at high rates, is relatively simple, since only load need be monitored.
3. Buckling is eliminated without the need of constraining members near the crack.
4. Cracking rate is related linearly to displacement rate.

KEY WORDS: fracture toughness, crack propagation, plane stress, brasses, aluminum alloys, double cantilever beam specimen, strains, stresses, loads (forces), measurement, evaluation, tests

The fracture toughness of materials that crack under a condition of plane stress, unlike those that fracture under a condition of plane strain, cannot be described by a single value. Plane strain fractures extend so rapidly that the critical value of stress intensity factor, K_{IC}, is essentially independent of the manner in which K_i changes with crack length, a. In plane stress fracturing, on the other hand, cracking is sufficiently slow that fracture instability depends on both the material, that is, its crack growth resistance, K_R, and the K_i characteristics of the structure containing the crack. This relationship between the curve, K_R versus a, and the curve, K_i versus a, for a structure, is shown in Fig. 1. The point of instability, K_C, occurs when the stress intensity factor at the crack tip, K_i, begins to increase more rapidly than K_R, that is, when

$$\partial K_i/\partial a_{\ \sigma=\sigma_c} = (\partial K_R/\partial a)_{\sigma=\sigma_c}$$

[1]Director of research and research engineer, respectively, Materials Research Laboratory, Inc., Glenwood, Ill. 60425.

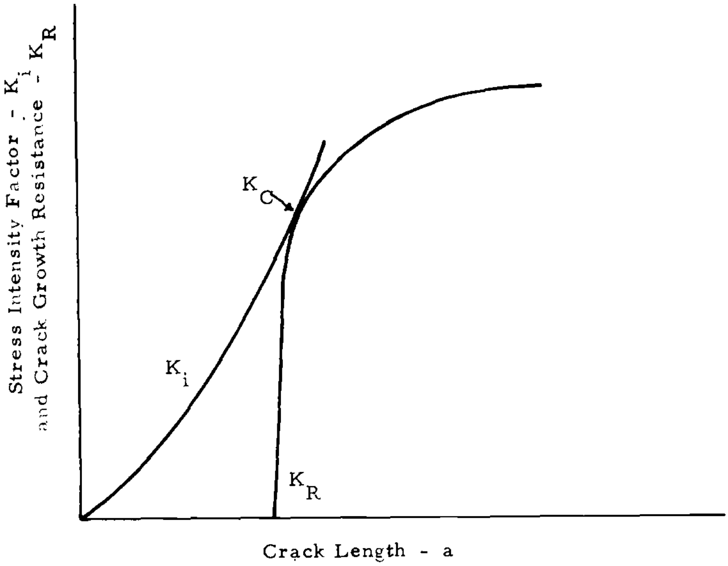

FIG. 1–*Relationship between structure characteristics* (K_i) *and material property* (K_R) *to develop fracture instability* (K_C).

The K_R-curve beyond the point of instability, of course, is not defined. Consequently, the specimen type selected for the measurement of K_R-curves should be one in which K_C is delayed, at least until an equilibrium condition for crack extension has occurred. This requirement suggests the use of specimens in which K_i either decreases or remains constant with increasing a, rather than one in which K_i increases with a. That is, the specimen should have a negative or zero K_i gradient with crack length. The most commonly used test for plane stress testing is a center-notched, remotely loaded, wide panel. Since this has a positive K-gradient, unstable cracking occurs after only a modest amount of crack extension. Carman and Irwin have shown that by the proper selection of the ratio of crack-length to specimen width, W, the amount of crack extension prior to instability can be increased,[2] but even with the optimum ratio of a/w, the amount of stable cracking is still quite limited.

Heyer and McCabe have adopted a modified compact tension specimen to the measurement of K_R-curves by the use of wedge loading.[3] Since such a constant displacement specimen has a negative K-gradient, crack extension is always stable, and the complete K_R-curve can be defined by this method. Because the wedges apply a compressive load, however, the specimens tend to buckle, and this tendency increases as the thickness of the test material decreases.

[2]Carman, C.M. and Irwin, G.R., "Relationship of Crack Opening Stretch and Thickness Contraction to R Curves for Evaluating Fracture Toughness," Frankfort Arsenal Report R-2029, Dec. 1971.

[3]Heyer, R.H. and McCabe, D.E., "Plane Stress Fracture Toughness Using a Crack-Line-Loaded Specimen," National Symposium on Fracture Mechanics, Aug. 1969, to be published *Journal of Engineering Fracture Mechanics.*

This paper describes an adaptation of the tapered-double-cantilever beam specimen to the measurement of K_R-curves particularly for very thin sheets. For this specimen, like the one used by Heyer and McCabe, cracking is stable allowing for the collection of the complete K_R-curve. Unlike the Heyer-McCabe specimen, however, the load is applied in tension rather than compression so that buckling is avoided in even the thinnest members. In this specimen, K_i is independent of a, and simply proportional to the load. Hence, the specimen, when applied to plane stress testing, might best be referred to as a ZKG (for zero K-gradient) specimen.

Specimen Development

Double-cantilever-beam (DCB) specimens, tapered so as to make K_i independent of a, have been used for measuring plane strain initiation and arrest toughness, stress corrosion cracking rates and crack growth rates in fatigue in both monolithic materials and adhesive joints. In those applications where data collected with this specimen could be compared with similar data collected by using compact tension or bend specimens, the scatter bands of data overlapped, indicating that in plane strain testing, at least, the tapered DCB specimen gave satisfactory results.

Designing a specimen shape in which K_i is independent of a is based on the definition

$$K_i = P_i \sqrt{\frac{E}{2B_n} \frac{\partial C}{\partial a}} \tag{1}$$

where

P_i = load,
E = Young's modulus,
B_n = thickness of specimen on crack plane, and
C = specimen compliance.

The specimen is contoured such that $\partial C/\partial a$ is a constant,[4] and it is then convenient to write the latter as

$$\frac{\partial C}{\partial a} = \frac{8}{Eb} m$$

where

B = gross thickness of the specimen and
m = shape factor having the dimensions of in.$^{-1}$. It is frequently found that the calculated value of m is not sufficiently accurate so that an experimentally determined value, based on compliance measurements, is generally used. The symbol for this experimental shape factor is m'.

Hence

$$K = 2P\sqrt{\frac{m'}{B_n B}} \tag{2}$$

When thick sections are contoured in this fashion and an opening load

[4]Mostovoy, S., Crosley, P.B., and Ripling, E.J., *Journal of Materials*, Vol. 2, No. 3, 1967, p. 661.

applied, the crack tends to veer out of the desired plane of extension. To prevent this, side grooves are added to the specimen so that B_n becomes sufficiently less than B to force cracking to occur along the center plane of the specimen. Of course, such side grooves are not practical for thin sheets. Further, if the loads required to cause crack extension were applied through holes in thin sheets, it would be difficult to prevent upsetting of the holes and buckling of the sheet.

To avoid these problems, the specimen is made up as an adhered sandwich in which heavy members are glued onto the test material, and the compliance characteristics of the specimen are determined by the shape of the glued-on members. A drawing of such a sandwiched specimen is shown in Fig. 2. The end of the specimen away from the loading holes is built up as a solid in order to withstand the compressive load that occurs at this location on application of the opening load. It is this solid end that prevents buckling of the sandwiched test section.

For the thin materials tested to date, 0.016 and 0.032-in.-thick brass and aluminum alloys, the glued-on cover-plates were 0.250-in.-thick aluminum alloy. These cover-plates and the test material are first machined separately to the shape shown in Fig. 2, after which all three pieces are properly cleaned prior to gluing with an epoxy adhesive to form the sandwich. Alignment during gluing is forced by means of pins in the loading holes and the back aligning hole. The portion of the test material that will be exposed after assembly, and on which adhesive is not required, is covered with Teflon tape prior to cleaning. This protects the region where the crack is expected to grow from any adverse effects of the cleaning solution. The tape is not removed until after the specimen is glued so that it also prevents any excess glue from getting on the test region of the specimen. For the specimen to perform satisfactorily, the adhesive joint must be able to transmit the applied load in shear. Fortunately, epoxy has excellent shear strength so that for test panels as thick as 0.062 in., there has been no trouble with glueline failures for well made joints, so long as the tests are not conducted at elevated temperatures. For high temperature tests, of

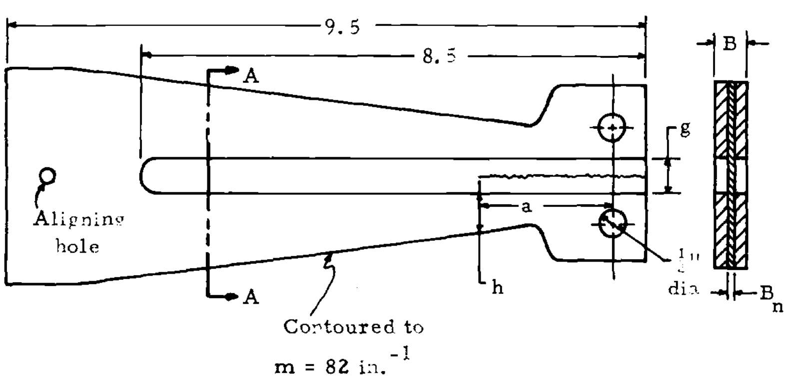

FIG. 2–*Fracture toughness test specimen.*

course, high temperature adhesives are required. When glue failures do occur, the large bending stress on the crack plane causes the crack to veer off the center. If there is a short unbonded section, the crack will deviate from the desired plane of extension only over the length of the unbonded region, and then with further extension the crack will return to the midplane. Apparently, the total specimen when properly adhered acts like a monolithic specimen with extremely deep side grooves.

The first program on which this specimen type was to be used was concerned with the effect of cracking rate, $\dot{a}$, on the K_R-curve. The ZKG specimen is well suited for such a study since at constant load, the cracking rate is proportional to the crosshead displacement rate

$$\frac{dC}{da} = \text{constant} = \frac{8m'}{EB}$$

since

$$C = \Delta/P$$

where

$$\Delta = \text{crosshead displacement,}$$

at constant load, P,

$$\frac{dC}{da} = \frac{1}{P}\frac{d\Delta}{da}$$

hence

$$da = d\Delta(EB/8Pm')$$

or in terms of time derivatives

$$\dot{a} = (EB/8Pm')\,\dot{\Delta}$$

Specimens can be made of reasonable size with shape factors, m', that vary from about 3 to 90. Hence, the proportionality constant relating $\dot{a}$ and $\dot{\Delta}$ is varied readily if faster or slower cracking rates are needed within a specific range of Δ's. (As m' increases, P for constant K_i, decreases, however, so that the ratio of proportionality constants rather than being equal to m'_1/m'_2 for two different shaped specimens is actually equal to $\sqrt{m'_1/m'_2}$.

Specimen Characteristics

A large number of experimental compliance calibration curves were made using different types and thickness of sheet materials and different thicknesses of the aluminum alloy 2024-T351 as cover sheets. In all cases, the contour was based on a calculated value of $m = 82$ in.$^{-1}$. The procedure for compliance calibration was as follows:

1. The test sheets, sandwiched between two adhered cover plates were cut with a jeweler's saw in 1/4 to 1/2 in. intervals. After each cut, six compliance, C, measurements (that is, load versus displacement) were made.

2. The average values of these six measurements was plotted as a function of crack length to determine the range over which dC/da was constant. For the specimen whose dimensions are shown in Fig. 2, this linear behavior occurred between $a = 1.5$ and 4.5 in. A least square fit of the data within this range was made to calculate dC/da.

Two typical curves, C versus a, are shown in Fig. 3, and a tabulation of dC/da and m' for brass and aluminum, each in two thicknesses, is shown in Table 1. As yet, there is no analytical program for calculating dC/da for this specimen type so that it is necessary to experimentally evaluate m'. In spite of the fact that the measured values of m' are not identical with the m-values on which the contour is based, it is obvious that dC/da is constant over a wide range of a's as shown in Fig. 3.

The slot in the cover plates, that is, the opening over which the test material is free of the attachments, was chosen as 1/2 in. It is essential that this height be large enough so that no interaction of the attachments with the stress pattern developed at the crack tip can occur. A formal calculation of the plastic zone size would suggest that this opening must be larger than 1/2 in., but the intensification of stress associated with the crack tip would not be expected to extend over a distance greater than a few plate thicknesses in a direction perpendicular to the plane of the crack. For the 0.016 and 0.032-in.-thick plate, the 1/2-in. opening is greater than 30 and 15 times the plate thickness, respectively.

In spite of the fact that the opening is many times the plate thickness, it is prudent to determine experimentally whether or not the opening is large

TABLE 1–*Compliance characteristics of plane stress ZKG specimen (1/2-in-thick 2024-T351 aluminum cover plates,* m = *82 in.*$^{-1}$, 1/2 in. gap).

Material	Thickness, in.	Test Direction	dC/da, in./lb.	m', in.$^{-1}$
Brass	0.016	WR	13.1×10^{-5}	85.9
	0.032	WR	11.8×10^{-5}	81.5
Aluminum	0.016	RW	13.9×10^{-5}	89.5
		WR	13.7×10^{-5}	88.6
	0.032	RW	12.5×10^{-5}	83.4
		WR	12.8×10^{-5}	85.4

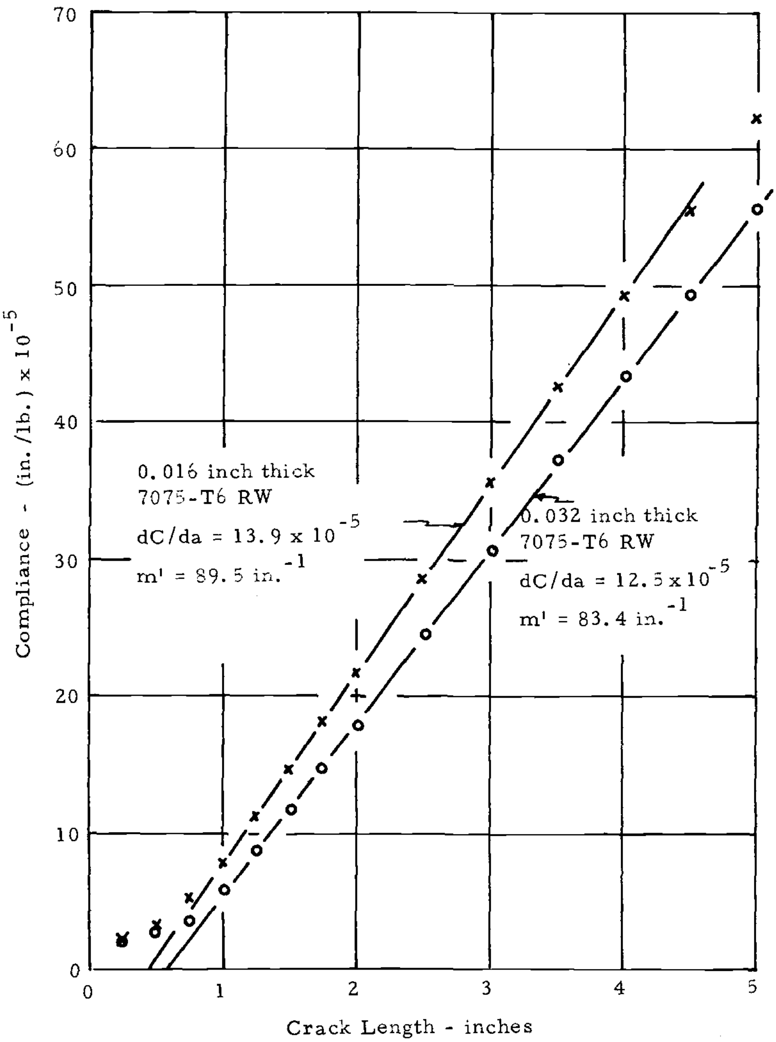

FIG. 3—*Compliance versus crack length for two specimens, both contoured to* m = *82 in.*$^{-1}$.

enough. The simplest way to do this is to measure the K_R-curve of one material with specimens having different sized openings. This was done for specimens having 1/8, 1/2, and 1-in. openings. All of these were machined to a contour calculated for m = 82 in.$^{-1}$ ignoring the contribution of the unsupported metal in the slot. Each of the three specimen shapes was first calibrated experimentally for $\partial C/\partial a$ to obtain the proper value of m' after which the K_R-curves were measured using 0.016-in.-thick aluminum as the test material. For all three openings, the scatterbands of the K_R-curves overlapped suggesting that openings between 1/8 and 1 in. were satisfactory for these specimens.

Typical Data

To compare the data collected with this ZKG specimen with wide plate data presented by Carman and Irwin, and with data collected by Heyer and McCabe using crack line loaded compact tension specimens, some tests were run on 0.065-in.-thick 7075-T6. The ZKG specimen was machined from one of the broken halves of a Carman-Irwin wide plate test specimen, and the K_R versus crack length curves for these three tests are shown in Fig. 4.

The ZKG K_R-curve was found to lie between the positive K-gradient specimen test of Carman and Irwin and the negative K-gradient specimen test of Heyer and McCabe. There is some reluctance to attach any significance to this rating since

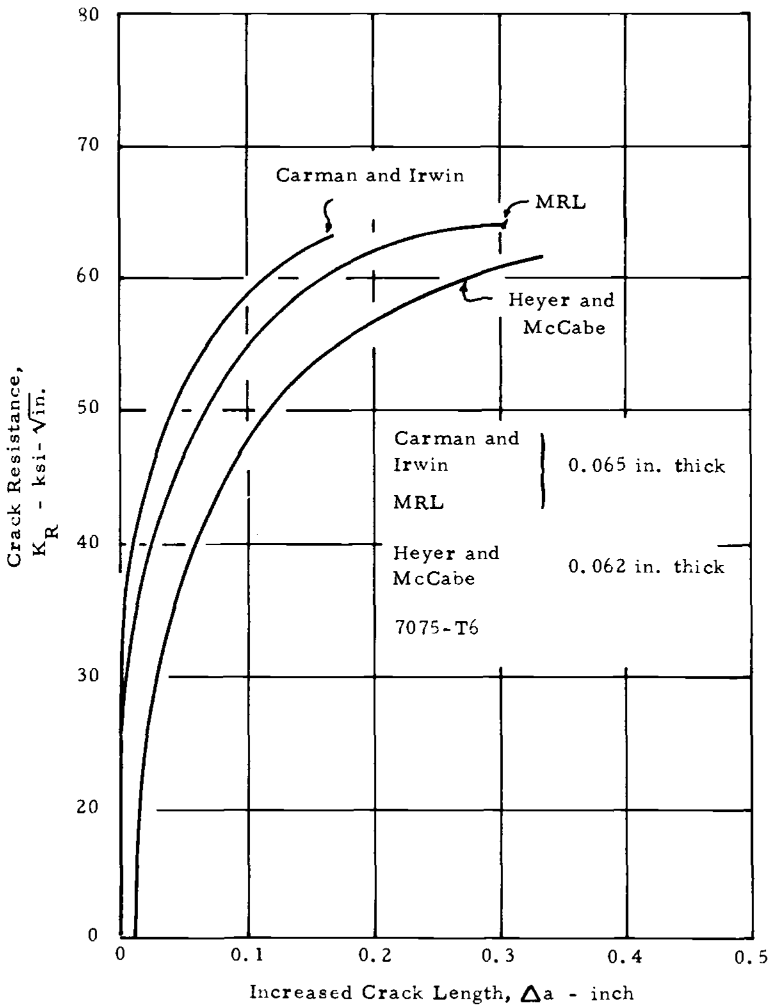

FIG. 4—*Comparison of K_R-curves obtained by Carman and Irwin (center-cracked panel) MRL (zero K-gradient specimen) and Heyer and McCabe (negative specimen).*

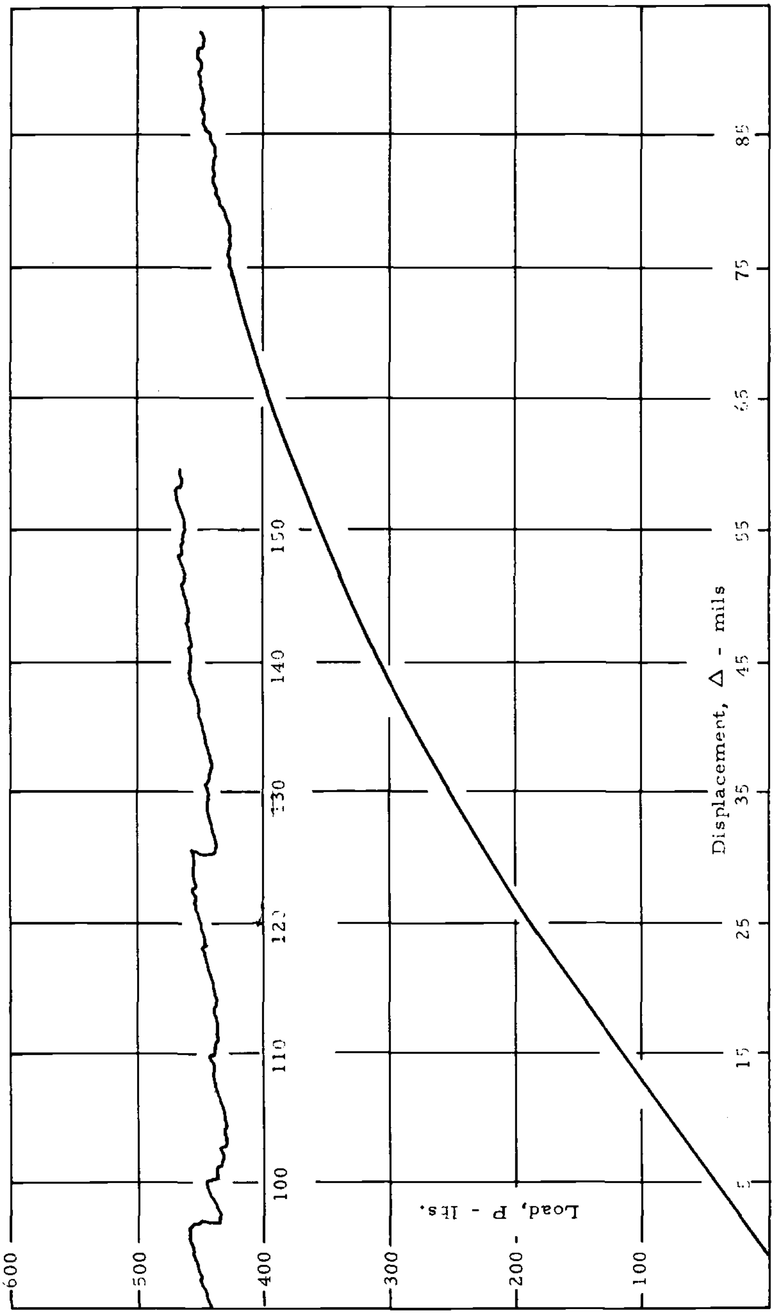

FIG. 5–*Typical load,* P, *displacement* Δ, *diagram obtained on 0.016-in.-thick brass tested in the RW direction.*

Carman and Irwin ran a series of tests on this same material, and found a scatterband that embraced all three of these curves. Nevertheless, these test results suggest that all three test procedures produce similar K_R-curves, and all three tests gave about the same value of K_R at the plateau: 65 ksi-$\sqrt{\text{in}}$.

In measuring K_R with the ZKG specimen, it is convenient to plot load, P, versus displacement, Δ , and if rates are important, load versus time as well. A typical load-displacement chart obtained on 0.016-in.-thick brass is shown in Fig. 5. Notice that after cracking starts, the load is relatively constant identifying a plateau value of K_R. The crack is not driven at a constant velocity within the plateau, however. Instead, cracking proceeds in a series of short jumps. Each of the peak values in the plateau regime is associated with the initiation of a short jump, and the trough that follows the peak is associated with an arrest. In plotting the K_R-values for equilibrium cracking in the plateau, it is necessary to show a band of values, the top of which indicates the initiation values and the bottom the arrest values.

It might also be mentioned that not all materials show a plateau as independent of crack length as the one shown here. Although all the brass specimens tested to date show this behavior, for the aluminum alloys there is a slight tendency for K_R to increase with crack length even after cracking has started.

Some typical test results obtained on a thin sheet of brass are shown in Fig. 6. The 0.016-in.-thick brass was tested in two directions, RW and WR at test temperatures of -70, +70, and +165 F. The value of K_R in the plateau is plotted as a band, the top of which represents initiation, and the bottom arrest, values. Rise time is defined as the time interval over which the load increases from zero to the load at which cracking starts. Assuming a K_R-value of 100 ksi-$\sqrt{\text{in}}$. the slowest tests (rise time = 100 s) would have a cracking rate of approximately 15 x 10^{-3} in./s. This is somewhat slower than the regime of static plane stress cracking. For the fastest tests, assuming the same value of K_R, the cracking rate would be approximately 3000 in./s.

Similar results for the aluminum alloy 7075-T6 in 0.016 in. thickness are shown in Fig. 7. Both of these materials are similar in that they get tougher with increased cracking rate. The brass, however, was highly anisotropic, that is, its properties in the RW direction were higher than those in the WR direction, while the aluminum alloy was reasonably isotropic.

Conclusions

In summary, a zero K-gradient specimen based on a modification of the tapered-double-cantilever beam appears to have certain advantages for plane stress testing of thin sheet. These advantages include:

1. The specimen is stable for all crack lengths allowing for the collection of the complete K_R-curve.
2. Buckling is eliminated without the need of constraining members near the crack.

3. Since only the load need be monitored, testing procedures are simple, and the instrumentation required to collect data, even at high rates, is relatively simple.

4. The cracking rate is related linearly to displacement rate so that the specimen is particularly useful for studying rate effects.

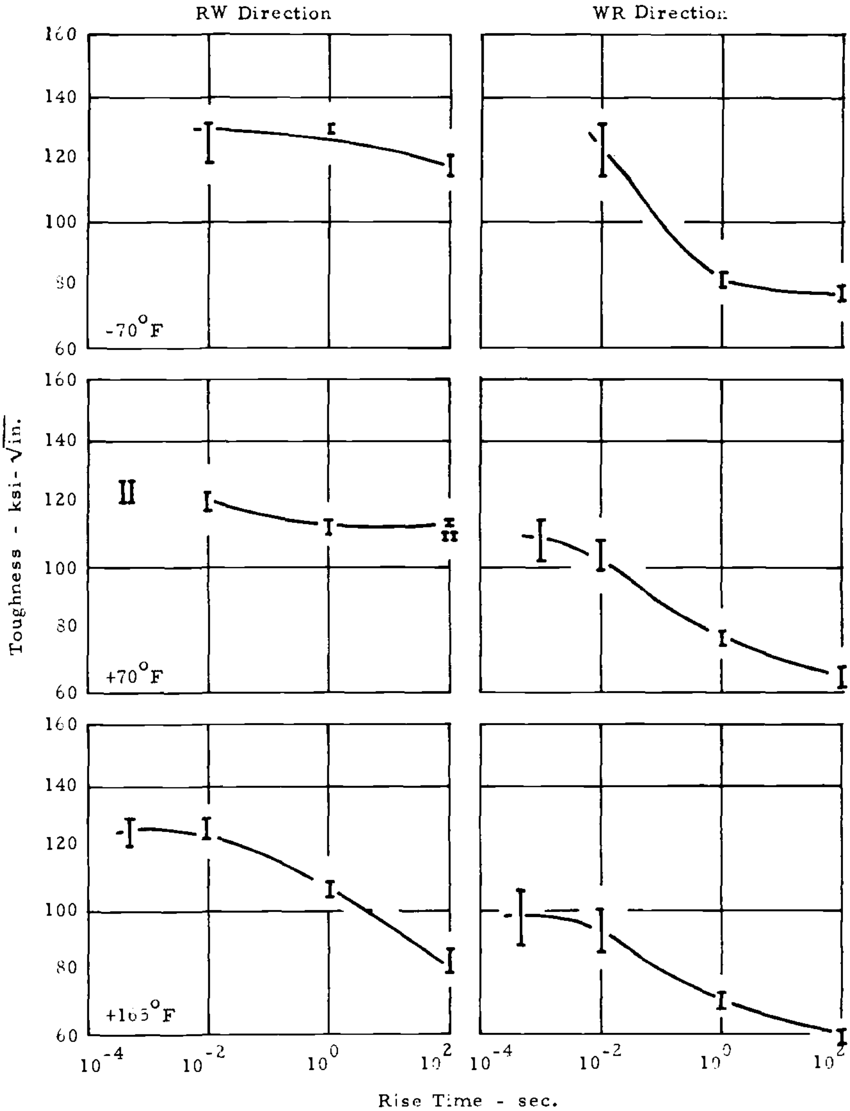

FIG. 6—*Toughness of 0.016-in. cartridge brass (spring temper) as a function of rise time.*

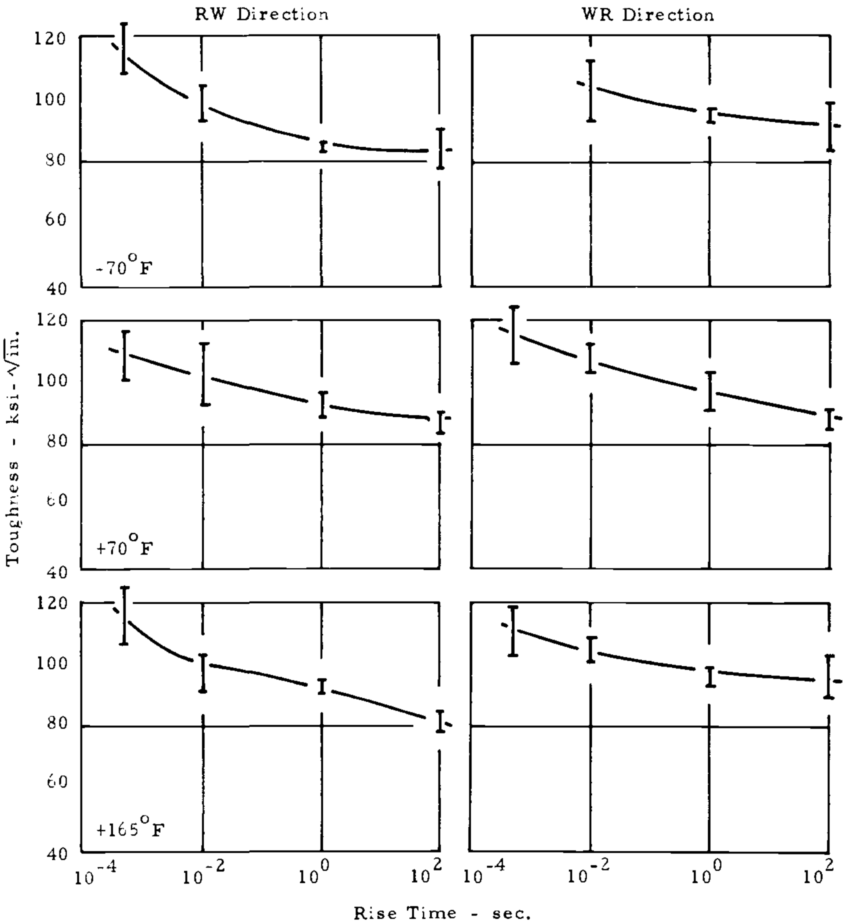

FIG. 7–*Toughness of 0.016-in.-thick 7075-T6 aluminum alloy as a function of rise time.*

R. W. Judy, Jr.,[1] and R. J. Goode[1]

Fracture Extension Resistance (R-Curve) Characteristics for Three High-Strength Steels

REFERENCE: Judy, R.W., Jr., and Goode, R.J., "**Fracture Extension Resistance (R-Curve) Characteristics for Three High-Strength Steels,**" *Fracture Toughness Evaluation by R-Curve Methods, ASTM STP 527,* American Society for Testing and Materials, 1973, pp. 48-61.

ABSTRACT: New procedures for characterizing the fracture extension resistance of ductile metals have been established. The fracture extension resistance curve (R-curve), which delineates the increasing rate of plastic work to cause crack propagation in nonbrittle metals, is determined by using dynamic tear (DT) test procedures. The resistance parameter is the slope of the R-curve.

The effect of thickness on the R-curve slope was investigated for three high-strength steels of high, intermediate, and low resistance to ductile fracture. R-curves were determined for each steel in the full thickness (1 in.) and for thicknesses of 0.625 and 0.325 in. The R-curve slopes showed good agreement for each section size, and a transition in the fracture mode from flat fracture at short crack extensions to the metal's characteristic degree of shear fracture for long extensions was observed for each steel. The data can be described by an exponential equation involving fracture energy, specimen cross-section dimensions, and a constant, R_p, which is proportional to the R-curve slope. For each steel, R_p is unaffected by changing specimen geometry, thus indicating it to be a material property.

KEY WORDS: crack propagation, fracture toughness, stresses, fracture properties, high strength steels, shear strength, shear stress, tests, evaluation

Recently, procedures based on the dynamic tear (DT) test have been evolved for characterizing the fracture extension resistance of structural metals [*1, 2, 3*].[2] The level of fracture extension resistance is expressed in terms of the resistance (R) curve slope, which defines the energy for fracture as a function of incremental crack extension. Increased R-curve slope is related to increased resistance to fracture extension for ductile metals; flat (no slope) R-curves are obtained for the case of brittle metals. Further it was shown that for steels, titanium alloys, and aluminum alloys the R-curve slope characteristics can be defined by an expression relating the fracture extension resistance energy-per-unit crack extension to the specimen geometry and a constant related to the inherent fracture resistance of the material.

This report describes the results of a study for three ductile high-strength

[1] Head, Structural Mechanics Section and head, Strength of Metals Branch, respectively, Metallurgy Division, Naval Research Laboratory, Washington, D.C. 20390.

[2] The italic numbers in brackets refer to the list of references appended to this paper.

steels in which it is shown that specific R-curve slope features are basic to a given material regardless of section size aspects. It also indicates that for a given material, accurate predictions of level of fracture resistance can be made by specimens of different geometries.

R-Curve Factors

The characteristic behavior of a metal under conditions of forced crack extension is modeled directly by the R-curve [*1, 4*]. Rising R-curves for ductile metals reflect the sequence of events at the crack tip in the initial phases of crack extension. Starting from a sharp crack with a straight front, the initiation of fracture is the same for all cases, that is, a high degree of constraint is present at the onset of crack extension. The breakdown of crack-tip constraint and the formation of crack-tip plastic zones are demonstrated by the transition from the flat fracture mode to some degree of oblique shear fracture. Flat fracture is a result of the plane strain constraint, while shear fracture results from the breakdown of constraint. Fracture mode transitions are illustrated in Fig. 1 for full shear *(top)* and part-shear/part-flat *(bottom)* fracture modes. The constraint to through-thickness deformation due to a triaxial stress state is a maximum at the center of the initial crack front; the initial plane strain crack extension takes place at the center, so that the shape of the advancing crack is either *V* or *U.* The length of the *V* section or the plane-strain "tongue" approximates the crack extension length for the initial R-curve rise. Metals with a high slope R-curve effect a rapid transition to full shear, plane stress fracture. After the transition to

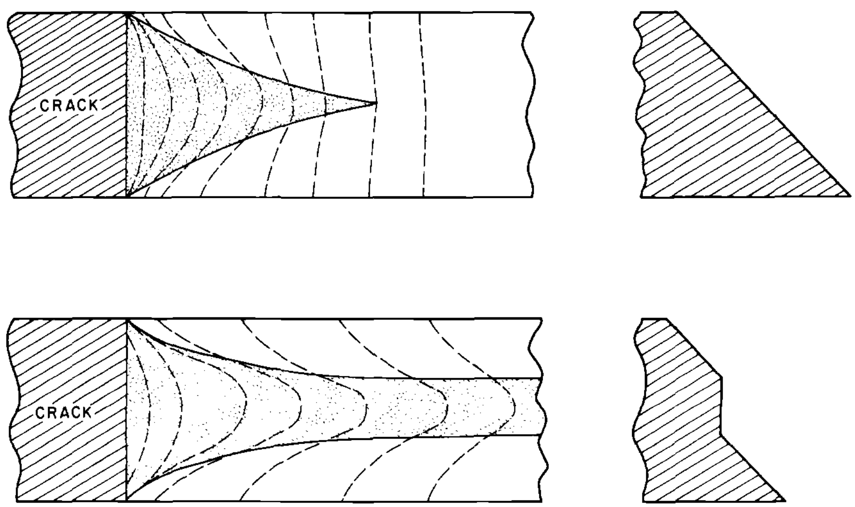

FIG. 1–*An illustration of the transition in fracture mode from initial plane strain constraint to full shear, plane stress fracture* (top) *and part-flat, part-shear mixed-mode fracture* (bottom). *The initial R-curve rise for ductile metals evolves from the transition from initial plane strain constraint to the degree of plane stress fracture propagation characteristic to the material.*

full shear is complete, the crack front becomes straight. Metals with a lower degree of ductility do not evidence a complete shear fracture mode but instead show a part-shear/part-flat fracture (mixed mode) resulting in a lower slope R-curve.

During the R-curve rise, the crack tip plastic zone also grows to its characteristic size, which is related to the intrinsic fracture resistance of the metal. This is evident in Fig. 2, which shows plastic zone development with fracture extension for both frangible *(top)* and ductile metals *(bottom)*. For the frangible case, the plastic zone is quite small and remains constant in size for continued unstable crack propagation. In ductile metals, through-thickness flow and yielding at the crack tip occur as a result of the constraint breakdown. In metals with a high degree of fracture resistance, the crack-tip plastic zone becomes very large and the yielding becomes a general rather than a local

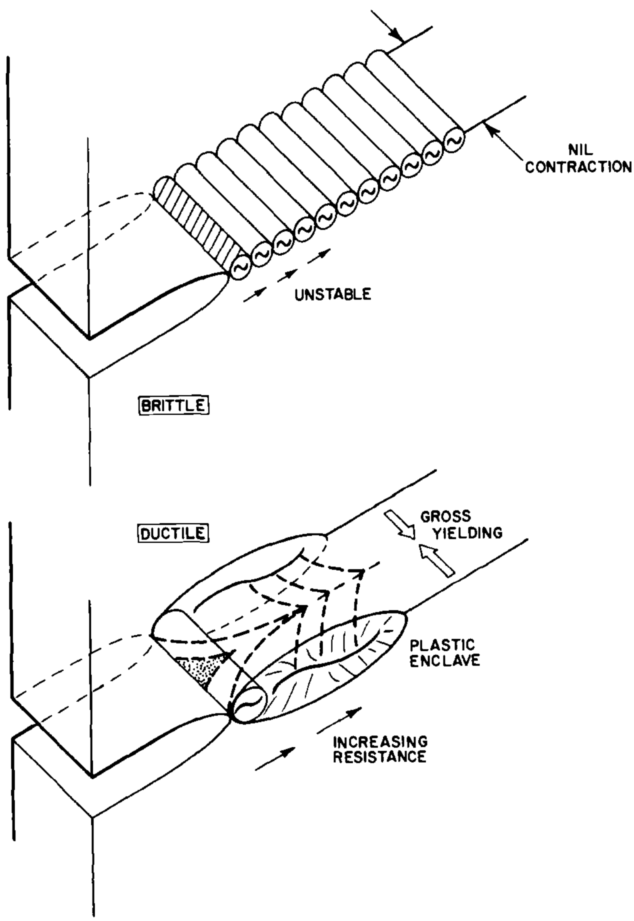

FIG. 2–*Schematic illustration of crack tip plastic zone formation with crack extension for brittle metals* (top) *and ductile metals* (bottom).

process. The breakdown of constraint and the through-thickness yielding result in the loss of the initial crack-tip acuity. All of these factors combine to require increases in energy to sustain the crack extension process.

R-curves for ductile metals are not expected to rise indefinitely. At some value of crack length, the transition is complete, and a constant plastic zone size that is typical for the metal is attained so that energy-per-unit extension required to continue crack propagation should become constant.

The important part of the R-curve is the initial rise. For metals in a wide range of fracture properties, the resistance to ductile fracture does not appear to differ significantly at small values of crack extension; however, large differences in fracture resistance become quickly apparent as the moving crack becomes longer. This is illustrated in Fig. 3 by schematic R-curve forms for metals of high

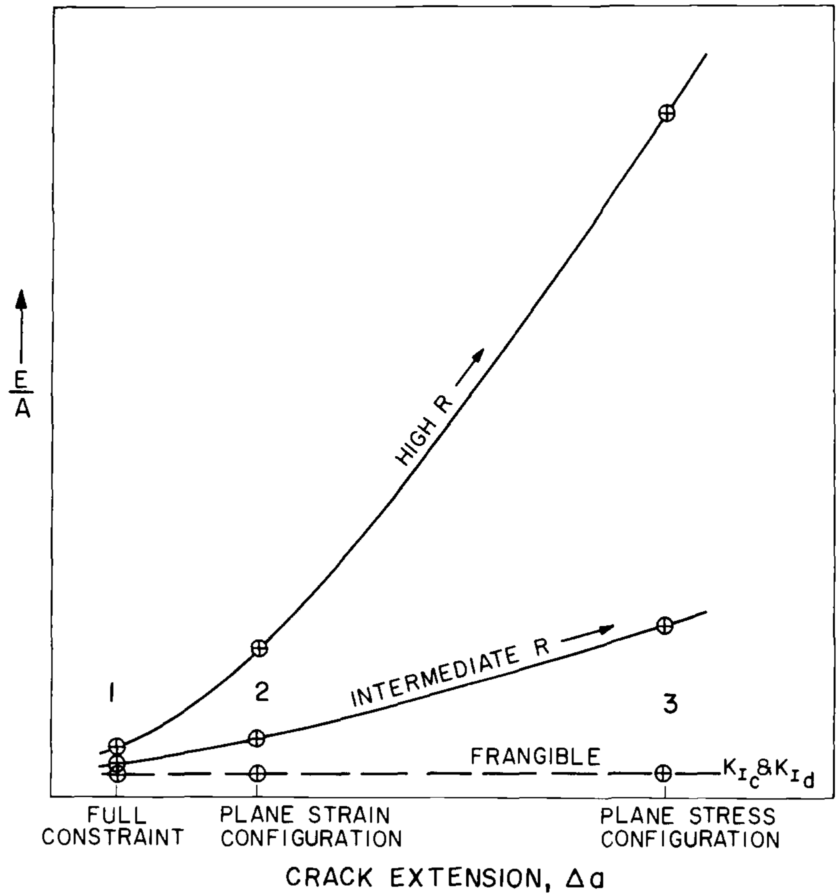

FIG. 3—*Schematic illustration of R-curves for metals of high and intermediate levels of resistance to ductile fracture and a frangible metal. The effect of crack tip constraint on the energy required for fracture extension is illustrated. The ability of different test methods to accurately present the true metals properties is related to the crack extension provided in each test specimen.*

R and low R characteristics and for a frangible metal. Full-constraint tests based on fracture initiation criteria (typically K_{Ic} tests), as depicted at Point 1, have very little ability to discriminate between the three metals. Plane-strain configuration tests of energy measurement type, such as the Charpy V, show limited ability for discrimination, while plane-stress type tests measuring energy for a significantly long crack extension accurately define the wide differences in fracture resistance that exist in these metals.

Dynamic Tear Test Procedures for Determining R-Curves

The dynamic tear (DT) test was designed [*5, 6*] to determine the fracture resistance of high-strength metals in different thicknesses over the full range of strength and toughness. Because the DT test provides a direct model of the crack extension process under conditions of maximum severity with respect to crack-tip acuity and dynamic loading and has the capacity for direct energy measurement, it was readily adaptable for R-curve determinations. The specimen is shown schematically in Fig. 4, along with dimensions of specimens used for this investigation. Adjusting the Δa dimension for a given specimen thickness permits determination of the R-curve by otherwise standard procedures. R-curves are plotted from simple energy-per-area calculations; this procedure does not permit separation of initiation and propagation energy, but instead

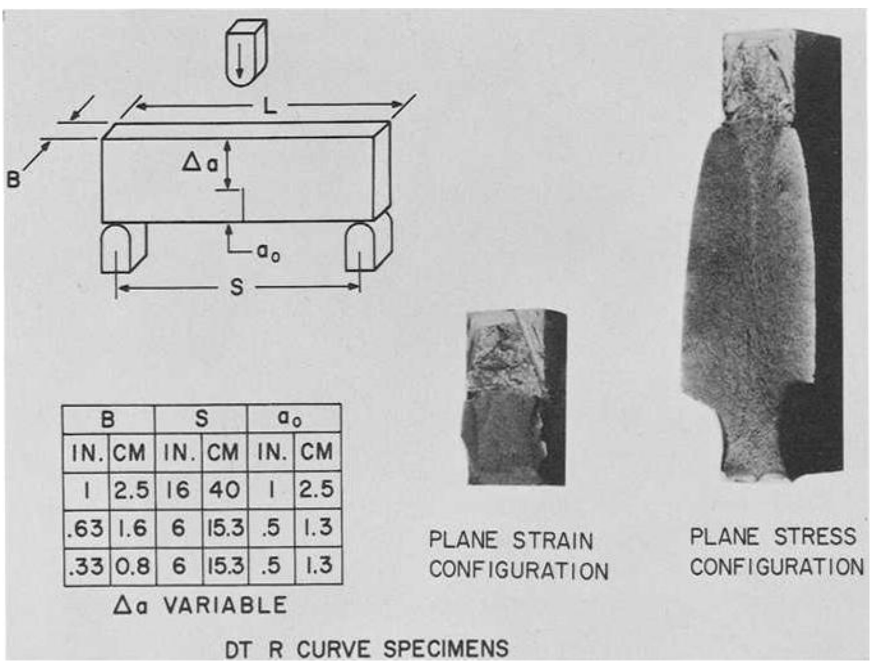

B		S		a_0	
IN.	CM	IN.	CM	IN.	CM
1	2.5	16	40	1	2.5
.63	1.6	6	15.3	.5	1.3
.33	0.8	6	15.3	.5	1.3

FIG. 4—*Dynamic tear test specimen adapted for R-curve studies. The dimensions refer to configurations used in this investigation. The fractures at the right of the figure illustrate the appearance of plane strain and plane stress fracture.*

integrates these into one value. Standard DT test specimens are of the plane-stress configuration type which permits development of the natural fracture mode. The DT R-curve test methods effectively model the fracture mode transition and place emphasis at the important initial R-curve rise.

Materials and Procedures

Three 1-in.-thick steels of nominal HY-80 composition with a wide range of strength and toughness properties were selected to study the effects of specimen thickness on the R-curve characterization. The test materials were coded according to their level of fracture resistance by H-high *R*, M-medium *R*, and L-low *R*. The chemical compositions of the three steels and their mechanical properties are given in Tables 1 and 2, respectively.

A series of DT type R-curve specimens of nominal thickness *(B)* 1, 5/8, and 3/8 in. were machined from each of the three test materials. Each series consisted of specimens of $\Delta a/B$ ratio of approximately 1, 2, 3, and 4, making the total of twelve specimens for each steel. The beam span was 16 in. for the 1-in.-thick tests and 6.5 in. for both the 5/8 and 3/8-in.-thick tests. The 1-in.-thick specimens had titanium embrittled electron-beam-weld flaws (a_0 in Fig. 4) that were 1 in. deep, and the 5/8 and 3/8-in.-thick specimens had 1/2-in.-deep machined notch flaws that were sharpened by a pressed knife edge to a depth of 0.007 to 0.009 in.

TABLE 1–*Chemical composition of steels used for R-curve studies.*

Code	C	Mn	Si	P	S	Ni	Cr	Mo
H	0.19	0.32	0.20	0.007	0.004	3.20	1.62	0.72
M	0.20	0.43	0.21	0.006	0.007	3.28	1.66	0.75
L	0.20	0.43	0.21	0.006	0.007	3.28	1.66	0.75

TABLE 2–*Mechanical properties of steels used for R-curve studies.*

Code	Yield Strength, ksi	Ultimate Tensile Strength, ksi	Reduction of Area, %	Elongation, %	Shelf DTE, ft · lb
H	144	159	61	18	6650
M	125	141	61	19	4390
L	162	185	48	14	1450

The DT R-curve specimens were fractured in pendulum type machines where possible and in drop-weight type machines when necessary due to the nonstandard geometry. All of the specimens were tested at temperatures where the fracture resistance was maximum, that is, above the temperature transition in fracture toughness. In conducting the tests, it was found that the 4:1 specimens of 5/8 in. thickness were excessively stiff, resulting in significant deformation at points of loading. For this reason, values for these specimens are not reported.

TABLE 3—*Test results.*

Thickness B, in.	Crack Run, Δa, in.	Fracture Energy, ft · lb	E/A, ft · lb/in.^{2}
Steel H:			
1.02	1.0	1330	1300
1.02	2.0	3300	1620
1.03	3.0	6550	2120
1.04	4.0	11400	2740
0.65	0.64	370	890
0.64	1.29	921	1130
0.64	1.87	1925	1620
0.35	0.43	102	627
0.34	0.79	218	810
0.34	1.17	399	1005
0.30	1.52	578	1270
Steel M:			
1.01	1.0	714	706
1.02	2.0	2086	1040
1.02	3.0	4388	1440
1.03	4.0	8000	1940
0.65	0.64	186	445
0.64	1.29	673	818
0.62	1.87	1363	1170
0.31	0.43	65	502
0.32	0.79	156	622
0.34	1.16	298	755
0.34	1.53	450	867
Steel L:			
1.03	1.2	353	286
1.03	2.0	714	346
1.03	3.0	1454	430
1.04	4.0	2468	594
0.64	0.63	92	230
0.60	1.29	246	324
0.63	1.88	550	465
0.34	0.43	37	252
0.36	0.79	78	279
0.36	1.19	163	379
0.35	1.52	255	476

Results

The fracture energy values and specimen cross-section dimensions are presented in Table 3. The R-curves for each steel are presented in Figs. 5, 6, and 7 for thickness values of 1, 5/8, and 3/8 in., respectively. In each figure, the R-curves show the same form and order, that is, in each case Steel H has the highest R-curve slope followed by Steel M, with Steel L having the lowest R-curve. The shape of the R-curves is independent of thickness. The fracture surfaces corresponding to the data points are also shown in Figs. 5-7. In each of these figures the transition in fracture mode (flat to shear) is apparent for each thickness. All plane-strain configuration specimens had a flat center with minor shear-lip formation. For Steels H and M, a transition to complete shear fracture was observed for all thicknesses. Steel L did not manifest full-shear fracture in any of the thicknesses tested, even at the 4:1 geometry; however, an increase in percent shear fracture can be noted for the thinner specimens. The natural fracture extension mode for this steel is part-shear/part-flat for all thicknesses above 3/8 in.

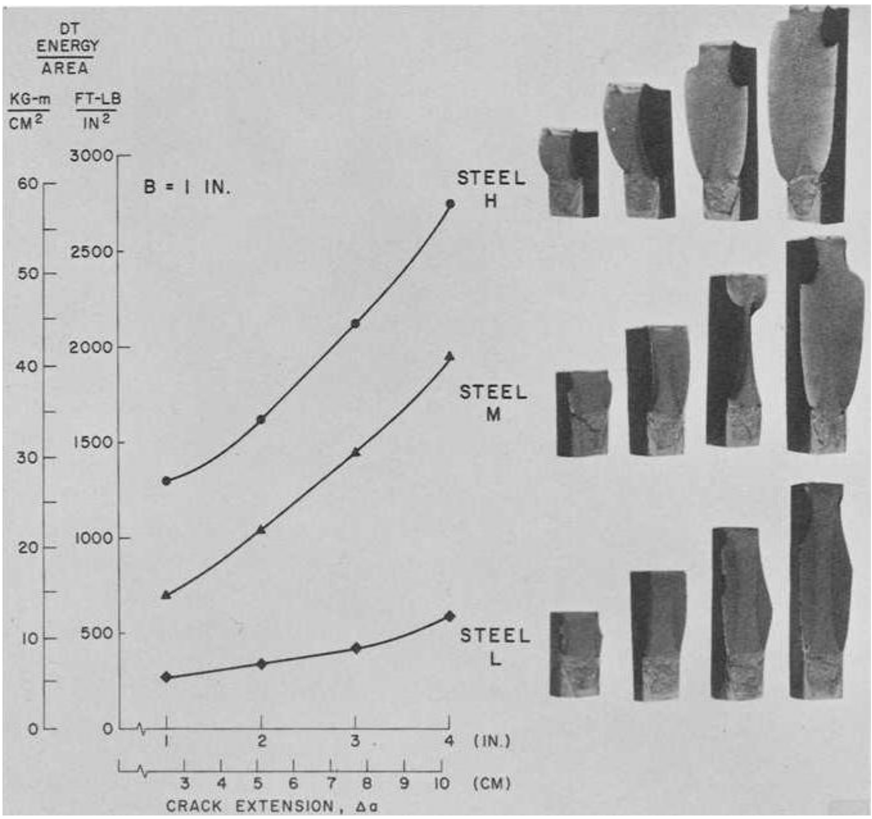

FIG. 5—*R-curves for the three test steels in the full 1 in. thickness. The fractures illustrate the transition in fracture mode for each steel.*

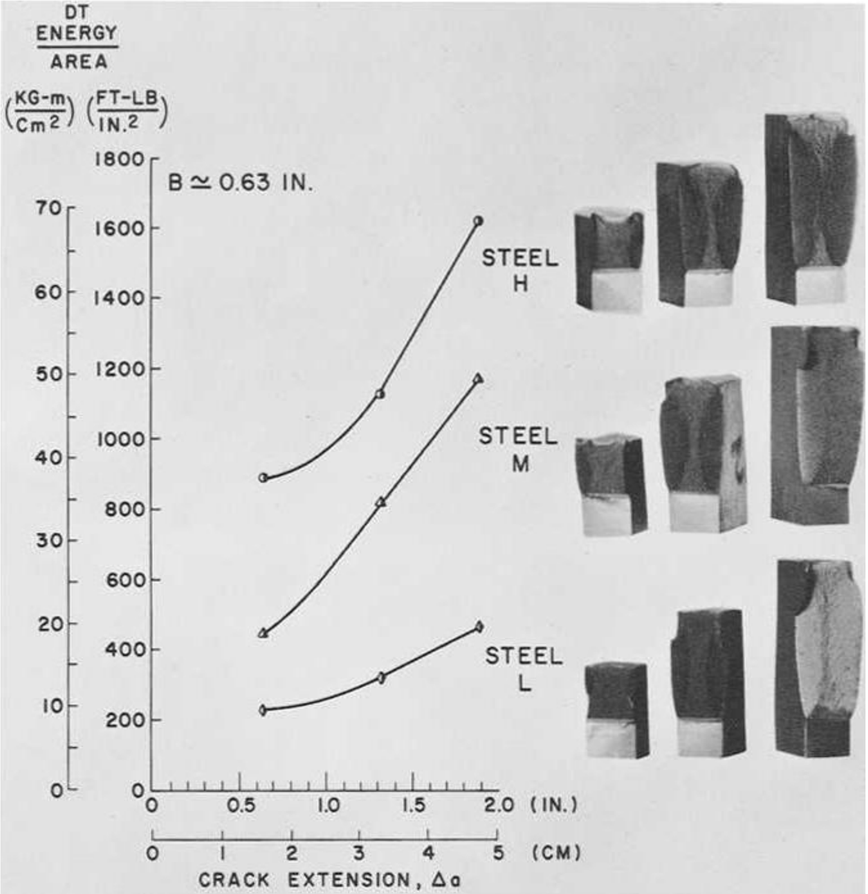

FIG. 6–*R-curves for the test steels in 5/8 in. thickness.*

Discussion

The physical significance of the R-curves for steels and other metals has been well defined in the references. It is necessary to demonstrate that the R-curve form is a characteristic of the material and that the effect of decreasing the thickness of the specimen below full plate thickness decreases the energy-per-area values but does not change the form of the R-curve. Figures 5-7 showed that the R-curves have the same form at each thickness, and the fractures illustrated the transition in fracture mode with increased fracture length for each steel at each thickness. Thus, the effect of decreasing specimen thickness is restricted to lowering the E/A-values, but the R-curve shape is unaffected.

A log-log plot of the fracture energy versus the crack run for all three steels, Fig. 8, demonstrates the geometric effects of specimen dimensions and the predictability of R-curve form. In Refs *1* and *7*, it was observed that an

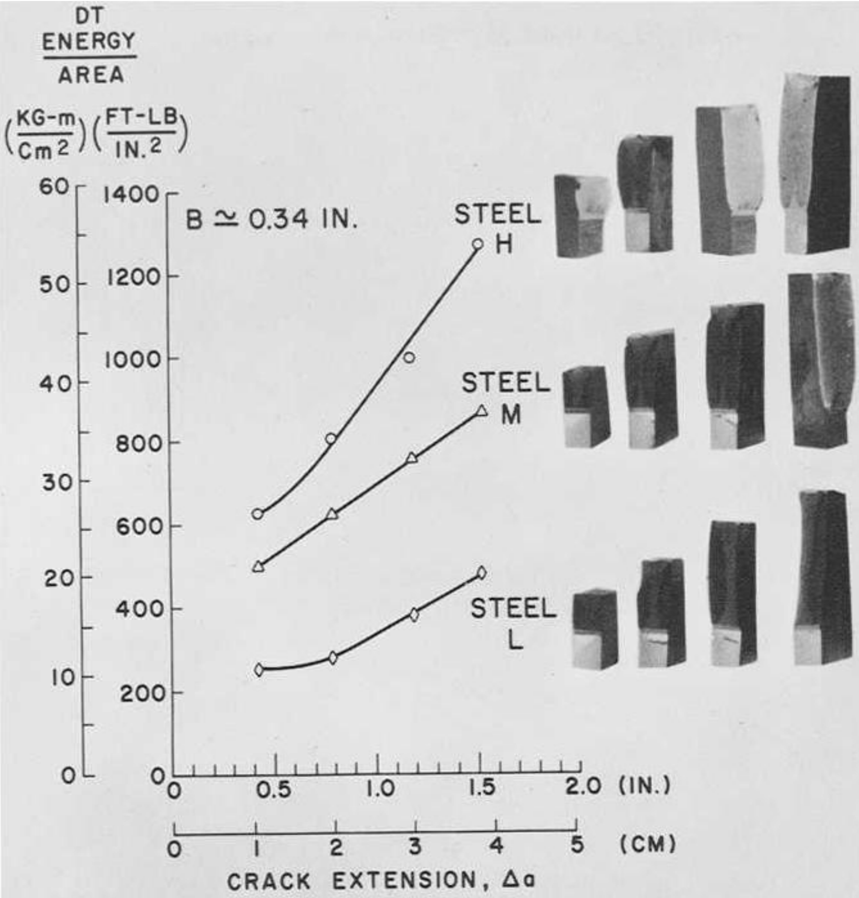

FIG. 7–*R-curves for the test steels in 3/8 in. thickness.*

exponential equation involving Δa, B, and a constant, R_p, could be used to describe the relationships between these factors. The plots in Fig. 8 are a family of parallel straight lines for each steel, which indicates that a single equation can be employed to describe this system. Note that the plane strain configuration (1:1) specimens do not fit the curves.

The equation $E = R_p\,(\Delta a)^x B^y$, where x and y are unknown exponents and R_p is a constant, which is associated with the inherent resistance to fracture of the material, describes the relation between DT energy and specimen geometry. The quantities R_p, x, and y can be determined for each steel. Exponent y is the slope of the families of parallel lines in Fig. 8. R_p and exponent x are determined by substituting the values of E at the intercepts of the curves where $\Delta a = 1$ into the equation and solving the resulting three equations in two unknowns for the best solution. Reasonably consistent values of x and y determined for all three steels by this procedure are shown on Fig. 8 and in Table 4. To isolate the

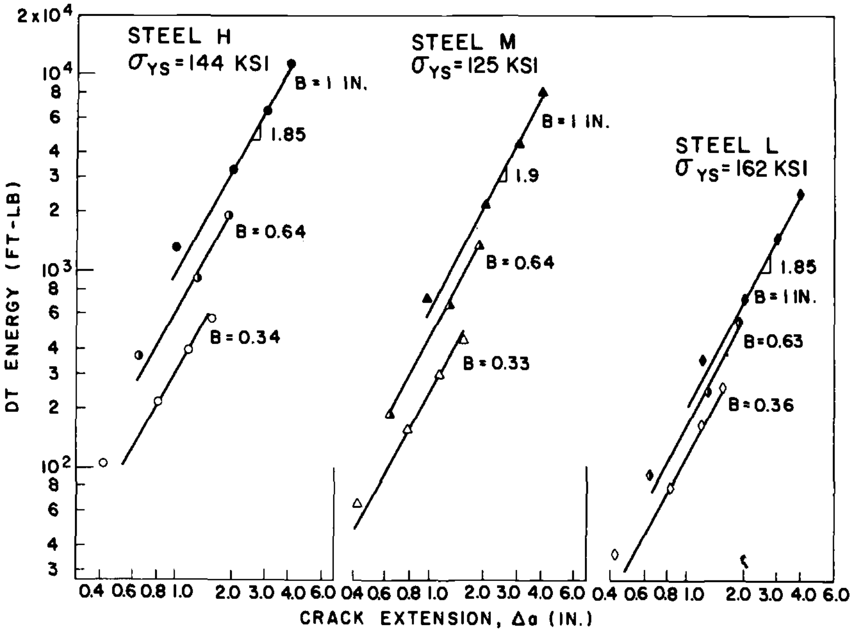

FIG. 8—*Log-log plot of the DT test data for three steels. Different* Δa *scales are used to prevent overlapping of the plots.*

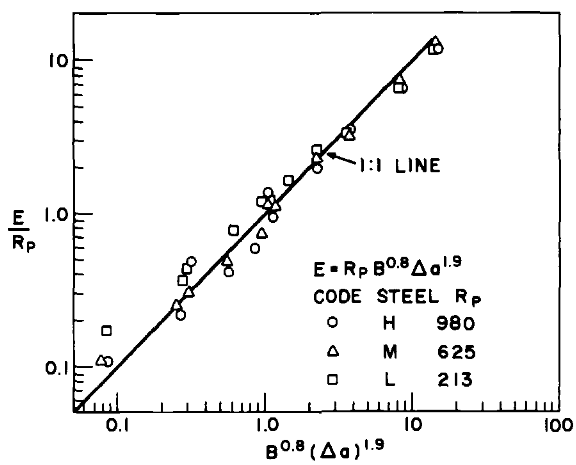

FIG. 9—*Illustration of the validity of the equation form. Exponents* x *and* y *are average values of 1.9 and 0.8, respectively.*

independent variables pertaining to geometry, the quantity $(\Delta a)^x B^y$, where x and y were average values of 1.9 and 0.8, respectively, calculated for each datum point, was plotted against the quantity E/R_p, Fig. 9. The agreement shown in Fig. 9 is very good when the normal variations in plate properties from specimen to specimen and expected variations due to experimental factors are considered.

TABLE 4– *Values of constants for plastic fracture equation.*

$$E = R_p \, \Delta a^x B^y$$

Steel	x	y	R_p
H	1.9	1.0	980
M	1.9	.9	625
L	1.9	.6	213

In previous work on two steels in sections sizes up to 3 in. thickness [7], the exponents in the equations were determined to be x = 2.0 and y = 0.5. For practical purposes, the exponents for the steels of this study approximate these values. This is illustrated in Fig. 10, which is a plot of E/R'_p versus $(\Delta a)^2 B^{0.5}$, where R'_p = the average value of R_p shown on the figure determined with the appropriate exponents. All the data points, including the 1:1 specimens, were used for this average; notice that the 1:1 specimens are all above the exact correspondence line in Fig. 10. Eliminating the 1:1 points and recalculating R'_p

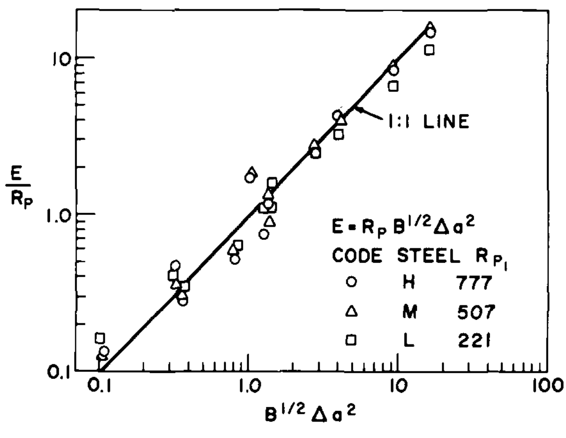

FIG. 10–*DT data fitted to the plastic fracture equation with exponents* x *and* y *equal to 2.0 and 0.5, respectively. All data included in this plot.*

results in the chart of Fig. 11, which shows the best correspondence of the three. Thus, the equation can be taken as $E = R_p(\Delta a)^2 B^{0.5}$ without any apparent effect on the capability to predict DT energy values as a function of specimen geometry. This is possible for these data because the values of exponent y in the range of 0.5 to 1.0 for the thicknesses involved are not as significant as the values of x. In other words, the effect of thickness on the energy for ductile fracture is of secondary importance to the effect of the length of the fracture.

The reasons why the 1:1 specimens do not fit the equations are not known exactly. One possible reason is that because of the small value of Δa in relation to the thickness, the compressive plastic zone formed under the striking tup interferes with tensile plastic zone formation during crack propagation. The significantly different stress field which exists for a large segment of the short specimen would not be a problem in specimens of larger Δa. This factor is part of the reason that short run fracture tests such as the C_v are not sensitive to differences in fracture resistance, as is illustrated by the inability of C_v tests to correctly define temperature transition curves for high-strength steels [*8*], etc.

It is necessary to show that R_p is a constant for each of the test steels because for each steel, the degree of R-curve rise is dependent only on R_p and the thickness involved. In comparing the fracture resistance of steels at a constant thickness, Fig. 5-7, the relationships between the different steels are reflected only as the relationships between the different R_p values. The fact that R_p corresponds to the intrinsic fracture resistance of each metal is underscored by the consistency of the geometrical factors shown for each steel, Figs. 9-11. It is important to note that the standard 5/8-in. DT specimen [*5*] has dimensions of $B = 0.625$ in. and $\Delta a = 1.125$ in. ($\Delta a/B = 1.8$), for which $(\Delta a)^2 B^{0.5} = 0.996$, or effectively 1.0. Thus, the standard 5/8-in. DT specimen can be used directly to determine the R_p-value.

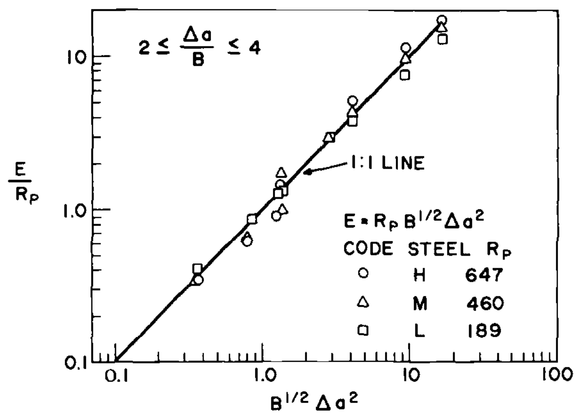

FIG. 11–*Same as Fig. 10 with the 1:1 geometry points omitted.*

Another item of interest in this study was the lack of any effect of specimen span on the energy measurements. Spans of 16 in. for the 1 in. thickness and 6.5 in. for the smaller specimens were utilized without an observable effect. This indicates that the fracture energy is dependent on the stress level that must be applied to cause metal separation, and thus the fracture energy for a given cross-sectional geometry–or R_p–is a property that is intrinsic to the metal. The limitations of beam span for valid DT testing are defined by stiffness factors.

The upper limit of usable Δa-values at a constant span is the point where excessive deformation at the loading points begins. For this study a $\Delta a/B$-value in excess of 4.0 would require an increase in the beam span to lower the forces required to attain the critical stress for fracture.

Summary

The most precise methods of defining conditions for fracture in structural design apply only to the least desirable materials. Linear-elastic fracture mechanics principles enable calculations of critical flaw sizes at specific stress levels only for those materials which fracture at elastic levels of stress. The vast majority of structures are fabricated from metals for which brittle fracture is not expected. For these applications, other methods of analysis must be derived.

The R-curve concept for ductile metals is based on the principle that the resistance to fracture increases with crack extension to the point of energy "saturation" due to plane-strain to plane-stress transition effects. Fracture extension resistance is modeled accurately by the R-curve from both the basic fracture mechanism aspect and the practical, structural design aspect. The descriptive parameter in this rationale is the slope of the R-curve; the easiest way to define this quantity is by impact tests of modified DT specimens.

One-in.-thick steels of high, medium, and low resistance to plastic fracture extension were tested in three different thicknesses to show that the R-curve is constant for each material. The R-curves showed good agreement for all three section sizes, and for each thickness the fractures demonstrated the constraint transition with increased crack extension. Curve fitting procedures showed that an exponential equation of form $E = R_p(\Delta a)^x B^y$ could be used to describe the system of equations for all three steels. Average values of the exponents were determined to be $x = 1.9$ and $y = 0.8$ for all three steels; this is in good agreement with values of $x = 2.0$ and $y = 0.5$ determined for other steels.

References

[1] Pellini, W.S. and Judy, R.W., Jr., "Significance of Fracture Extension Resistance (R-Curve) Factors in Fracture-Safe Design for Nonfrangible Metals," Welding Research Council Bulletin 157, Dec. 1970.

[2] Goode, R.J. and Judy, R.W., Jr., "Fracture Extension Resistance (R-Curve) Features in Fracture-Safe Design for Nonfrangible Aluminum Alloys," NRL Report 7262, Naval Research Laboratory, June 1971.

[3] Judy, R.W., Jr., and Goode, R.J., "Fracture Extension Resistance (R-Curve) Concepts for Fracture-Safe Design with Non-Frangible Titanium Alloys," NRL Report 7313, Naval Research Laboratory, Aug. 1971.

[4] Pellini, W.S., "Integration of Analytical Procedures for Fracture Safe Design of Metal Structures," NRL Report 7251, Naval Research Laboratory, 26 March 1971.

[5] Lange, E.A., Puzak, P.P., and Cooley, L.A., "Standard Method for the 5/8 Inch Dynamic Tear Test," NRL Report 7159, Naval Research Laboratory, 27 Aug. 1970.

[6] Puzak, P.P. and Lange, E.A., "Standard Method for the 1-Inch Dynamic Tear Test," NRL Report 6851, Naval Research Laboratory, 13 Feb. 1969.

[7] Lange, E.A. and Cooley, L.A., "Generalized Equation for Effect of Geometry in Plastic Fracture Resistance of A537-A Steel," Report of NRL Progress, Naval Research Laboratory, Nov. 1970, p. 38.

[8] Judy, R.W., Jr., Puzak, P.P., and Lange, E.A., *Welding Journal,* Vol. 49, No. 5, May 1970, p. 201-s.

C. M. Carman[1]

Plane Stress Fracture Testing Using Center-Cracked Panels

REFERENCE: Carman, C.M., "**Plane Stress Fracture Testing Using Center-Cracked Panels,**" *Fracture Toughness Evaluation by R-Curve Methods, ASTM STP 527,* American Society for Testing and Materials, 1973, pp. 62-84.

ABSTRACT: Three experimental techniques for developing the crack resistance curve and plane stress fracture toughness using center cracked panels are reviewed. One technique involving a plasticity characterization based on the crack opening stretch is discussed in detail.

Experimental data for a variety of materials and thicknesses are presented which show the equivalence of the various methods for determining the crack resistance curve.

KEY WORDS: crack propagation, fracture toughness, strains, stresses, loads (forces) measurement, aluminum alloys, stainless steels, fracture strength, fracture tests, evaluation

Nomenclature

Symbols

K	Parameter describing local elevation of elastic stress field ahead of the crack
$\mathcal{G}$	Elastic strain energy release rate
E	Young's modulus
δ	Crack opening stretch (or displacement)
σ	Tensile stress
τ	Shear stress
a	Half crack length in center-cracked panel specimen
v	Displacement in the y-direction
W	Specimen width
Y	Numerical function of a/W used to compute K-values
σ_{ys}	0.20 percent offset yield strength
r_{ys}	Radius of plastic zone at crack tip $\left[r_{ys} = \frac{1}{2\pi}\left(\frac{K}{\sigma_{ys}}\right)^2\right]$
B	Specimen thickness
P	Load
α	Constant

[1] Metallurgist, Materials Engineering Division, Frankford Arsenal, Philadelphia, Pa. 19137.

Subscripts

I	Designates opening mode of crack extension
III	Designates parallel shearing mode of crack extension
R	Resistance
TS	Tensile strength
T	Theoretical
CLWL	Crack-line wedge loaded
ksi	Kilopounds per square inch

The problem of plane stress fracture toughness testing began with the failure of relatively thin sections in structures such as solid propellant rocket motor cases. To calculate the plane stress fracture toughness, one must determine the stress and crack length at instability. This paper presents some of the basic concepts involved in plane stress fracture toughness and R-curve determination, together with three laboratory techniques for determining these properties.

Considerations of the Irwin-Griffith concept indicated that a relatively constant value of the critical elastic energy release rate, $\mathcal{G}_c$, would be obtained, regardless of specimen width. This value would be essentially independent of the crack length, a. This is illustrated in Fig 1*a*, where the crack resistance, R, of the material is shown as a constant, or slightly decreasing value, when plotted against the crack length, while the driving force curve is shown as an increasing function of a. Instability will occur at the intersection of these two curves. From this point on, the driving force exceeds the crack resistance, and unstable propagation of the crack occurs. However, experimental data obtained using specimens of various widths show that wider, more deeply notched specimens produce higher values of $\mathcal{G}_c$.

Irwin [*1*][2] has advanced two concepts to explain the observed increase of fracture toughness with specimen width. Plastic deformation associated with

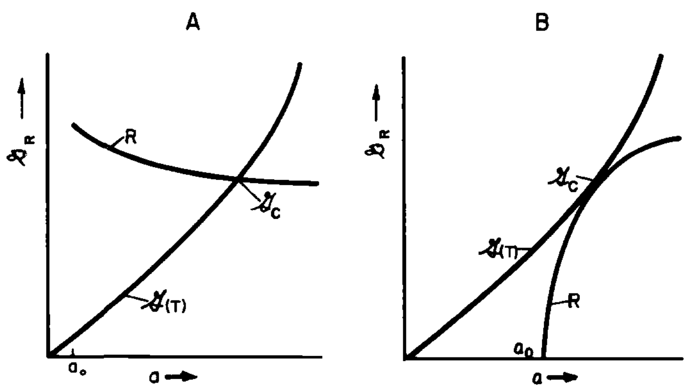

FIG. 1–*Schematic representation of crack instability.*

[2]The italic numbers in brackets refer to the list of references appended to this paper.

crack growth is essential to explaining the difference between actual fracture energy requirements and surface free energy. In this analysis, it is assumed that this plastic deformation forms a zone of relieved tensile stress immediately ahead of the crack in the plane of the sheet, so that the crack is effectively longer than its actual extent. A roughly constant effective extension of a short crack, as in a narrow specimen, produces a relatively larger disturbance both on the stress field and on the $\mathcal{G}_c$-value, than that of a long crack in a wide specimen. It was hoped that crack size corrections based on these observations would lead to constancy of fracture toughness.

The second concept states that the plastic zone, and thus, the fracture toughness, grow as the crack extends from a crack-simulating machined notch or from an actual fatigue crack. This concept presents the possibility that the fracture toughness, at instability, need not be constant and that instability may occur before an equilibrium maxium size of the plastic zone is attained. If one describes the growth of fracture resistance, R, as a simple convex upward curve from the initial crack, a_0, to a limiting level (Fig. 1*b*), fast fracture (instability) occurs at the point of tangency between it and the crack extension force curve, $\mathcal{G}_T$. The R-values to be subsequently described in this paper are the crack resistance values for nearly zero crack speed. Srawley and Brown [*2*] have clarified the conditions for crack instability. By definition, $\mathcal{G}_c$ is equal to the value of R at instability, and beyond this point $\mathcal{G}$ increases more rapidly with specimen deflection (e) than does R. In Fig. 1*b* the R-curve is determined as the applied $\mathcal{G}$. This practice is valid even though $\mathcal{G}$ and R represent distinctly different physical entities and have different functional relations to the subsidiary test variables, nominal stress (σ) and crack length (a).

The curve labeled $\mathcal{G}_{(T)}$ is calculated as a function of crack length using the maximum gross stress and the stress analysis of the specimen. At the instability point

$$\mathcal{G} = R \tag{1}$$

and

$$\frac{d(\mathcal{G} - R)}{de} = 0 \tag{2}$$

In a fracture toughness test as normally conducted, the value of only one point on the crack extension resistance curve is determined, namely, the instability point for the particular specimen used. This point is called $\mathcal{G}_c$. How nearly independent of crack length $\mathcal{G}_c$ will be for a group of tests on the same material, using specimens with different initial crack lengths, will depend upon the form of the R-curve for the material. To characterize the fracture toughness of a material thoroughly it will be necessary to determine the entire R-curve.

Experimental Procedure

The development of crack resistance curves requires direct or indirect knowledge of the history of stress and crack length up to the point of instability. Three experimental techniques are available for determining the stress and crack length relationship. The first technique involves direct measurement of the crack length and load during test. The second technique is concerned with the indirect measurement of crack length through the measurement of the change in the elastic compliance of the specimen. The third technique employs a plasticity characterization based on the crack opening stretch. All three experimental techniques were utilized in these studies.

The direct measurement technique can be readily applied to tests of relatively wide panels. The specimen employed for this phase of the investigation is shown in Fig. 2. A specimen width of 20 in. for the reduced section was selected for all tests. After a preliminary study, an initial crack length of 8 in. was selected as giving the most information concerning the crack resistance curve. The specimens were machined to the desired contour, and the 8-in. slot was cut in the center by electrodischarge machining. An additional sharper notch was cut at the tip of the slot by electrodischarge machining using 0.0015-in.-thick foil. This procedure results in a square notch tip of approximately 0.003 in. width. This tip was sharpened to a root radius of 0.001 in. by means of a hardened steel razor blade. Normark et al [3] have shown that this notch sharpness is

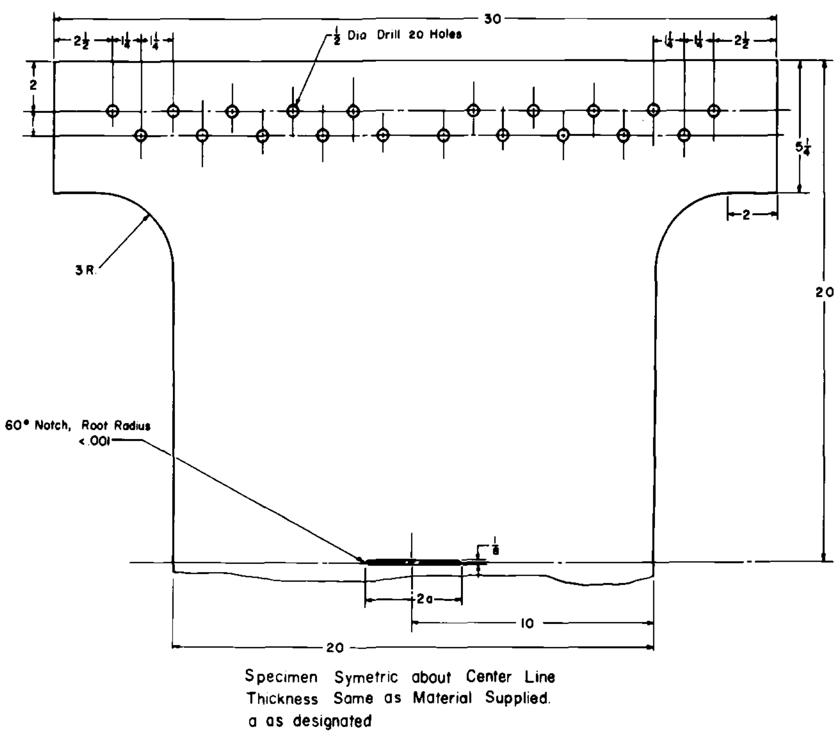

FIG. 2–*Twenty-in.-wide panel specimen.*

equivalent to fatigue cracking for most high strength aluminum alloys.

The wide panel tests were conducted on a 300 000-lb tensile machine. These specimens were pin-loaded through special adaptors. Lubricated face plates were used to prevent buckling during the test. An assembled specimen is shown in Fig. 3.

The crack length and load were recorded by means of two high speed motion

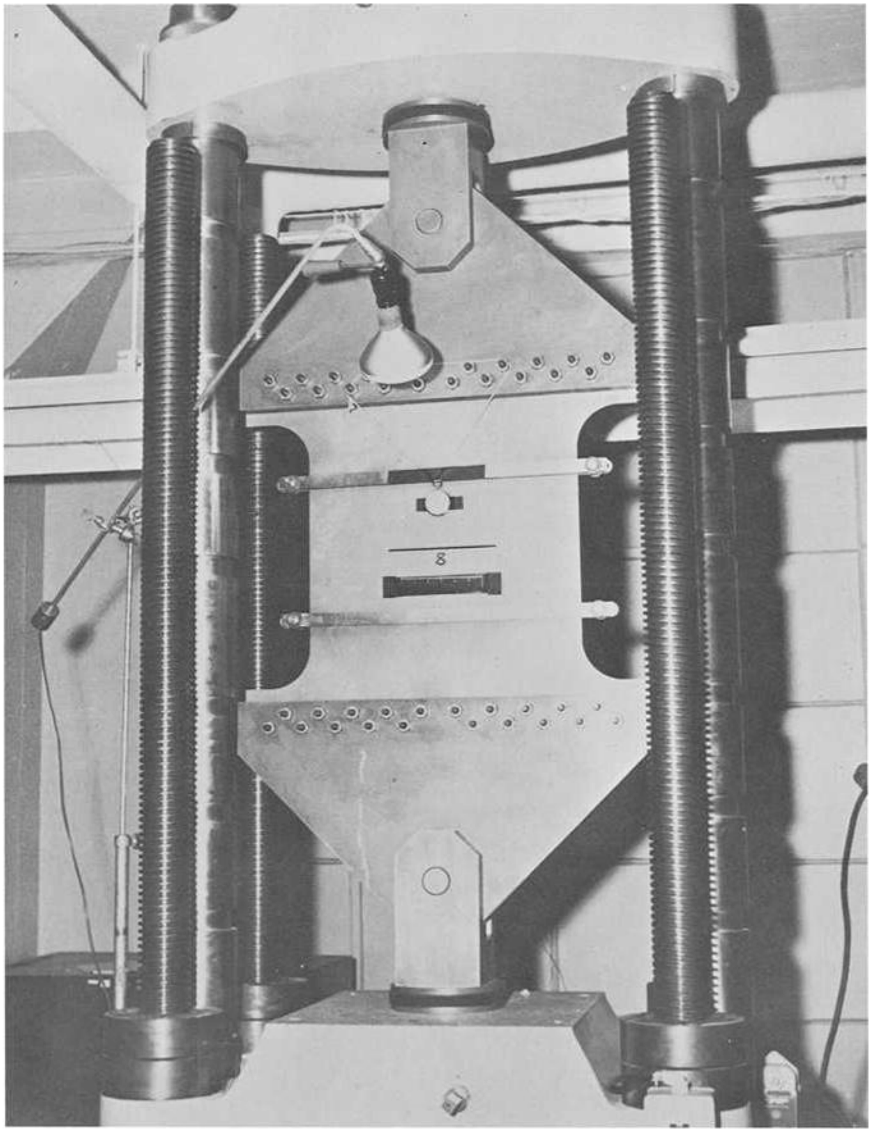

FIG. 3—*Assembled 20-in.-wide panel specimen ready for test.*

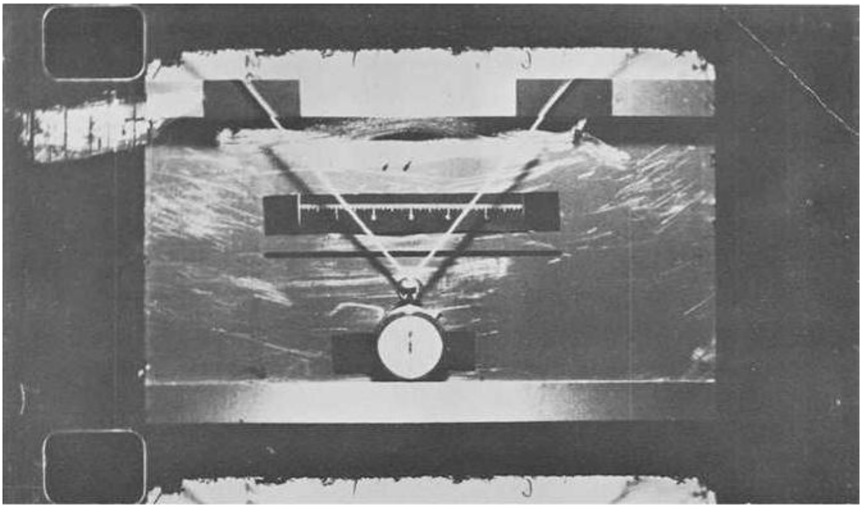

FIG. 4–*Photograph of crack just prior to instability in 1/8-in.-thick 7075-T6 aluminum alloy. Photograph of the center 10 in. of the specimen.*

picture cameras operating at 24 frames per second. One camera recorded the crack length and the other photographed the loading dial. The relationship between the two motion picture films was established by synchronized stopwatches on the specimen and loading dial.

A motion picture frame is reproduced in Fig. 4, showing the crack length just preceding instability for 1/8-in.-thick 7075-T6 aluminum.

The indirect method of crack length measurement involves detection of the change in elastic compliance of the specimen with crack extension. The most common experimental technique involves displacement measurements (ν) in a plane normal to the crack plane. Early work on the problem of displacement measurements resulted in the development of several types of gages.

These early gages were suitable for narrow specimens but would be difficult to use with wide specimens. Consequently, it was decided to determine if the double cantilever beam gage recommended for plane strain fracture toughness testing could be used for this purpose. A series of calibration specimens having various crack lengths were machined from 9-in.-wide by 1/8-in.-thick 7075-T6 aluminum alloy panels. These specimens were loaded so that the net section stress did not exceed one half the yield strength, and the ratio of crack opening displacement to load was measured at the center line. A plot of the experimental data in terms $E\nu/\sigma W$ versus $\pi a/W$ is shown in Fig. 5. The theoretical curve is based on a Westergarrd periodic crack stress field analysis for displacement in the Y-direction. The nature of the agreement between the experimental and the theoretical curves shows that the technique should give reliable data. The offset between the experimental and theoretical curves is approximately the same as that reported by other investigators [*5, 6*].

The third technique, introduced by Wells, [*7*], uses the crack opening stretch

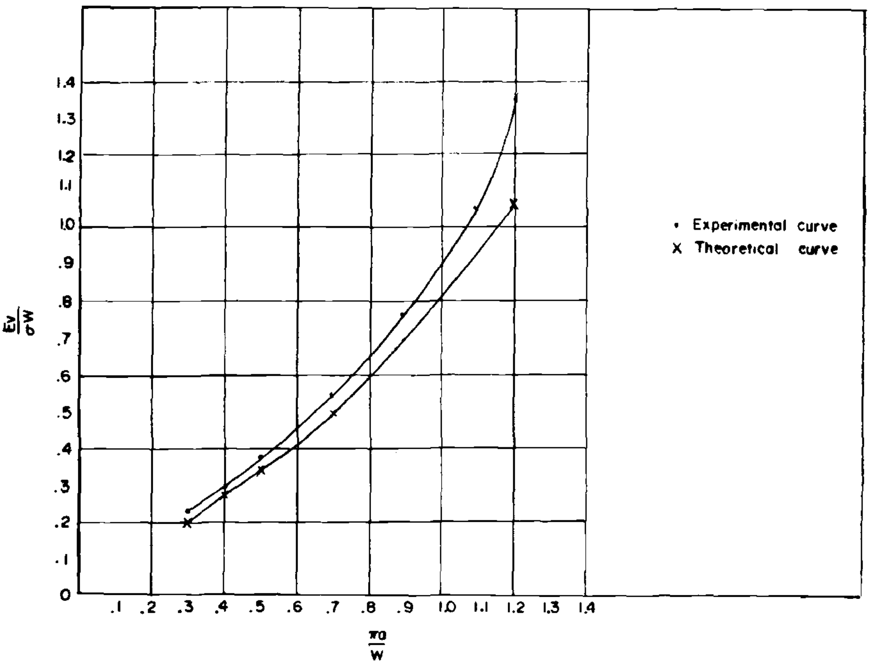

FIG. 5—*Calibration curve for double cantilever beam clip gage.*

(δ) to provide a plasticity-type characterization for the fracture process zone at the leading edge of a crack. Initially δ was pictured as an opening displacement discontinuity at the leading edge of the crack, as would be predicted for elastic-plastic behavior corresponding to zero work hardening. A substantial loss of simplicity occurs if the assumed stress-strain relationship permits representation of various amounts of strain hardening. However, studies with Mode III elastic-plastic analysis models possessing adjustable amounts of strain hardening suggested that δ could be taken as the opening of the crack at the intersection of the elastic-plastic boundary with the crack surface, (Fig. 6) and that the concept would be defined with adequate precision for calculation purposes so long as the yield point was defined sharply in the assumed stress-strain relationship [*8*].

Direct measurement of δ in metals is possible only when the crack is modeled as a narrow slit with smooth surfaces. For crack simulating notches of this kind one can use an opening displacement gage such as was developed at the British Welding Institute [*9*] especially for these measurements. However, if the crack simulating groove is "sharpened" by low amplitude fatigue, or if the crack is natural, as might be formed, for example, by a run arrest segment of fracture produced at low temperature, then direct experimental measurements of the crack opening stretch are not feasible using known techniques. Furthermore, in the case of crack simulating grooves which permit crack opening stretch measurements by methods similar to that of Ref *9*, it is impractical to position

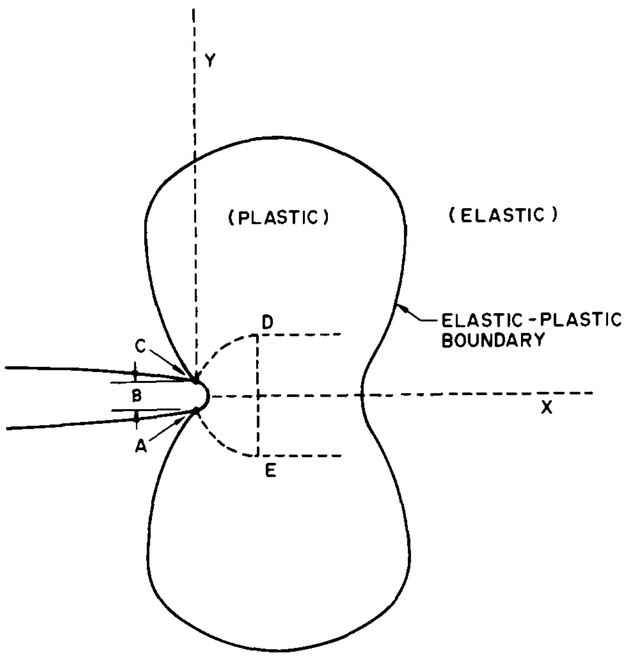

FIG. 6—*Schematic representation of plastic zone surrounding the crack tip.*

the gage so that the measurement is exactly at the intersection of the elastic-plastic boundary with the surfaces of the crack simulating groove. Thus, for purposes of comparing experimental measurements to calculations, it would be a natural choice to make the root radius of the leading portion of the crack simulating groove large enough so that plastic deformation at the surfaces of the groove would be nearly restricted to the leading root radius contour. The localization of yielding thus achieved in the experiments would provide a plausible basis for use of simple, nonstrain-hardening analysis model for the theoretical calculations.

The practical purpose of the crack opening concept is to provide a plasticity type characterization for the small fracture process zone directly adjacent to the leading edge of the crack. For a natural crack, this zone is a region in which the methods of elastic-plastic continuum analysis may not be applied in any simple way. The complications are due to geometric irregularities at the crack front, to small scale microstructural inhomogeneities, and to the existence of finite strains and rotations. Furthermore, for a through-the-thickness crack in a plate, the characterization must be interpreted on the basis of a through-the-thickness average. Thus, the most attractive characterization ideas would represent the leading edge strain condition as a gross average in such a way that extension of the analysis procedure into the fracture process zone itself can be avoided. The crack opening stretch is such an idea because δ can be computed, in principle, as the integral around the elastic-plastic boundary of the component of the elastic limit strain normal to crack.

Other than from the strip model, exact calculation of δ for opening mode (or tensile) crack problems have not been done. However, Mode III cracks, in addition to the strip model, elastic-plastic analysis models developed by McClintock and by Rice [*10*] are applicable and have received considerable study. From these, in the case of a relatively small plastic zone

$$\delta = \alpha \frac{\mathcal{G}_{\text{III}}}{\sigma_y} \tag{3}$$

where $\mathcal{G}_{\text{III}}$ is the crack extension force and σ_y is the elastic limit yield stress. The coefficient α is unity for the strip model and is $4/\pi$ for the Mode III elastic-plastic treatment. When the strip model is applied to an opening mode crack, in the limit of a small enough plastic zone

$$\delta = \frac{\mathcal{G}}{\sigma_y} \tag{4}$$

where $\mathcal{G}$ is the opening mode crack extension force and σ_y gives the magnitude of the closure stresses assumed to act along the "strip" plastic zone. In studies by Wells [*8*] which employ the δ concept, Eq 4 is always assumed. When the size of the plastic zone is not "relatively small" in comparison to crack and net section sizes, the validity of Eq 4 could be questioned unless $\mathcal{G}$ is computed with a suitable, plasticity adjustment of the crack size. $\mathcal{G}$ then becomes essentially equivalent to the J-integral [*10*].

Studies of a central crack in a plate of finite width have been made [*11*] using both the strip and Mode III elastic (perfectly) plastic models. There it was shown that Eq 3, with α constant, remained valid within about 3 percent so long as the average net section stress was substantially less than σ_y and the ratio of crack size to plate width was not too small for an approximate-tensile-analog interpretation. In order to obtain this result, the values of $\mathcal{G}$ in Eq 3 were computed using a plasticity corrected crack size. This localized plastic flow at the crack tip results in crack face displacements greater than would be predicted by a strictly elastic analysis. To account for this a virtual crack extension, r_y is added to the physical crack length. This effective crack length produces displacements consistent with the elastic analysis.

It is clear from the preceding discussion that any satisfactory definition of δ must be computationally simple. We are concerned here only with calculations of δ for situations similar to those for which the approximate validity of Eq 3 was established in Ref *9*. Since the tensile equivalent of Eq 3 which has received most use is Eq 4, it will be assumed in this report that Eq 4 provides satisfactory estimates of δ for given values of applied tensile load and effective crack size.

The state of strain in the fracture process zone is controlled to some extent by the influence of specimen geometry upon the general shape of the plastic zone. However, it is almost completely dominated by the discontinuity at the crack front, and this fact suggests that a one-parameter characterization of the fracture process zone has good possibilities for a wide range of usefulness. The neglect of "state of stress" by the crack opening stretch characterization method will perhaps limit the range of usefulness of the concept. However, it is probable that trials of the concept in various applications will in time suggest both the degree of stress state influence and ways of adjusting the concept so as to take account of such influences where they are of significant magnitude. A similar comment applies to characterization of the fracture process zone by means of thickness contraction methods.

Characterization of the Fracture Process Zone by Thickness Contraction

From the viewpoint of practical considerations, a plasticity type characterization should possess three qualities. (1) There should be some overlap of the method with K-value characterization, in the case of relatively small and enclosed leading edge plastic zones, such that across the range of overlap the linear-elastic and plasticity type characterizations are essentially equivalent. (2) The quantity used for characterization should be satisfactory on physical grounds as indicative of fracture toughness relative to onset of rapid fracture. (3) The quantity used for characterization should be available either by direct measurement or, indirectly, by calculation using observations of load and effective crack size. The crack opening stretch concept satisfies these requirements if one accepts Eq 4 as discussed in the previous section.

For the fracture problems under consideration in this paper, a substantial plate thickness reduction is present at the position of the fracture process zone. In fact, measurement of thickness contraction adjacent to the leading edge of the crack can be considered as potentially capable of providing a satisfactory plasticity type characterization. With regard to requirement (3), in contrast to the crack opening stretch, direct measurements are clearly possible.

With regard to requirements (1) and (2), the idea of using thickness contraction measurements was introduced by Burdekin [*12*] who showed that a near equality existed between thickness contraction and δ-values for $2r_{ys}$ larger than half of the plate thickness. Burdekin's test plates possessed crack simulating notches of a type which permitted use of the Welding Institute gage as discussed previously. Thus the δ values as well as the thickness contraction were observed directly. In a subsequent investigation by Rooke and Bradshaw [*13*], the measurement of thickness contraction was assisted by making a Wood's metal replica of the "dimple" indentation adjacent to the leading edge of the crack. The quantity listed as the thickness contraction test result was the thickness contraction at the deepest position within the dimple. Values of δ were obtained using Eq 4. The results tended to verify Burdekin's findings.

The theoretical grounds for the observed near equality between thickness contraction and δ can be pointed up with the aid of Fig. 6. We assume first that the plastic zone size, $2r_{YS}$, is much larger than the plate thickness, B. Next we assume that plastic instability toward thickness reduction has concentrated most of the plastic strain into a furrow extending forward from the crack, with a vertical height (DE in Fig. 6) which is nearly equal to the plate thickness. Because of the tendency of the plastic strain to focus at the leading edge of the crack, the opening stretch of the crack (shown as AC in Fig. 6) must be nearly equal to the y-direction displacement separation of positions D and E of Fig. 6. If we neglect x-direction extensional plastic strain and assume constant density during deformation, then the average thickness contraction along DE must be nearly equal to δ. As this figure suggests, there are additional plastic strains above and below the plate thickness contraction furrow which also contribute to the size of δ. However, the thickness contraction in the region between DE and the crack tip is not uniform. Furthermore, a proportionality of the plastic strain magnitude to K^2 is expected on general grounds, where $K^2 = E\mathcal{G}$. Similar results have been obtained by Hahn and Rosenfeld using another argument [14].

The results of Burdekin, Rooke and Bradshaw, and those reported here, can not be predicted in any exact sense by the reasoning just provided. However, one can see these results are at least plausible. Furthermore, the averaging procedure applied to thickness contraction measurements within the region $ADEB$ of Fig. 6, could be adjusted considerably without loss of proportionality of the resulting thickness contraction to K^2. Thus, it would seem that a thickness contraction measurement method providing results proportional to δ across a substantial range of plasticity properties possesses good development possiblilities. Although extension of such measurements into the range where $2r_{ys}/B$ is less than unity is limited, an adequate overlap range exists within which the K-value characterization as well as thickness contraction measurements are applicable and appropriate.

Experimental Results and Discussion

The materials used in this investigation were high-strength aluminum alloys of the 7000 series, 2000 series, and PH14-8Mo steel.

The crack resistance curves for 7000 series of aluminum alloys tested as both 4 and 20-in.-wide panels are shown in Figs. 7, 8, and 9. These curves show the same general characteristics, namely, a rapid increase in fracture resistance with crack extension until instability is reached. These crack resistance curves show essentially the same shape regardless of the specimen width or thickness except for deviations as instability is approached. Comparison of the solid curves (calculated with plastic zone correction) with the dotted curves (without plastic zone correction) shows very little difference; therefore, the curves calculated with the plastic zone correction will be reported for this family of alloys.

In the example of 7075-T6 alminum alloy, the critical value of $\mathcal{G}$ increases as the specimen thickness decreases. This behavior would be anticipated since the size of the plastic zone relative to plate thickness increases as the plate thickness is reduced. The critical value of $\mathcal{G}$, as determined by both panel widths, is essentially the same.

Esentially the same comments can be made concerning the crack resistance

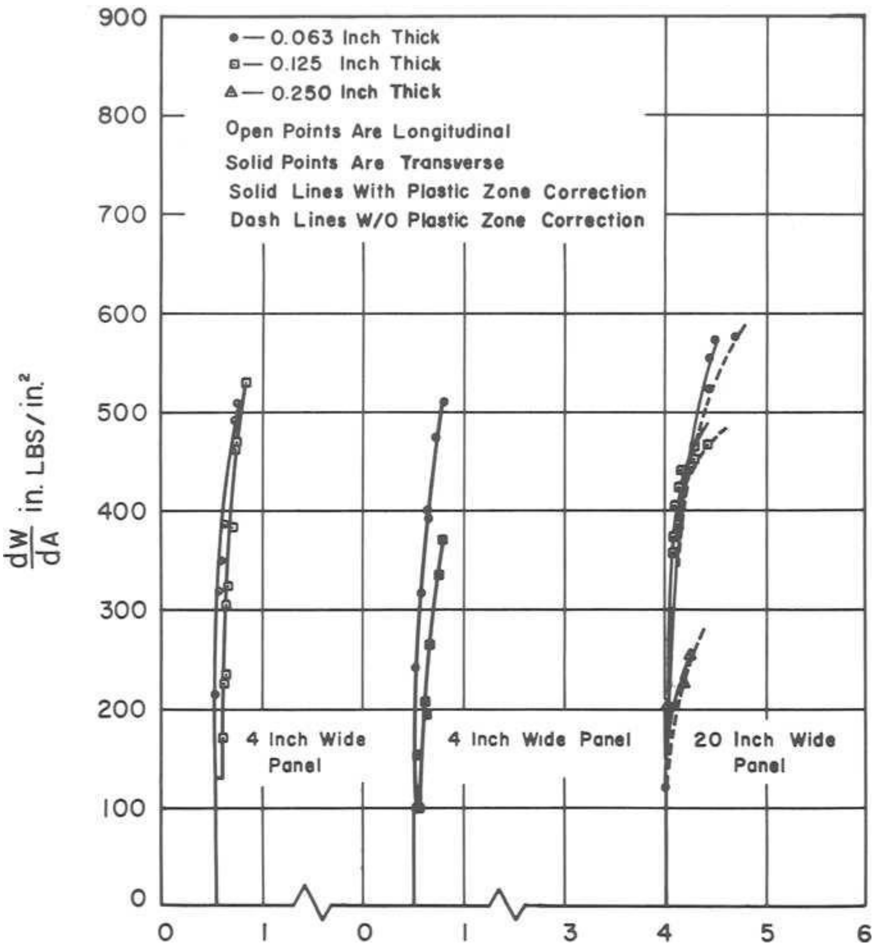

FIG. 7—*Crack resistance curves for 7075-T6 aluminum alloy.*

curves for 7079-T6 aluminum alloy as were made for the 7075-T6 aluminum alloy.

The crack resistance curves for 7178-T6 aluminum alloy are normal except for the ¼-in.-thick by 20-in.-wide specimen, which showed a higher value of fracture toughness than the other specimens. Metallographic examination of the specimens showed extensive delamination of this specimen, thus accounting for its higher fracture toughness.

The crack resistance curves for the 2000 series of aluminum alloys are shown in Figs. 10, 11, and 12. The data for the 20-in.-wide specimens of 2014-T6 aluminum alloy are valid data. The remaining data are considered lower bound values, since the ratio of net section stress to yield strength exceeded 0.80. The high fracture toughness and low yield strength make it very difficult to obtain

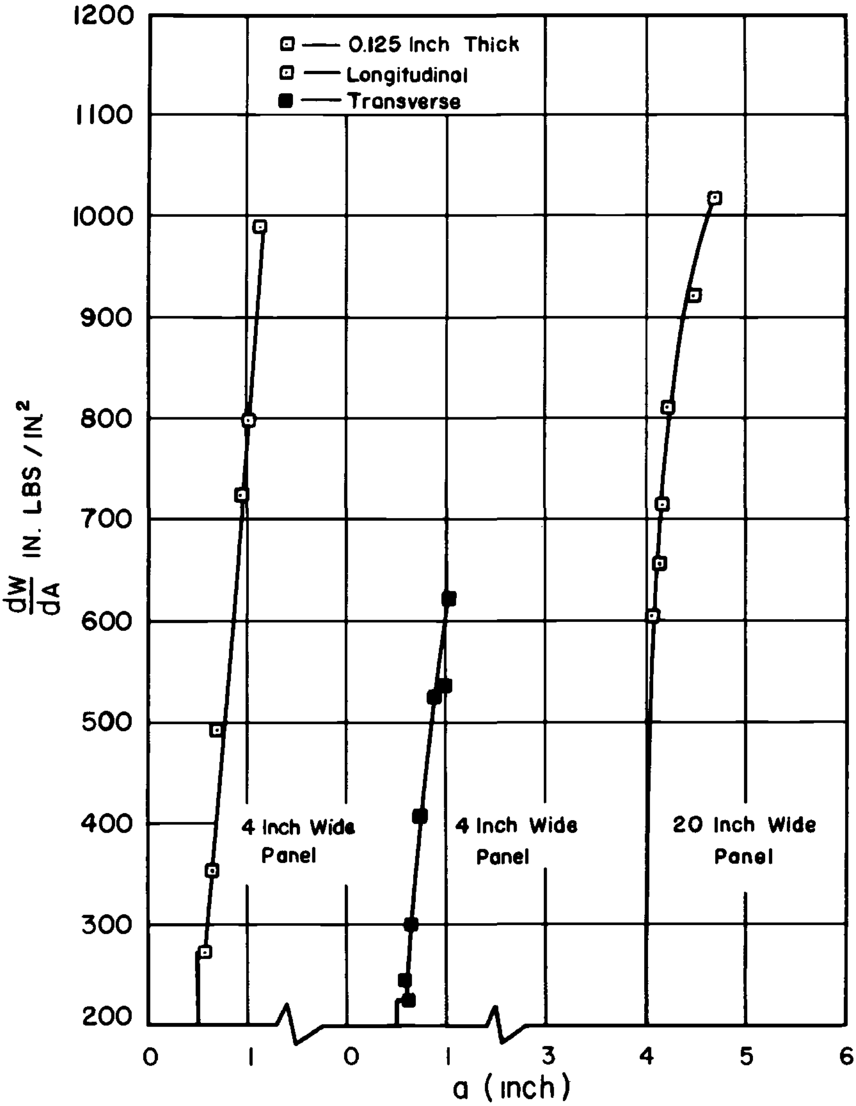

FIG. 8—*Crack resistance curves for 7079-T6 aluminum alloy.*

valid data for the 2219-T81 and 2024-T4 aluminum alloys. In view of these difficulties, it is somewhat surprising that linear elastic fracture mechanics can evaluate these materials as well as it has.

Having considered the linear elastic approach, it is now appropriate to determine what can be done with the plasticity type of study. The specimens were 9-in.-wide centered-cracked panels and were pre-cracked prior to testing by fatiguing at low stress levels. The fracture toughness tests were conducted using

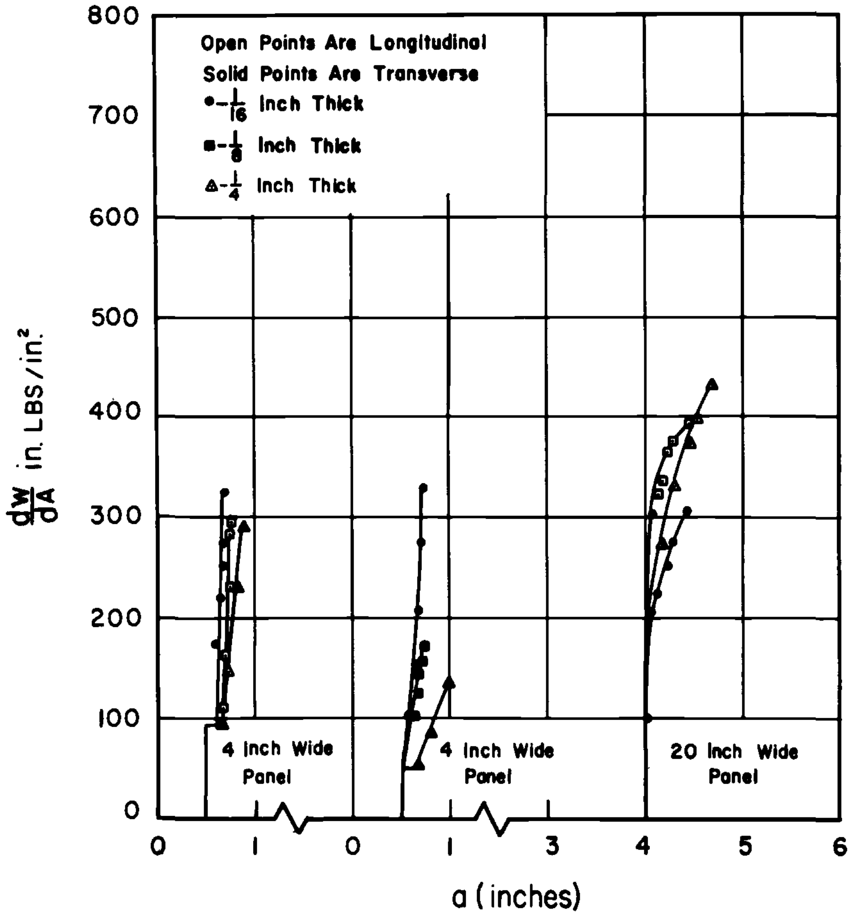

FIG. 9—*Crack resistance curves for 7178-T6 aluminum alloy.*

an MTS closed-loop, servo-controlled, testing machine. The equipment was operated in displacement control using a displacement rate of 50 μin./s. The displacements in the y-direction were measured using the double cantilever beam clip gage. The readout was in terms of load and vertical displacements. Buckling restraints, as shown in Fig. 13, were used to maintain flat sheet conditions. The effective crack length was determined from the displacement readings. The K-value was calculated from this effective crack length and load.

The thickness contraction was measured with a dial gage device. Loading was halted while the thickness contraction measurements were made. Each measurement attempted evaluation of thickness contraction at the deepest point in the dimple adjacent to the leading edge of the crack. In presentation of results the thickness contraction is interpreted as equal to δ. For comparison to K_R (from load and effective crack size), additional K-values were computed from δ using the equation

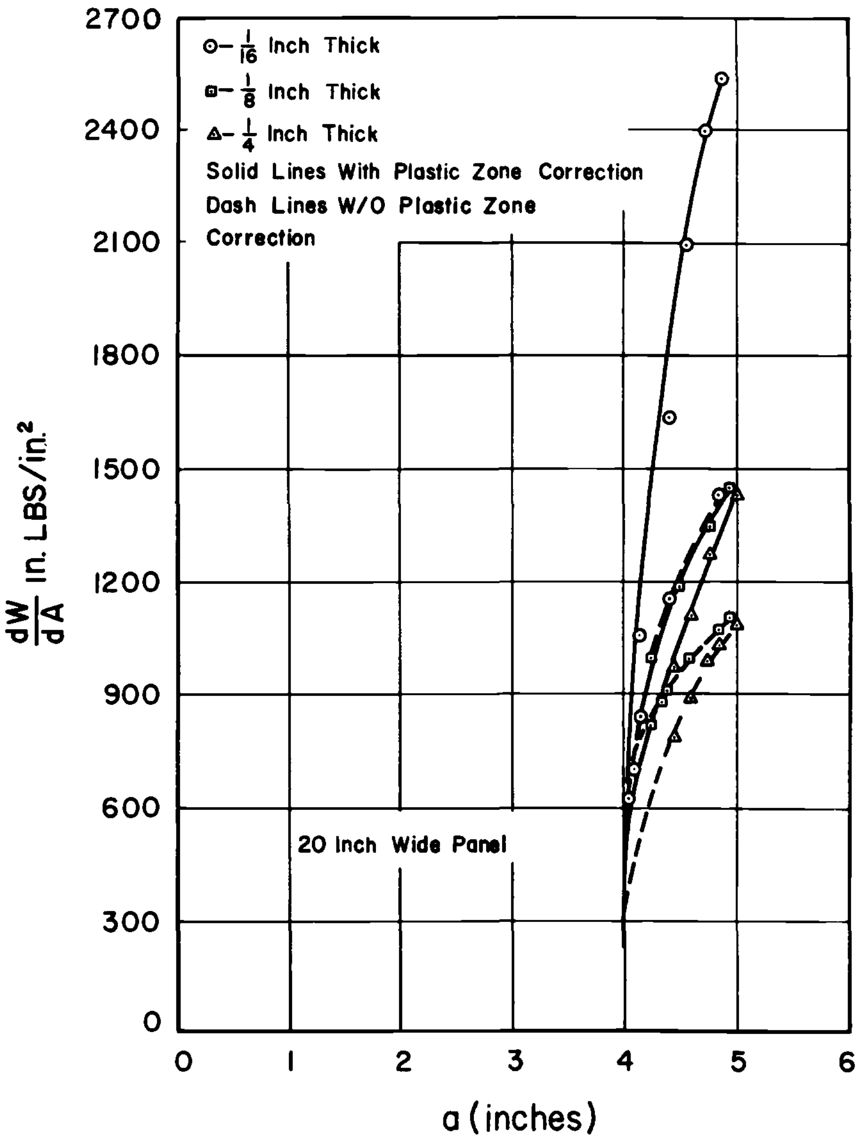

FIG. 10—*Crack resistance curves for 2024-T4 aluminum alloy.*

$$K(\delta) = \sqrt{E \sigma_{ys} \delta} \tag{5}$$

The data are presented in the form of crack resistance curves in which K_R and $K_{(\delta)}$ are plotted as a function of effective crack length. The crack resistance curves for the 1/16-in.-thick 7075-T651 aluminum alloy are shown in Fig. 14.

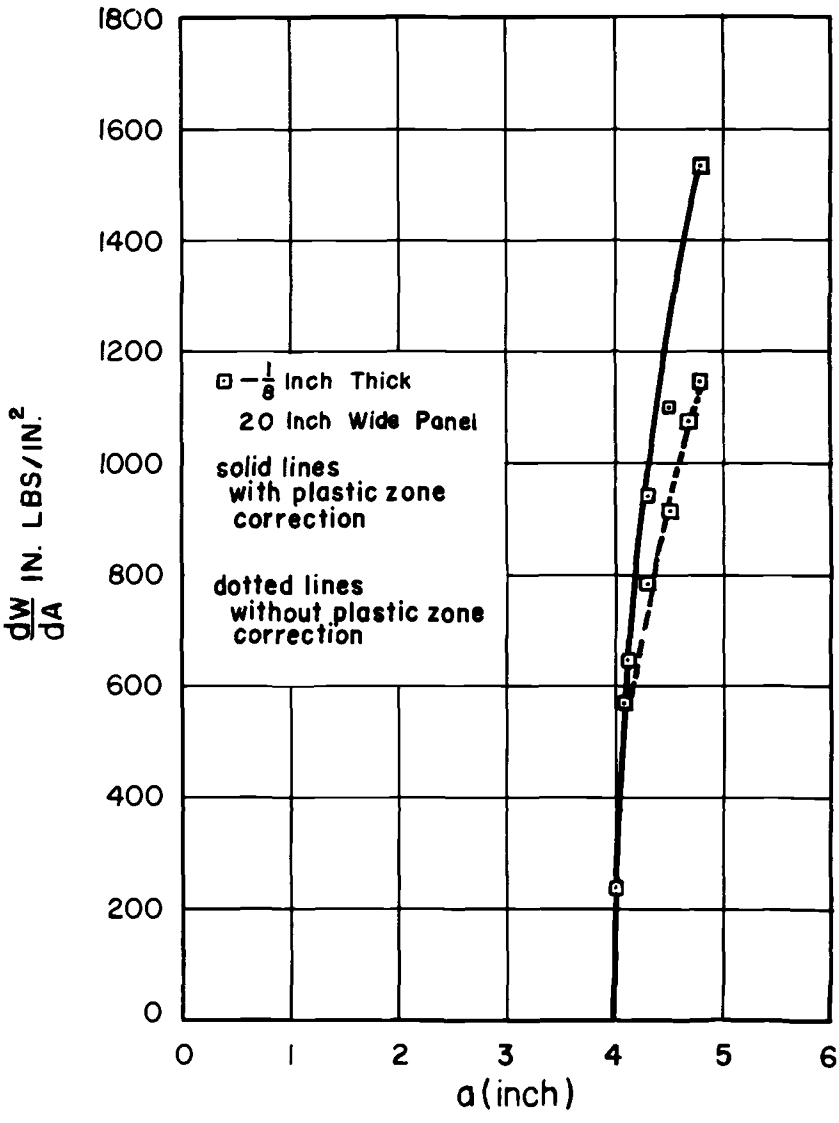

FIG. 11—*Crack resistance curve for 2219-T81 aluminum alloy.*

Also included in this figure are data obtained by Heyer and McCabe [*15*] for the same material using their crack line wedge loaded specimen. It will be noted that all of the R-curves for this material are in reasonable good agreement. The R-curve determined by the crack line wedge loaded specimen show a high plateau which would be expected from a negative K-gradient specimen. The crack resistance curves for 1/8-in.-thick 7075-T651 aluminum alloy are presented in Fig. 15, in which $K(\delta)$ deviates from K_R by less than 7 percent.

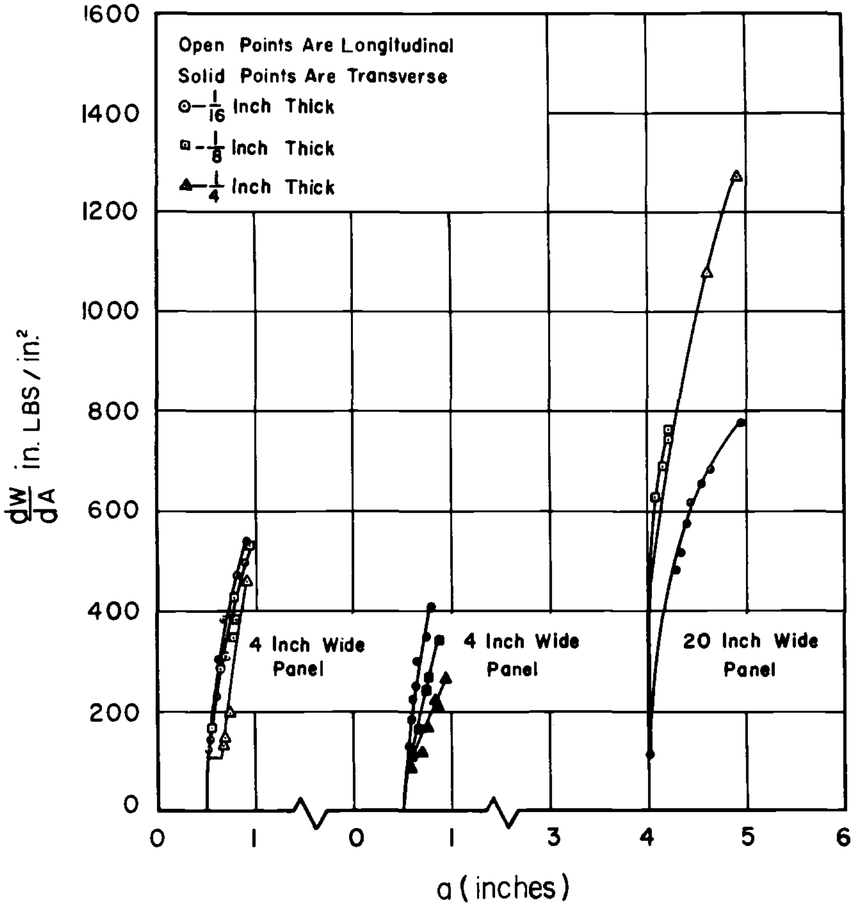

FIG. 12—*Crack resistance curves for 2014-T6 aluminum alloy.*

Comparison of the data for the 1/16 and 1/8-in.-thick 7075-T651 aluminum alloy shows that the 1/8-in.-thick specimens exhibited somewhat greater stable crack extension than the 1/16-in.-thick specimens and a higher value of K_c.

Crack resistance curves for 0.048-in.-thick PH14-8Mo SRH 950 stainless steel alloy are presented in Fig. 16. The R-curves determined from the center cracked panels (K_R and $K(\delta)$) are in good agreement with the data of Heyer and McCabe [*16*].

The crack resistance curves for 1/16-in.-thick 2024-T351 aluminum alloy presented in Fig. 17 show fair agreement between K_R and $K(\delta)$ for each specimen, but the variation between specimens is substantial.

Conclusions

Crack resistance curves may be developed from test data using large center

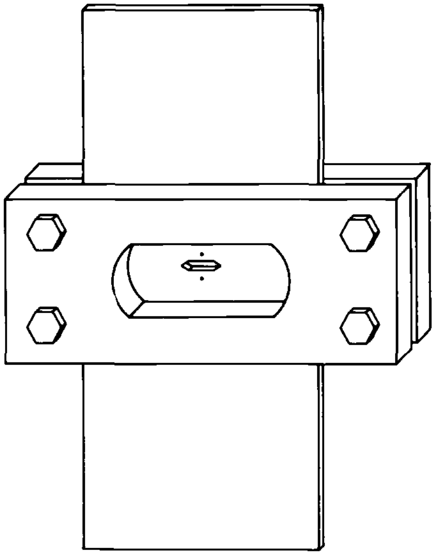

FIG. 13–*Buckling restraints used to maintain flat sheet conditions.*

cracked panels. These data may be readily analyzed by means of linear elastic fracture mechanics. The crack length may be determined directly by means of motion pictures or indicated by means of specimen compliance. However, these experiments were not completely satisfactory for low-strength, high-toughness alloys.

Crack resistance curves developed from plasticity considerations, that is, based on the crack opening stretch concept, were shown to be in good general agreement with R-curves based on an effective crack size obtained through compliance techniques. The method was consistent for metals in a variety of thicknesses and conditions, so long as the net section stress on the specimen was kept reasonably below that which causes general yielding.

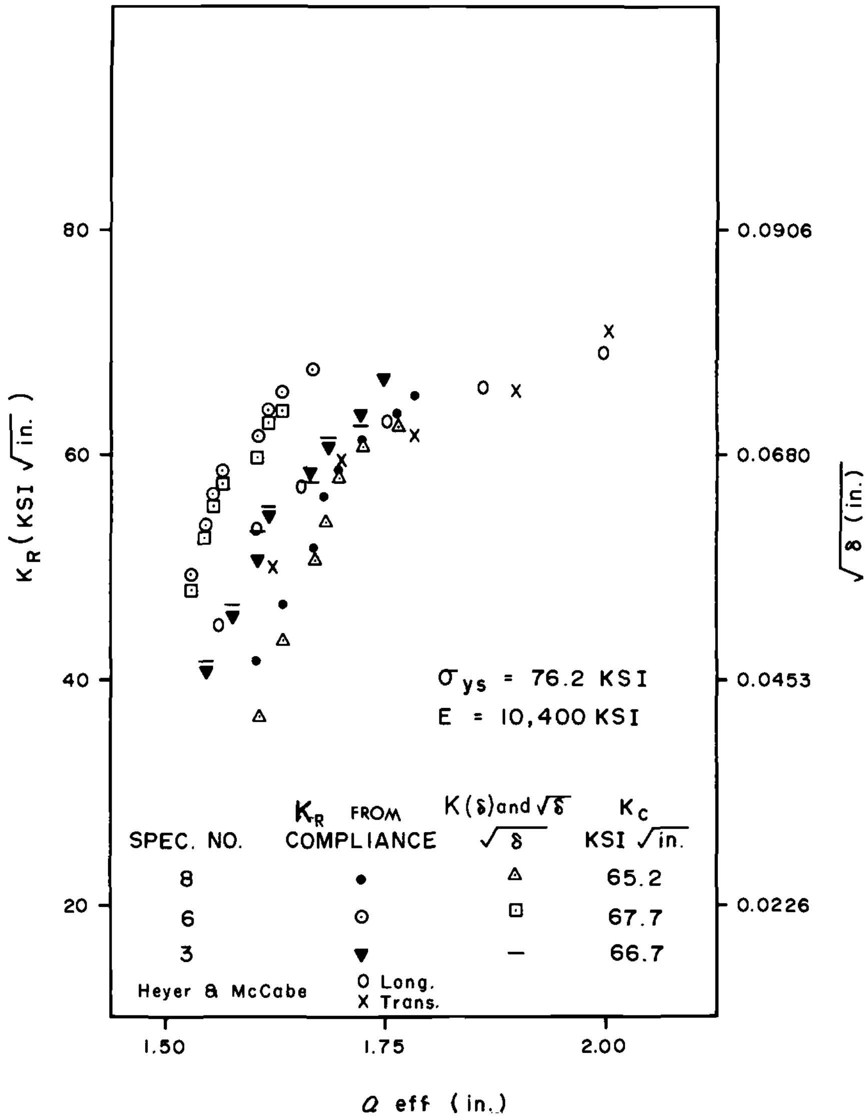

FIG. 14—*Crack resistance curves for 1/16-in.-thick 7075-T651 aluminum alloy.*

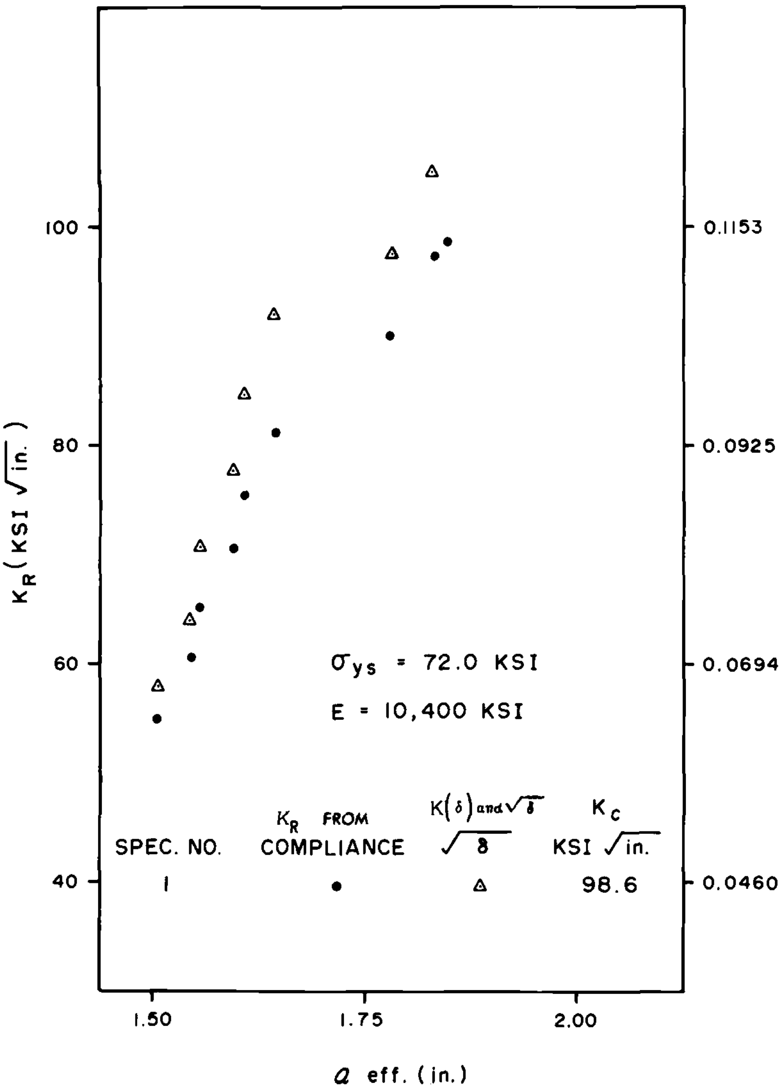

FIG. 15—*Crack resistance curves for 1/8-in.-thick 7075-T651 aluminum alloy.*

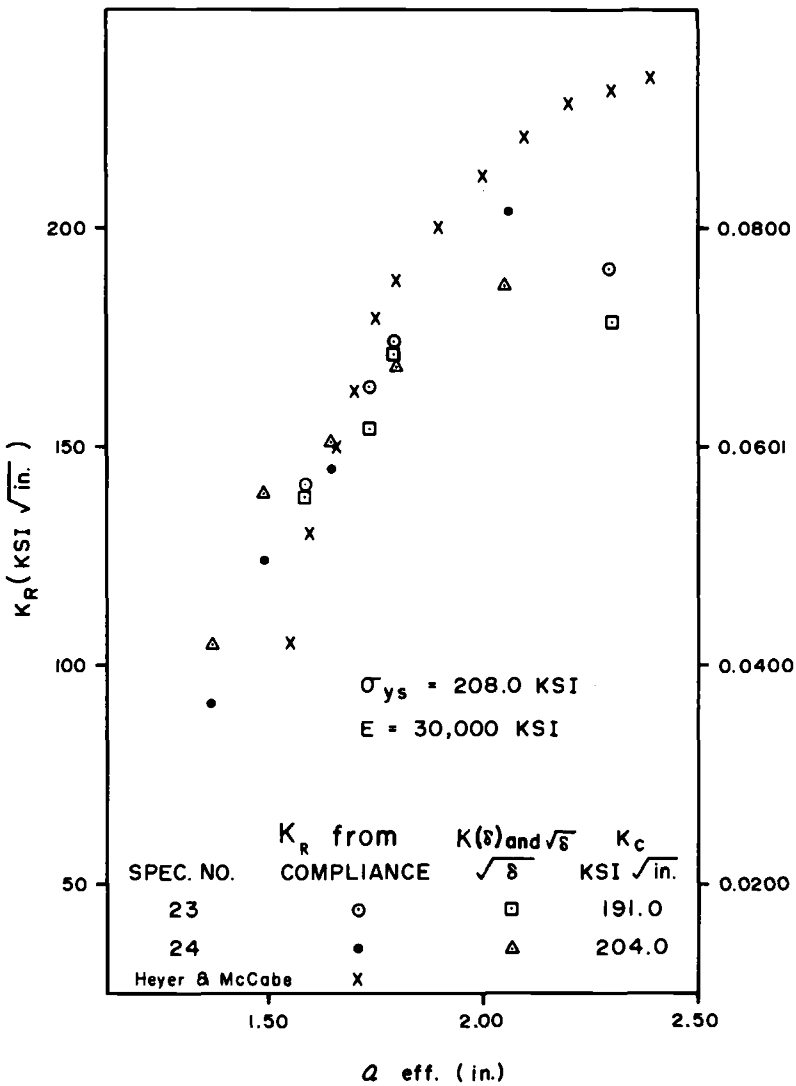

FIG. 16—*Crack resistance curves for 0.048-in.-thick Ph14-8Mo SRH 950 stainless steel alloy.*

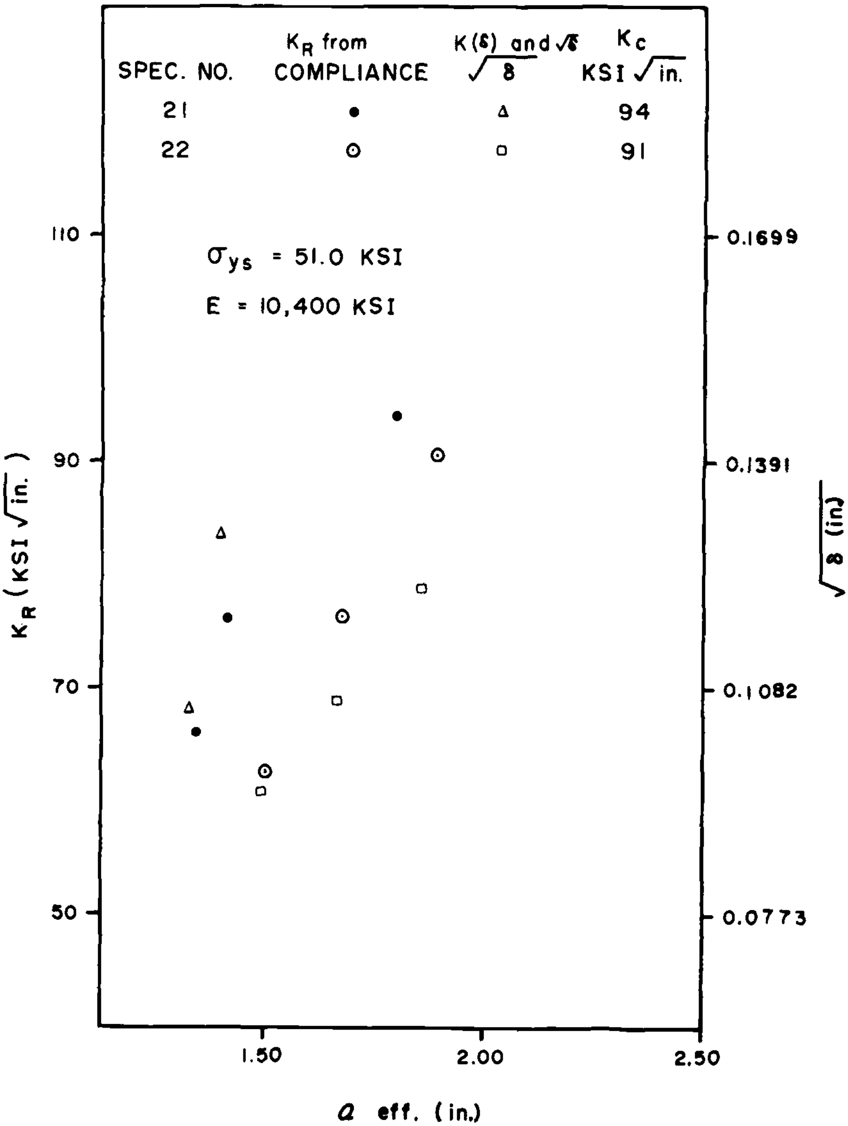

FIG. 17—*Crack resistance curves for 1/16-in.-thick 2024-T351 aluminum alloy.*

References

[1] Irwin, G. R. "Fracture Testing of High Strength Sheet Material Under Conditions Appropriate for Stress Analysis," Report No. 5486, Naval Research Laboratory, July 1960.

[2] Strawley, J. E. and Brown, W. F., "Fracture Toughness Testing," NASA Technical Memorandum TMX-52030, National Aeronautics and Space Administration.

[3] Normark, G. E., Lifka, B. W., and Kaufman, J. G., "Fracture Toughness, Fatigue-Crack Propagation and Corrosion Characteristics of Aluminum Alloy Plates for Wing Skins," Aluminum Company of America Quarterly Report, 3 June 1964 to 3 Sept. 1964, Contracts AF 33 (167)-11155 and AF 33 (615)-2012.

[4] Irwin, G. R., "Fracture Testing of High-Strength Sheet Materials Under Conditions Appropriate for Stress Analysis," Report No. 5486, Naval Research Laboratory, July 1960.

[5] Boyle, R. W., "A Method for Determining Crack Growth in Notched Specimens," *Materials Research and Standards*, Aug. 1962.

[6] Zinkham, R. E., "Anisotropy and Thickness Effects in Fracture of 7075-T6 and T651 Aluminum Alloy," *Engineering Fracture Mechanics*, Vol. 1, Aug. 1968.

[7] Wells, A. A., "Notched Bar Tests, Fracture Mechanics, and the Brittle Strength of Welded Structures," *British Welding Journal*, Vol. 13, 1965.

[8] Wells, A. A., "Application of Fracture Mechanics at and Beyond General Yielding," *British Welding Journal*, Nov. 1963.

[9] Burdekin, F. M. and Stone, D. W., *Journal of Strain Analysis*, Institute of Mechanical Engineering, Vol. 1, No. 2, 1966, p. 145.

[10] Rice, J. M., *Mathematical Analysis in the Mechanics of Fracture*, Vol. 2, Academic Press, New York, 1968, p. 191.

[11] Irwin, G. R., Lingaraju, B., and Tada, H., "Interpretations of the Crack Opening Dislocation Concept," Report No. 358, Fritz Engineering Laboratory, 2 June 1969.

[12] Burdekin, F. M. and Wells, A. A., private communication.

[13] Rooke, D. P. and Bradshaw, F. S., "A Study of Crack Tip Deformation and a Derivation of Fracture Energy," Second International Conference on Fracture, Brighton, England, 1969.

[14] Hahn, G. T. and Rosenfield, A. R., "Local Yielding and Extension of a Crack Under Plane Stress," *Acta Metallurgica*, Vol. 13, March 1965.

[15] Heyer, R. and McCabe, D., private communication.

[16] Heyer, R. and McCabe, D., "Plane-Stress Fracture Toughness Testing Using a Crack-Line-Loaded Specimen," Third National Symposium on Fracture Mechanics, Lehigh University, Bethlehem, Pa., Aug. 1969.

A. M. Sullivan,[1] *C. N. Freed,*[2] *and J. Stoop*[1]

Comparison of R-Curves Determined from Different Specimen Types

REFERENCE: Sullivan, A. M., Freed, C. N., and Stoop, J., "**Comparison of R-Curves Determined from Different Specimen Types,**" *Fracture Toughness Evaluation by R-Curve Methods, ASTM STP 527*, American Society for Testing and Materials, 1973, pp. 85-104.

ABSTRACT: Crack growth resistance curves (R-curves) have been obtained by testing center-cracked tension specimens (CCT) of three aluminum alloys, one titanium alloy, and two steels. Direct comparison is possible for four of these alloys with R-curves determined from crackline loaded (CLL) specimens.

Some differences between the two specimens are found in the reported values of K_c. These appear to be a direct consequence of the type of stress-crack length relationship noted during testing. In tough material tested using the CCT specimen, the crack grown first under a rising load but finally continues to extend at a constant load. Since this constant load crack growth marks the end of structural integrity, its recognition is crucial to a rational interpretation of fracture resistance. The CCL specimen type does not discriminate between the changes in crack growth behavior observed for these tough materials. Further, it is shown that fatigue precracking may influence the amount of crack growth prior to instability even though the final value of K_c remains unchanged.

No evidence of variation in the K_c-value with initial crack length has been observed over the range of slit lengths investigated.

KEY WORDS: crack propagation, fracture toughness, titanium alloys, aluminum alloys, structural steels, strains, stresses, loads (forces), steels, tests, evaluation

Fracture of structural materials and fail-safe design are still problems of abiding concern. Furthermore, although both are ramifying, they are in a very real sense interconnected, since, unless fracture toughness can be assessed in some form useful for design, it cannot be incorporated therein. Recognition that materials and structures will contain flaws and that these cracks or defects impair load-bearing capacity required definition of the degree of impairment. This definition can be provided through the basic parameters of linear-elastic fracture mechanics (LEFM) which define load or crack length or both for material failure.

The fact that geometric variables attendant upon measurement of fracture toughness were minimized under conditions of plane strain (thick section material) led initial research emphasis in this direction. Now, however, with the experience gained, it is appropriate to reexamine the problem of assigning

[1] Head, Fracture Mechanisms Section, and metallurgist, respectively, Strength of Metals Branch, Metallurgy Division, Naval Research Laboratory, Washington, D.C. 20390.

[2] Lawyer, Mobile Source Enforcement Division, Environmental Protection Agency, Washington, D.C. 20024.

fracture toughness values to thin sheet material essentially under conditions of plane stress. Facets of this problem include particularly the influence of specimen dimensions on K_c, crack growth measurement, and the concept of a crack growth resistance, or R-curve.

Crack Growth Resistance Curve

The R-curve concept, first promulgated in 1960 [*1*],[3] suggests that a unique relationship exists between the crack growth resistance, R, manifested by a metal sheet and the amount of crack extension ($\Delta a = a - a_0$). This relationship, determined for each material, will characterize the material in terms of toughness. Points of tangency between such a curve and curves of $\mathcal{G}$ evaluated for constant stress then define specific instability conditions for finite width structures. This concept, tabled for some years, is now undergoing serious evaluation [*2,3*]. Particularly, the work of Heyer and McCabe [*4*] utilizing the crack-line-loaded (CLL) specimen is continuing to provide R-curves for a spectrum of metal alloys.

If the crack resistance curve, hereafter referred to as the R-curve, has a unique shape for each material (of a given thickness) and is independent of initial crack length, specimen geometry, and boundary loading conditions, it can be considered a fracture toughness signature of the metal. A geometry independent R-curve can be a useful tool to engineers engaged in failure-safe design. Through the use of a numerical solution, the designer can ascertain the tangency point between the crack driving force curve and the R-curve and, therefore, compute the stress intensity at commencement of unstable crack propagation. Since the equation which describes the crack driving force curve will approximate the stress distribution and boundary loading conditions of the structure, the tangency point will provide the critical stress-crack length relationship applicable to the structure at the onset of brittle fracture. Catastrophic failure can be prevented through a structure design which will preclude any stress-crack length relationship that may occur in service from approaching the critical relationship.

Materials

The fracture toughness of six structural sheet metals was investigated: three aluminum alloys, one titanium alloy, and two steels. All of the sheet was 0.063 in. thick with the exception of the PH 15-7 air melt stainless steel (0.052 in.) and 7475-T61 aluminum (0.090 in.). The mechanical property data and heat treatments are presented in Table 1; fracture toughness properties in Table 2.

Experimental Parameters

Center-cracked-tensile (CCT) sheet specimens have been employed throughout the investigation at the Naval Research Laboratory (NRL), as this specimen is representative of a structural prototype element. As mentioned before, other

[3] The italic numbers in brackets refer to the list of references appended to this paper.

TABLE 1—*Mechanical properties.*

Material	Alloy	Fracture Direction	Yield Strength, σ_{ys} at 0.2% offset, ksi	Ultimate Tensile Strength, ksi	Elongation, %	Heat Treatment
Aluminum						
	7075-T6	WR	76.5	88.5	11.0	
	7475-T61	WR	73.3	80.2	13.0	
	2024-T3	WR	50.0	69.8	17.0	
Steel						
	4130	WR	169.5	193.0	3.8	austenize: 1575 F, 1 h, water spray temper: 700 F, 30 min, air cool
	4130	WR	178.4	226.1	5.2	austenize: 1575 F, 30 min, water spray temper: 500 F, 30 min, air cool
	15-7 PH[a]	WR	212.0	. . .	. . .	heat: 1750 F, 10 min cool: air cool to room temperature cool to -100 F, 8 h
	15-7 PH[a]	RW	219.1	229.4	5.2	reheat: 1050 F, 1 h
Titanium						
	6Al-4V	WR	151.1	156.3	1.0	solution anneal: 1700 F, 20 min, water spray age: 975 F, 8 h, air cool

[a] Donated and heat treated by Armco Research Laboratory.

specimen types can also be employed [2,3]. Figure 1 depicts the specimen together with the gage used to measure crack opening (COD). Specimen width, W, was varied (Table 1), the length to width ratio of the aluminum alloys being equal to 3. For the heat-treated materials, titanium alloys and steel, the restricted size of the heat-treating equipment limited the sheet length to 12 to 15 in. To achieve the desired total testing length, $L/W = 3$, heat-treated extension tabs of the same material were fastened to the central specimen with bolts. Previous tests on foreshortened aluminum specimens that were lengthened by extension tabs in this manner have demonstrated that the value of K_c was unaffected [5]. The PH 15-7 specimens were heat treated at Armco, and only the 20-in.-wide specimen required extension with end tabs.

The center slit in the CCT specimen was produced by an electric discharge (elox) method. The root radius of the slit tip was typically 3 to 5 mils, which

TABLE 2—*Fracture toughness properties.*

Material	Alloy	Fracture Direction	Yield Strength, ksi		Slit Tip	Width, in.	Specimen Geometry CCT, K_c, ksi$\sqrt{\text{in.}}$	Specimen Geometry CLL, K_c, ksi$\sqrt{\text{in.}}$
Aluminum								
	7075-T6	WR	76.5	Lot 1	elox	12	65.2	...
	7075-T6	WR	76.5	Lot 2	elox	12	61.2	...
	7075-T6	WR	76.5	Lot 2	elox-sharp	12	61.0	...
	7075-T6	WR	76.5	Lot 2	elox-fatigue crack	12	59.0	63.0
	7475-T61	WR	73.3		elox	12	88.4	118.1
	2024-T3	WR	50.0		elox	12	97.2	86.0
						15	97.2	...
						20	102.7	106.0
Steel								
	4130	WR	169.5		elox	12	160.0	...
	4130	WR	178.4		elox	12	140.8	...
	15-7 PH	WR	212.0		elox	11	117.8	90.0
	15-7 PH	WR	212.0		elox	12	109.8	...
	15-7 PH	WR	212.0		elox	20	137.6	90.0
	15-7 PH	RW	219.1		elox	5	222.0	...
	15-7 PH	RW	219.1		elox	10	243.3	...
	15-7 PH	RW	219.1		elox	12	258.5	...
	15-7 PH	RW	219.1		elox	20	294.2	...
Titanium								
	6Al-4V	WR	151.1		elox		74.4	...
	6Al-4V	WR	151.1		elox-fatigue crack		86.1	...

could be decreased to 1 mil by a second elox operation with a fine electrode. Some specimens were also fatigued to assess the influence of slit-tip sharpness on K_c and the R-curve. When stable crack growth preceded fracture, earlier work has shown the crack to be sufficiently acute to eliminate crack of slit-tip radius as a variable [*6*].

Within the slit is placed a beam displacement gage instrumented with a 4 strain gage circuit. Upon loading, the borders of the slit are displaced, and cracks will initiate at the slit tips along a plane perpendicular to the applied stress. The displacement gage monitors the crack-opening displacement (COD) via an electrical readout to an X-Y recorder; a previous calibration between COD and crack length enables calculation of crack length at any load level during the test [*5*]. Stable crack growth occurs from each slit tip until the total crack reaches a critical length for the applied stress, whereupon unstable crack propagation

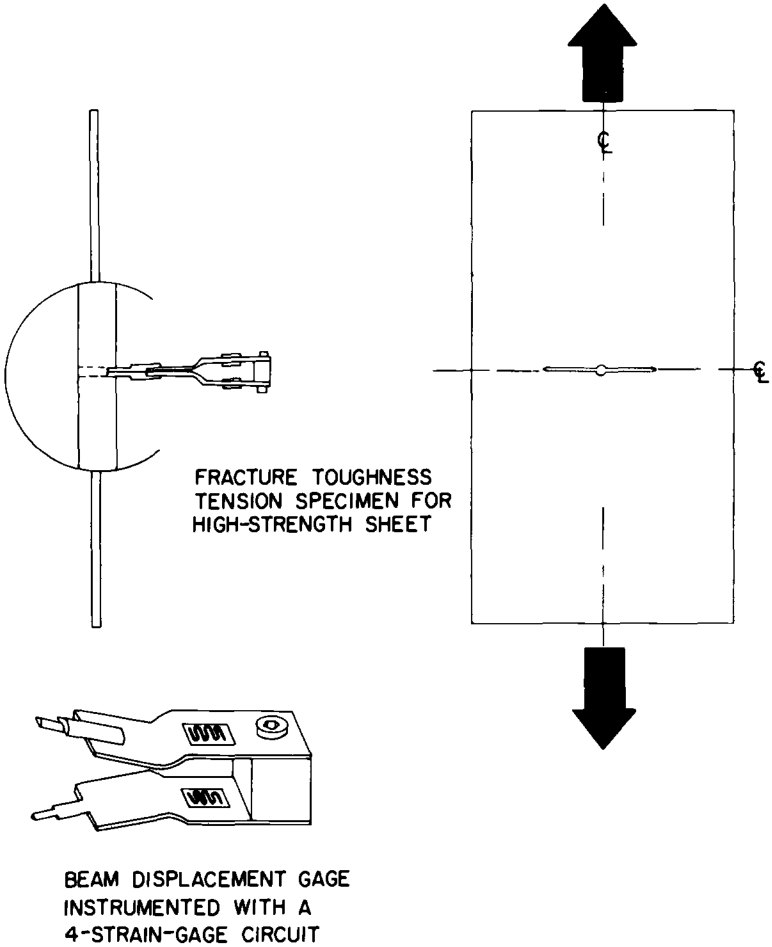

FIG. 1—*Center-cracked tension specimen and displacement gage used to monitor crack opening displacement.*

ensues and the specimen fractures. The crack length and stress at the onset of instability are used to calculate K_c, which utilizing the CCT specimen is equal to K_R (critical). With other specimen types, various, mathematical relationships are used to determine K_R (critical).

Data Reduction

To analyze load-COD data curves:

(*a*) A line is drawn through the "best fit" part of the straight line portion of the curve; this locates the origin and eliminates occasional "start-up" errors.

(*b*) Straight lines are then drawn from the origin to the loading curve at selected intervals of COD.

(*c*) The inverse slope, COD/P, of these lines is now determined. At NRL, the lines are drawn with a drafting instrument from which angles can be read; the cotangent of the angle will give the value required when appropriate units are supplied (that is, multiply by 45-deg chart values).

(*d*) This number is then normalized to give $[EB(\mathrm{COD})]/P$.

(*e*) The initial crack length being known, the value of $[EB(\mathrm{COD})]/P$ is read from the calibration curve and compared with the initial crack length value read from the chart. Frequently small differences will be observed due to shifts in alignment or of probe positioning. The difference between the calibration value and the observed value is then added (or subtracted) from all measured values of $[EB(\mathrm{COD})]/P$ read from the chart.

(*f*) These values are then referred to the calibration curve and $2a/W$-values read off. Simple arithmetic easily gives crack length values.

(*g*) Gross stress, σ_G, is computed for the various load values as load/unnotched area, P/BW.

Load P and crack length $2a$ now being known from the test record, K_c is calculated from a modification of the Isida equation [7]

$$K_c = \sigma_G \sqrt{a}\, f\, 2a/W$$

where

$$f\, 2a/W = 1.77\ [1 - 0.1\ (2a/W) + (2a/W^2)].$$

This expression has been found accurate to within 1 percent over the range $0 < 2a/W > 0.6$. This equation is preferred over the commonly used Irwin-Westergard tangent formula since it more properly satisfies the boundary conditions for the specimen. Further polynominal expressions are more convenient for incorporation into data-reduction computer programs.

Discussion of R-Curves

As originally introduced, R was defined as equivalent to $\mathcal{G}$ since both are essentially energy concepts. However, since the stress intensity terminology—K-value—is now more commonly used, it has seemed reasonable to present these curves as K_R versus Δa. Comparison of R-curves determined by both the CCT and CLL specimens is possible for four of the six materials tested.

Aluminum 7075-T6

Two lots of this alloy were utilized; Lot 1 represents material stored for a number of years, while Lot 2 sheet is newly acquired. In Fig. 2*a* data points are displayed representing R-curves for specimens manifesting a spectrum of initial ($2a_0$) crack length values. An average curve has been drawn culminating in the K_c-value of 65.2 ksi $\sqrt{\text{in.}}$ for Lot 1 material. This average is based on more than 20 tests not all of which are plotted. The Armco R-curve for this alloy indicates that greater crack growth is obtained with the fatigue pre-cracked CLL specimen

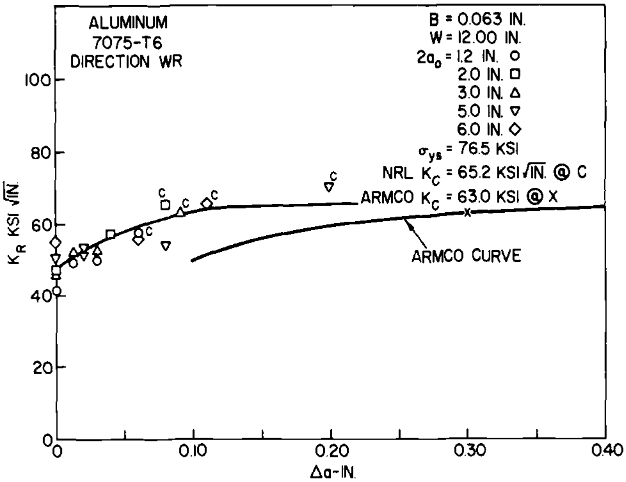

FIG. 2a—*Crack growth resistance* K_R *for aluminum alloy 7075-T6 plotted as a function of crack growth* $\Delta a = a - a_0$. K_c *indicated by "C" for CCT specimens, and by "X" for CLL specimens (Armco). Radius of the slit tips was 0.003 to 0.006 in.*

although the K_c-value of 63 ksi$\sqrt{}$in. is compatible with the CCT data.

The effect of notch acuity (slit tip radius) on K_c and the R-curve was studied. Some specimens were prepared with the original elox slit tip (radius ≈ 0.00 in.) and then re-eloxed to produce an extension of about 0.060 in. This extension is 0.002 in. wide with a tip radius of 0.001 in. Data from the sharp elox slit seen in Fig. 2*b* for Lot 2 material again show less crack growth than the Armco curve. Curves produced from the fatigued CCT specimens in Fig. 2*c* for Lot 2 aluminum demonstrate crack growth more nearly comparable to the CLL

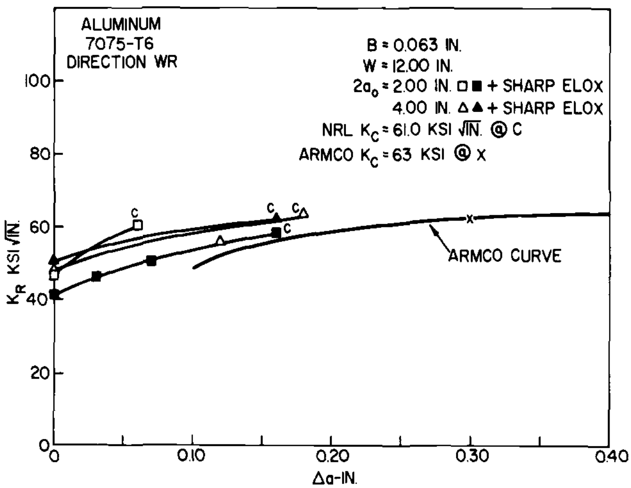

FIG. 2b—*As Fig.* 2a; *slit tips extended by a sharp elox slit (0.06 in. long; 0.002 in. wide) tip radius of about 0.001 in. Amount of crack growth similar to that in Fig.* 2a.

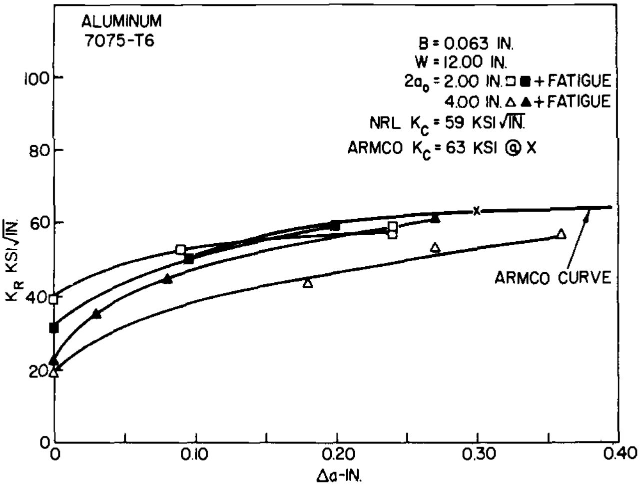

FIG. 2c—*As Fig.* 2a; *slit tips extended by a fatigue crack. Amount of crack growth prior to instability has increased to that of CLL specimen.*

specimen. In these latter cases of Lot 2 material, values of K_c = 61 and 59 ksi$\sqrt{}$in. are commensurate with unpublished data on Lot 2 material using the blunter elox slit in which K_c = 61.2 ksi$\sqrt{}$in.

Aluminum 7475-T61

The data for this tougher aluminum alloy are shown in Fig. 3. Although curves for both the CCT and CLL specimens virtually overlap, the amount of crack growth prior to instability differs markedly and is reflected in the lower K_c-value

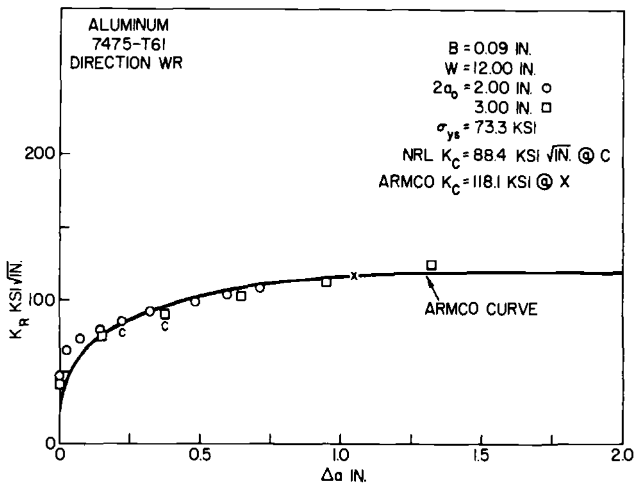

FIG. 3—*Crack growth resistance* K_R *for aluminum alloy 7475-T61 plotted as a function of* Δa. *Instability value of* K_c *indicated by "C" for CCT specimens and by "X" for CLL specimens. Armco (CLL) curve fits CCT specimen R-curve but* K_c*-values differ.*

for the CCT specimens. Considered dependent upon the crack growth behavior observed, the implications of this observation are discussed more fully in another section of this report.

Aluminum 2024-T3

Tested in two widths, W = 12.0 in., Fig. 4*a*, and W = 20.0 in., Fig. 4*b*, the curve shapes for this alloy show comparability of CCT and CLL data points. Again, however, the K_c-values differ. The Armco curve indicates an effect of

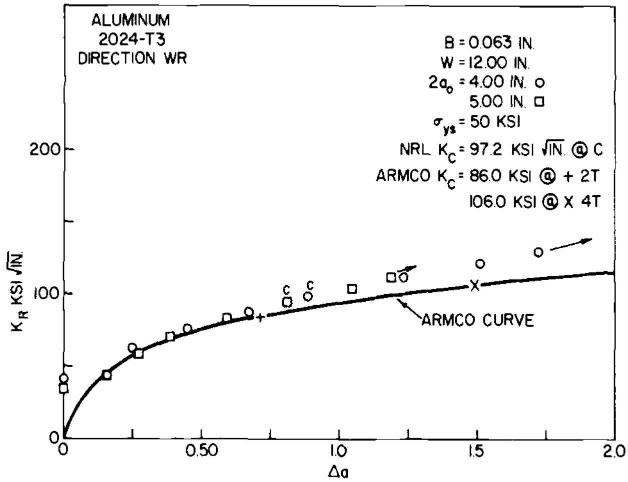

FIG. 4*a*—*Crack growth resistance* K_R *for aluminum alloy 2024-T3. Instability value of* K_c *indicated by "C" for 12-in.-wide CCT specimen, and "X" for CLL specimen. Arrows indicate crack growth beyond limit of CCT calibration curve. R-curves from both specimen geometries are close fitting but* K_c*-values differ.*

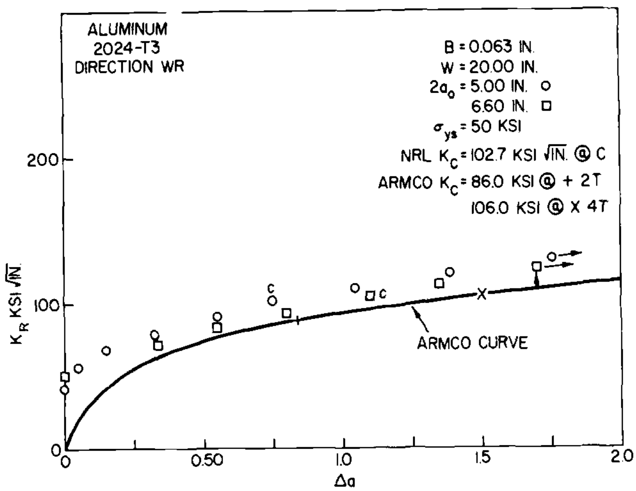

FIG. 4*b*—*As Fig.* 4a *but width* W = *20 in. Although Armco curve is slightly low, it is probably within normal scatter range.*

width which is not apparent with the CCT specimen. The width of the CLL specimen can be considered equivalent to one half the CCT specimen. K_c for the 2T (5-in.-wide) CLL specimen is evaluated as 86 ksi$\sqrt{\text{in.}}$, while that of the 4T (10-in.-wide) specimen is 106 ksi$\sqrt{\text{in.}}$

Steel PH 15-7

The effect of sheet width on K_c and the R-curve was investigated for this alloy together with that of fracture direction. As evidenced by Fig. 5*a*, WR direction, (fracture path parallel to the rolling direction) curves for the CCT specimen lie significantly above that of the CLL data and the K_c-value is higher. It is interesting to note that the narrower CCT specimens lie further from the Armco curve. In the tougher RW direction, Fig. 5*b*, not tested successfully by the CLL specimen, considerable scatter is observed and a width effect is indicated. Again, the widest specimen produces the lowest curve. The K_c-values are spread over such a broad range that no characteristic value can be cited.

Steel 4130

This alloy steel was heat treated to the two yield strength levels of 169.5 and 178.4 ksi. Several initial slit lengths were investigated for each strength level; the results being displayed in Fig. 6. Data for the varied slit lengths of the lower strength material can be represented by a single R-curve, Fig. 6*a*. The scatter apparent in the curves for the higher strength level material, Fig. 6*b*, does not indicate any definite trend towards an effect of initial crack length. No CLL data are available for comparison.

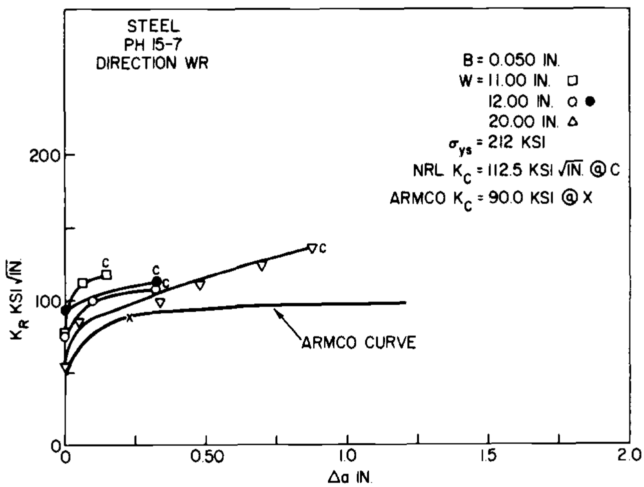

FIG. 5*a*—*Crack growth resistance* K_R *for stainless steel PH 15-7 (air melt) direction WR. Instability value of* K_c *indicated by "C" for CCT specimen and by "X" for CLL specimen. Inexplicably high* K_c*-value noted for 20-in.-wide CCT specimen.*

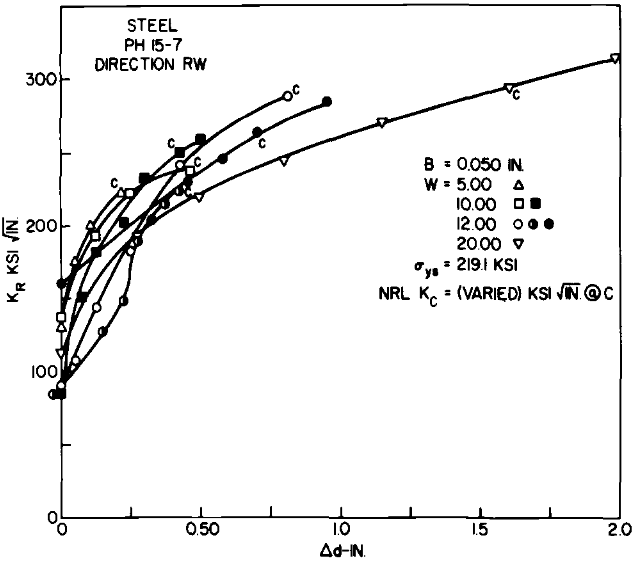

FIG. 5*b*—*As Fig. 5*a; *direction RW. Note influence of specimen width on the R-curve for this high toughness fracture direction as reflected by broad* K_C *scatter.*

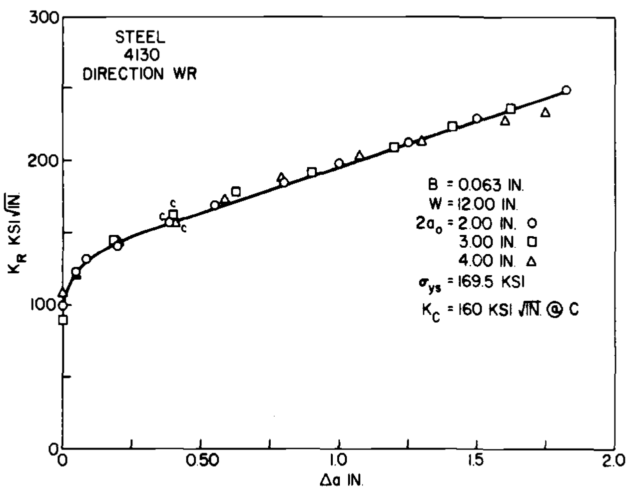

FIG. 6*a*—*Crack growth resistance* K_R *for 4130 steel,* σ_{ys}*=169.5 ksi. Instability values of* K_c *indicated by "C".*

Titanium 6Al-4V

The effect of initial slit length upon the R-curve shape is again observed with the longest initial slits producing the lowest curves. The one fatigue precracked specimen exhibits no increased crack growth prior to instability. Two distinct types of fracture behavior, as will be later shown, were observed for this

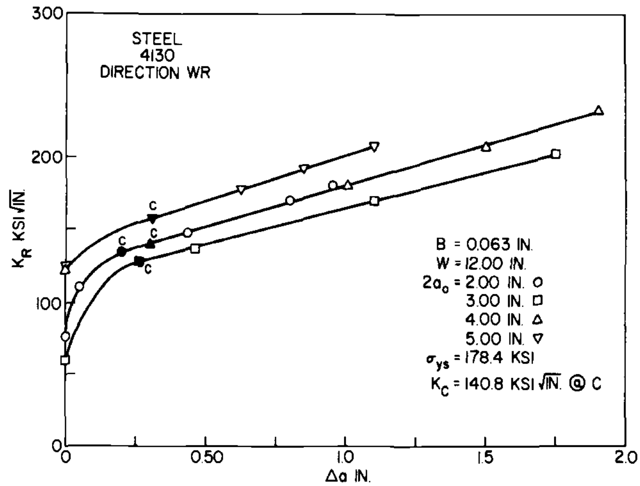

FIG. *6b–As Fig. 6*a; *σ_{ys} = 178.4 ksi.*

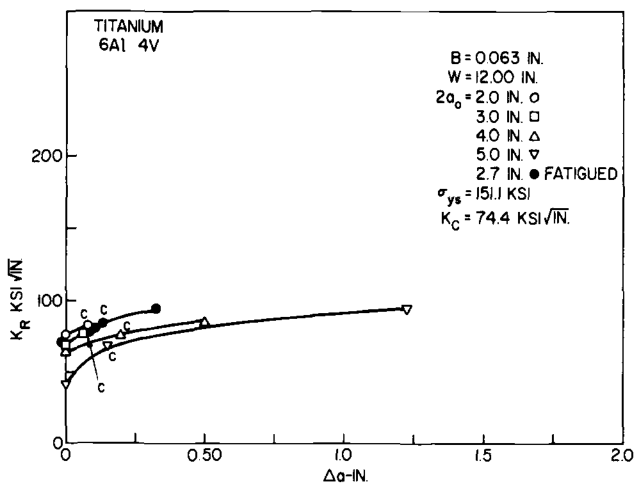

FIG. 7–*Crack growth resistance for titanium alloy 6Al-4V. Instability values of* K_c *indicated by "C".*

material. Again no CCL specimen data are available for comparison with the R-curves of this alloy shown in Fig. 7.

Discussion of Crack Growth Behavior

Examination of load-crack growth records for these materials has shown two types of crack extension behavior which are schematically illustrated in Fig. 8. The upper boundary of Region I defines the load required to initiate growth at the crack tip; in Region II, the crack propagates under a continually rising load. If the load is held constant in this region, growth ceases. For the more brittle

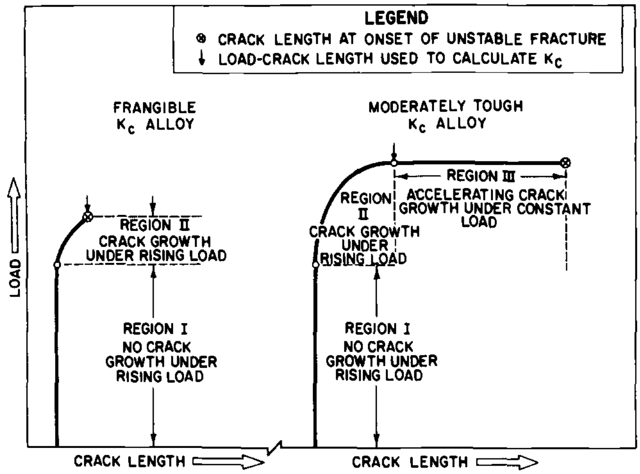

FIG. 8—*Schematic illustration of two types of crack extension behavior; one in which final separation occurs at some value of the rising load; the other in which final separation occurs after a period of crack growth under a constant load.*

alloys, propagation under the rising load continues until the combination of load and crack length becomes critical and unstable fracture ensues.

While tougher alloys also exhibit Regions I and II behavior, final separation does not occur at the end of Region II. Instead, at this point, the load remains constant while the crack grows at an accelerating rate; this type of growth is designated as Region III. Noted previously by Brock [*8*] and Campbell [*9*], it was suggested that both the K-level at commencement of Region III and at final specimen separation are relevant damage criteria. However, Srawley and Brown [*2*] define instability as occurring at either the maximum load value or an inflection point of load versus crack extension of zero slope, for example, $dP/d2a = 0$. Practically, it seems reasonable that the start of Region III behavior (crack growth under constant load) marks the limit of structural integrity. Therefore, the crack length at this position, the start of Region III, is used to calculate K_c for materials exhibiting such behavior.

Data from which the previously discussed R-curves were obtained, gross stress, σ_G, plotted against crack length, $2a$, are presented. In addition, crack growth curves calculated from the CLL specimen R-curve data are included. This calculation can be accomplished for an assumed crack length ($2a_0$) and width (W) by adding values of Δa to a_0, calculating first $2a/W$, and finally σ_G from the relationship:

$$\sigma_G = \frac{K(@f\,\Delta a)}{\sqrt{a}\,(2a/W)}$$

A hyperbolic curve denoting the stress value for the constant (average) K_c-value of the material is also drawn in each figure. Since this is computed for the infinite sheet equation,

$$\sigma_G = \frac{K}{\sqrt{\pi a}}$$

some stress values for the finite sheets tested will lie below the curve. A diagonal straight line across each figure represents a limiting net stress level equal to the material yield stress.

Aluminum Alloys

In Fig. 9 the stress-crack length curve of 7075-T6 computed for the CLL-Armco specimen rises to a maximum value; the CCT data curve also rises to a maximum value at which final separation occurs. The instability value is identified readily, and, as noted previously, the K_c-values compare closely.

Unlike 7075-T6, in Fig. 10, Region III behavior is noted for the tougher 7475-T61 alloy in which crack growth is observed during constant gross stress. The K_c-value of 118.1 ksi$\sqrt{}$in. reported for the CLL specimen (see X in Fig. 10) is seen to fall at the end of the constant stress region; at the start of Region III a K_c-value of 105 ksi $\sqrt{}$in. is obtained. This value, however, is still higher than that obtained from the CCT specimen in which K_c = 88 ksi $\sqrt{}$in.

Other data [*10*] indicate a value of K_c = 85 ksi $\sqrt{}$in. for this alloy. It should be also noted that when the specimen used by Heyer and McCabe is loaded in tension rather than crack-line loaded, a K_c-value of 110.6 ksi$\sqrt{}$in. is calculated, and no region of crack growth under constant load is observed [*11*].

Similarly for 2024-T3 aluminum, Fig. 11, Region III behavior is noted. The instability point recorded for the CLL specimen is at the beginning of Region III

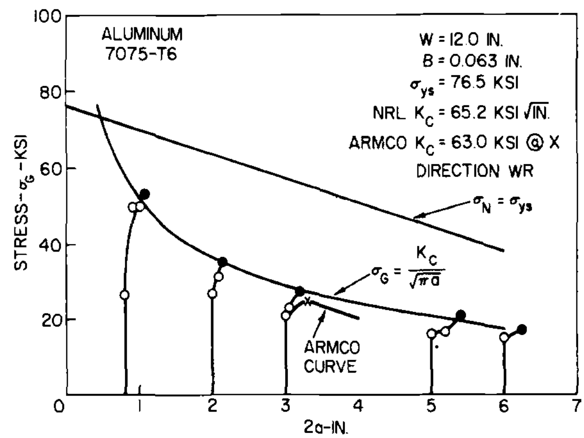

FIG. 9—*Gross stress, σ_G, (equivalent to load) plotted against crack length, 2*a*, for aluminum alloy 7075-T6. Note crack growth to instability under rising load and well defined in maximum constructed Armco curve. Instability location marked by solid symbols.*

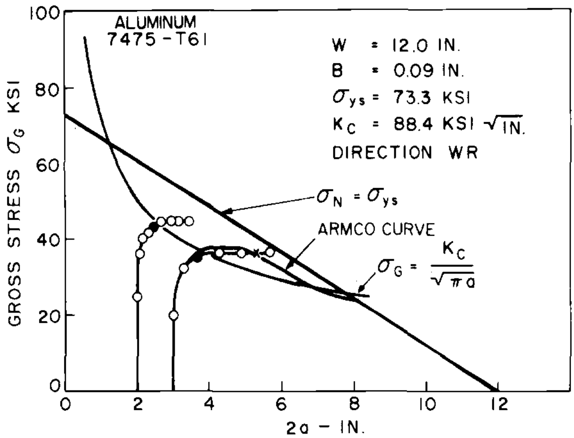

FIG. 10—*Gross stress, σ_G, plotted against crack length,* 2a, *for aluminum alloy 7475-T61. Note region of crack growth under constant gross stress (equivalent to constant load) and similar region in constructed Armco curve. Instability location marked by solid symbols.*

in Fig. 11*a*, the narrower specimen, but occurs after considerable constant load crack growth in the wider specimen, Fig. 11*b*. K_c-values for the 12-in.-wide CCT specimen (avg K_c = 97 ksi $\sqrt{}$in.) are calculated from stress values which just exceeded the material yield stress but correspond well to those of the 20-in.-wide specimen (K_c = 102 ksi $\sqrt{}$in.) for which the instability stress was lower than the yield stress.

Steels

Little indication of crack extension at constant load is seen for PH 15-7, Fig. 12, save for the 20-in.-wide specimen in the RW direction (not shown). For 4130

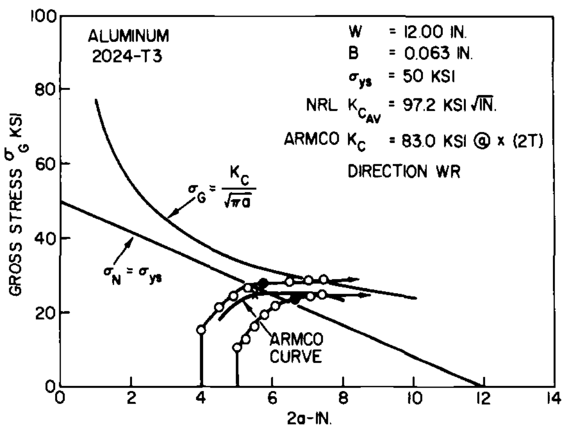

FIG. 11*a*—*Gross stress, σ_G, plotted against crack length, 2a, for aluminum alloy 2024-T3 (specimen width 12 in.). Note region of crack growth under constant stress and similar region in constructed Armco curve. Instability location marked by solid symbols. Although the CCT specimen at instability manifested $\sigma_N > \sigma_{ys}$, a K_c-value compatible with that from the wider specimen is obtained.*

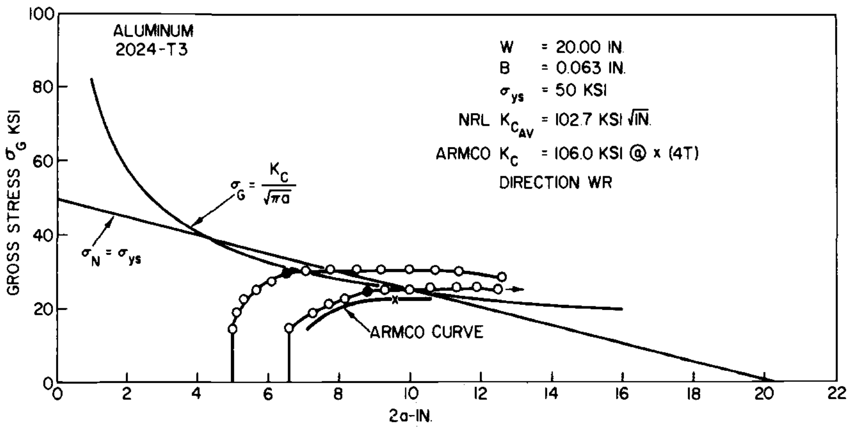

FIG. 11*b–As Fig. 11*a *but W = 20 in. At instability,* $\sigma_N < \sigma_{ys}$.

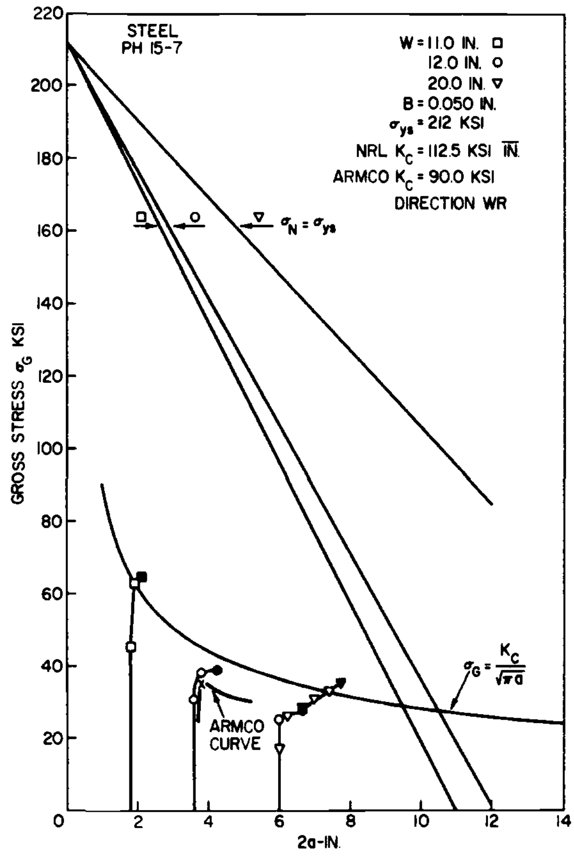

FIG. 12–*Gross stress,* σ_G*, plotted against crack length,* 2a, *for stainless steel PH 15-7 (air melt), direction WR. Similar to Fig. 8, the curve shows that crack growth to instability occurs under rising load only and is reflected in well defined maximum of Armco curve. Apparent shape of 20-in.-wide specimen curve is somewhat abnormal and may indicate an experimental anomaly. Instability location marked by solid symbols.*

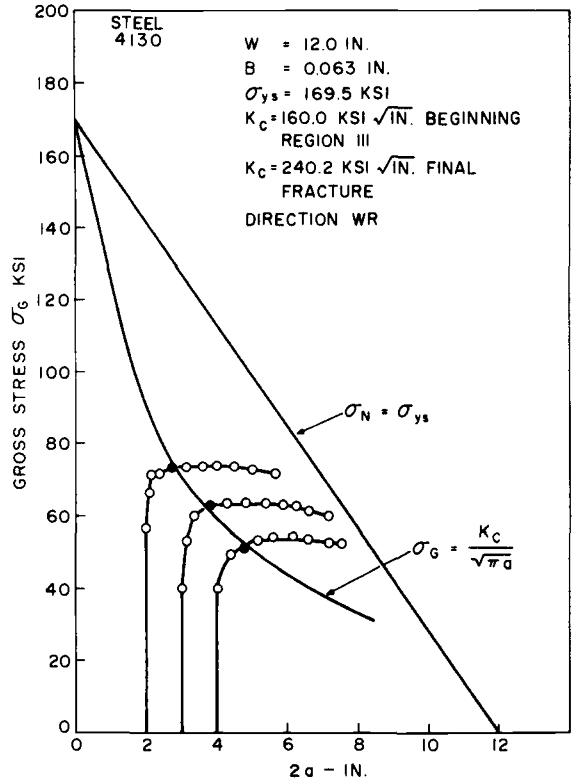

FIG. 13*a*–*Gross stress, σ_G, plotted against crack length, 2a for 4130 steel (σ_{ys} = 169.5 ksi). Region of crack growth under constant load terminates in final separation before yield stress is reached in specimen net section. Instability location marked by solid symbols.*

steel Region III behavior is common to both yield stress levels, Fig. 13*a* and *b*, and crack extension at constant load is considerable. Here both instability and final separation occur at net stress values below that of general yield, showing that Region III behavior is not a phenomenon associated with general yield in the specimen. This was not true of the aluminum alloys 7475-T61 and 2024-T3.

Titanium

Both types of crack extension behavior are found with Ti-6Al-4V, Fig. 14. Specimens with longer initial crack lengths show Region III behavior as well as those with the fatigued short crack while specimens with short initial slits fracture as soon as maximum load is reached.

Conclusions

1. Since structural integrity is lost once a crack starts to propagate under constant load, a definition of instability as occurring at the start of the Region III load-crack length relationship is considered to be mandatory.

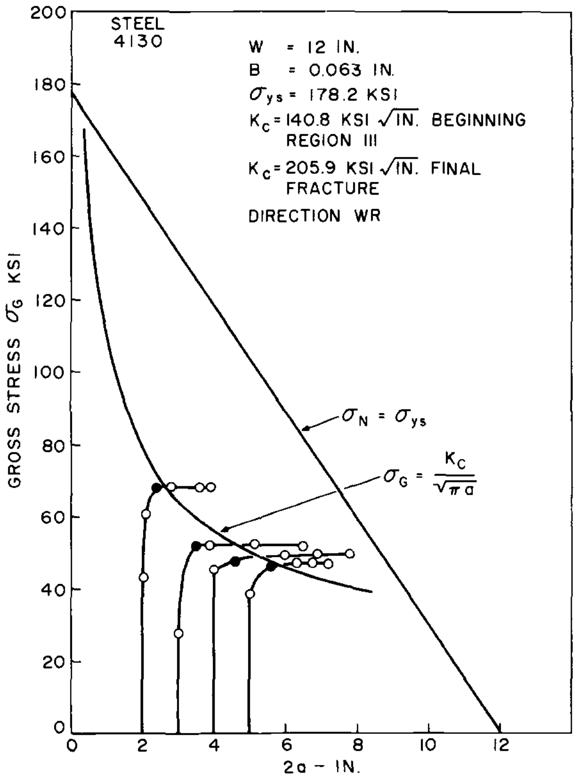

FIG. 13*b*–*As in Fig. 13*a; σ_{ys} = *178.4 ksi.*

2. Mathematical tangents to R-curves produced by either the CCT or the CLL specimen are not sufficiently discriminatory in identifying the location of the start of Region III behavior; this location must be checked by data plots of σ_G versus $2a$.

3. The CCT specimen, therefore, is preferred since, where applicable, the location of Region III behavior is readily identified from the raw data, whereas for the CLL specimen a conversion computation must be made.

4. No effect of slit tip radius on the K_c-values was observed for 7075-T6 aluminum which exhibited stable crack extension preceding fracture. However, fatigue pre-cracked specimens exhibited greater crack growth prior to instability.

5. K_c-values appear independent of the initial crack length for aluminum alloys over the range investigated. Some scatter is evident for one of the strength levels of 4130 and Ti-6Al-4V, but no discernible trend was observed.

6. Specimen width does not influence K_c for 2024-T3 when $W > 12$ in. Earlier work indicated a similar independence of K_c and width for 7075-T6 for specimens as narrow as 6 in. A possible R-curve width dependence was observed for PH-15-7 stainless for CCT specimens as wide as 20 in.

7. An inverse relationship between K_c and yield strength was observed in the materials where comparisons of different strength levels were made, namely, in the aluminum alloys and in 4130 steel.

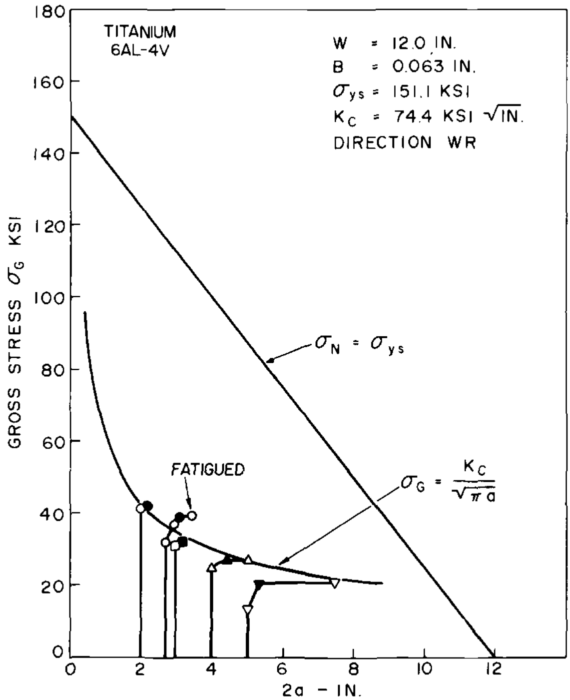

FIG. 14—*Gross stress, σ_G, plotted against crack length, 2*a*, for titanium alloy 6Al-4V. Instability location marked by solid symbols. Note here both types of crack extension behavior.*

References

[1] Krafft, J. M., Sullivan, A. M., and Boyle, R. W. in *Proceedings*, Crack Propagation Symposium, College of Aeronautics, Cranfield, England, Vol. I, 1961, pp. 8-28.

[2] Srawley, J. E. and Brown, W. F., Jr. in *Fracture Toughness Testing and Its Applications, ASTM STP 381*, American Society for Testing and Materials, 1965, pp. 133-245.

[3] Clausing, D. P., "Crack Stability in Linear Elastic Fracture Mechanics," *International Journal of Fracture Mechanics*, Vol. 5, No. 3, Sept. 1969.

[4] Heyer, R. H. and McCabe, D. E., "Plane Stress Fracture Toughness Testing Using a Crack-Line-Loaded Specimen," Third National Symposium on Fracture Mechanics, Bethlehem, Pa., Aug. 1969.

[5] Sullivan, A. M. and Freed, C. N., "The Influence of Geometric Variables on K_c Values for Two Thin Sheet Aluminum Alloys," NRL Report 7270, Naval Research Laboratory, 17 June 1971.

[6] Broek, D., "The Residual Strength of Aluminum Sheet Alloy Specimens Containing Fatigue Cracks or Saw Cuts," Technical Report NRL-TR M. 2143, National Aerospace Laboratory, Amsterdam, 1966.

[7] Brown, W. F., Jr., and Srawley, J. E., *Plane Strain Toughness Testing of High Strength Metallic Materials. ASTM STP 410*, American Society for Testing and Materials, 1966.

[8] Broek, D. in *Aerospace Proceedings*, 1966, pp. 811-835.
[9] Campbell, J. E., "Mechanical Properties of Metals," *Defense Metals Information Center Review*, 15 Jan. 1971.
[10] Alcoa Aerospace Technical Information Bulletin, Series 71, No. 6, 1971.
[11] Heyer, R. H. and McCabe, D. E., "Test Method–Fracture Toughness Measured by Crack Growth Resistance," Research and Technology Report, Armco, 27 Jan. 1971.

Matthew Creager[1]

A Note on the Use of a Simple Technique for Failure Prediction Using Resistance Curves

REFERENCE: Creager, Matthew, "**A Note on the Use of a Simple Technique for Failure Prediction Using Resistance Curves,**" *Fracture Toughness Evaluation by R-Curve Methods, ASTM STP 527,* American Society for Testing and Materials, 1973, pp. 105-112.

ABSTRACT: The use of resistance curves in the prediction of catastrophic failure in a structure normally requires the determination of the point of tangency between the resistance curve and the applied stress intensity versus crack length curve evaluated for the failure stress. Since the failure stress is unknown *a priori* a number of iterations or interpolations or both are necessary. This is often a cumbersome task. A simple procedure utilizing a transparency is presented which enables the critical stress intensity factor based on final crack length, the critical stress intensity factor based on initial crack length, and the failure stress to be found directly without iteration or interpolation.

KEY WORDS: crack propagation, fracture toughness, stresses, loads (forces), panels, predictions, failure

The primary reason for developing a failure theory is to predict the loads which will cause catastrophic failure in structural components. This note is concerned with minimizing the effort required to accomplish that task when a resistance curve approach must be taken.

Theory of Failure

No theory of failure will ever be exact; to do that, at least a quantum mechanics description of each structure under consideration would be necessary. A useful (in the engineering sense) theory is one which enables sufficiently accurate predictions to be made with a minimum of complexity in the actual construction of the prediction. This is probably the primary reason for the wide acceptance of the Irwin crack tip stress intensity factor approach to failure prediction. It is an approach which uses a single loads geometry parameter (K) to predict the response of a crack to applied loads. Often, this parameter can be compared to a single material parameter (K_{Ic}), and a reasonably accurate failure prediction can be made.

This, unfortunately, is not usually the case for thin metal sheet structures. The existence of extensive slow stable growth (under monotonic loading) prior to instability and catastrophic failure results in a significant complication. Here

[1] Engineering consultant, Canoga Park, Calif. 91304.

rather than a single material parameter, a material curve (K_r) representing essentially an infinity of points is apparently necessary to make an accurate failure prediction. Not only is the necessary input information more extensive, but the actual failure prediction is more complex due to the presence of an unknown in addition to the failure load. The crack length (or alternatively the stress intensity factor) at instability is not known *a priori.* Thus, rather than the single failure criteria for plane strain structure

$$K \geq K_{Ic}$$

two criteria must be satisfied in structures for which a significant amount of slow stable growth takes place

$$K \geq K_r \quad \text{and} \quad \frac{\partial K}{\partial a} \geq \frac{\partial K_r}{\partial a}$$

New Prediction Technique

For this reason general design curves using the resistance curve concept are difficult to generate. However, a simple technique has been developed which makes the task of failure prediction easier. The technique is highly efficient as long as an elastic analysis is appropriate. It is not as helpful when there is yielding at locations other than the crack tip (in a reinforcement, for example).

Usually the graphical procedure for predicting the failure stress using a resistance curve concept consists of: plotting a number of K versus crack length curves of different load levels; superimposing the resistance curve; and

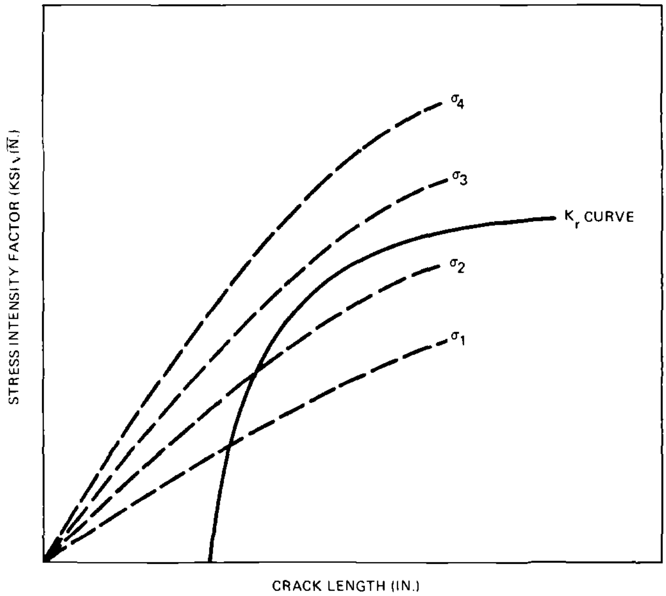

FIG. 1—*Resistance curve failure prediction.*

interpolating (or plotting additional curves) between the curves to get the failure load (see Fig. 1). This procedure has proven useful even for complex structures, as is seen in Fig. 2.

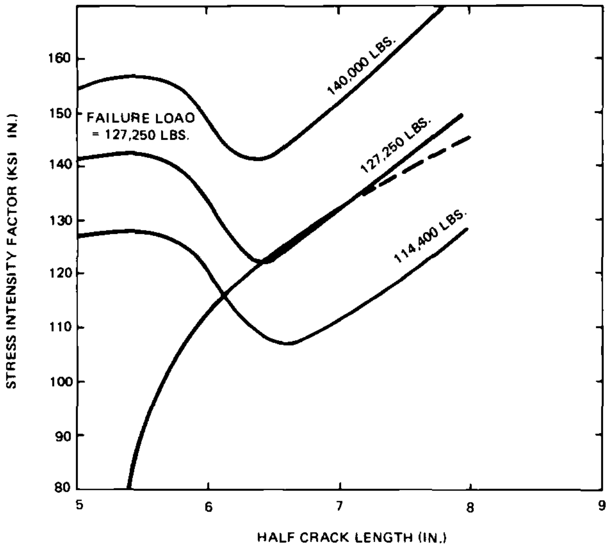

FIG. 2–*Failure prediction, reinforced panel (footnote 4).*

Procedures

The new technique consists of simply plotting resistance curves and stress intensity structural coefficient curves on semilog paper and superimposing the curves to find the point of tangency. The stress intensity coefficient is defined as all of the expression for the stress intensity factor except the load term. That is, if $K = \sigma\alpha$, α is the structural stress intensity coefficient (for example, for a wide center cracked panel α is $\sqrt{\pi a}$.) Once the point of tangency of these curves is determined, the K at instability (K_c), the K based on initial crack length and load at instability (K_0), and the load at instability can be immediately read from the curves. The following example will clarify the procedure.

For an infinitely wide center cracked panel $K = \sigma\sqrt{\pi a}$, therefore $\alpha = \sqrt{\pi a}$. This is plotted (along with finite width panels) on a semilog grid in Fig. 3. Figure 4 represents what would be a transparency of a typical resistance curve (K_r) also plotted on a semilog grid. If an initial crack length is chosen and the $\Delta a = 0$ line (on the K_r-curve) is aligned with the crack length on the α plot, a tangency point can be found by vertically moving the curves relative to one another. Since $\sigma = K/\alpha$ and $\log \sigma = \log K - \log \alpha$; the value of the stress at instability is read from the K_r-curve ordinate at the line corresponding to $\alpha = 1$ ($\log \alpha = 0$). K_c is simply the value of K_r at the tangency point, and K_0 is the value of the K_r-curve where the α-curve crosses the ordinate. This is schematically shown in Fig. 5.

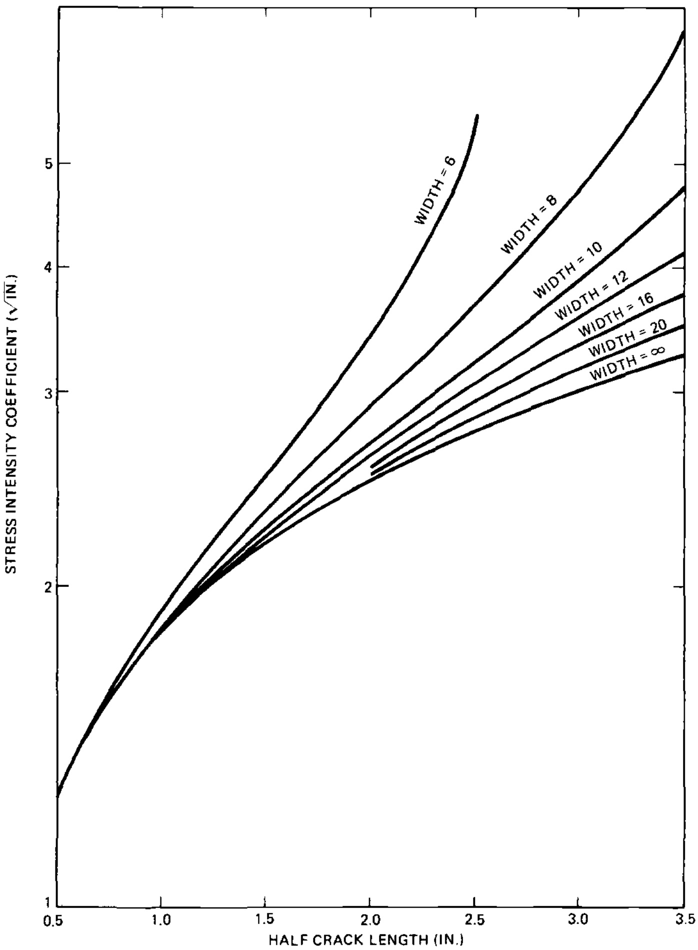

FIG. 3—*Stress intensity structural coefficient, center cracked panel.*

It can be seen that using this technique allows the rapid computation of a prediction that is normally tedious to make. For example, using Fig. 3 and the transparency, the failure stress for panels with an initial half-crack length of 2 in. and various panel widths can be quickly evaluated by simply moving the transparency vertically to give Table 1.

Even if the relationship between the stress intensity factor and the applied load is nonlinear this approach (using log plots) can be used as an aid in the necessary interpolation. Figure 6 shows an α-curve for a reinforced panel[2] where the reinforcements yield as the crack grows beyond them. α is defined by the

[2]Liu, A. F. and Creager, M., "On the Slow Stable Crack Growth Behavior of Thin Aluminum Sheet," 1971 International Conference on Mechanical Behavior of Materials, Kyoto, Japan, 1971.

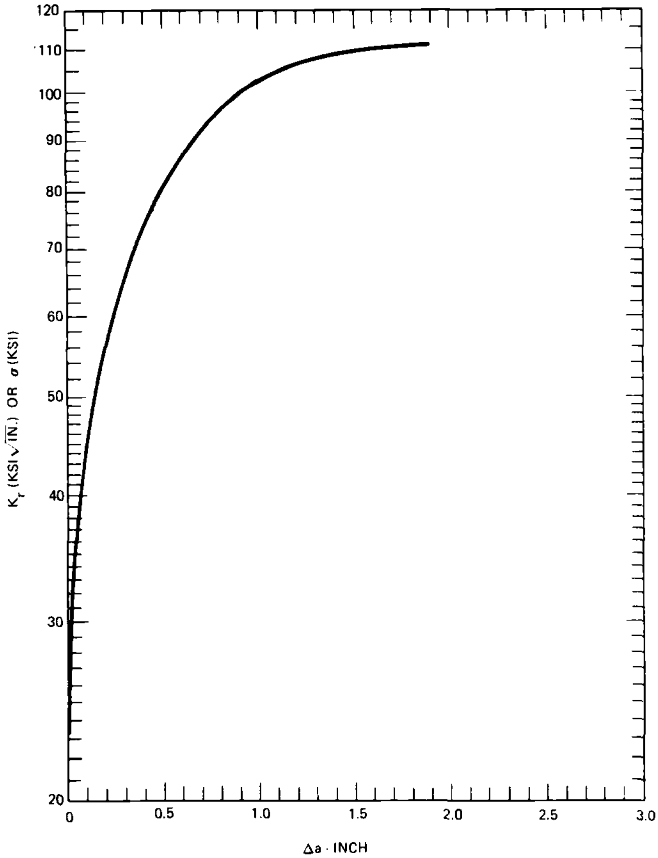

FIG. 4—K_r-*curve.*

TABLE 1—*Example predictions.*

W	$\sigma_{failure}$	K_c	K_o
∞	33.5	104	84
20	32	103	82
16	30.5	102	79
12	29	100	76
10	27	96	73
8	22.5	91	66

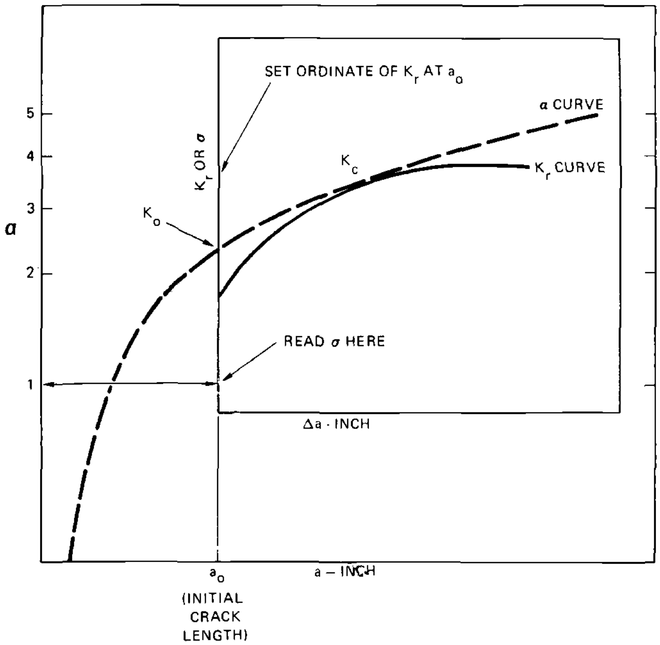

FIG. 5—*Schematic of prediction procedure.*

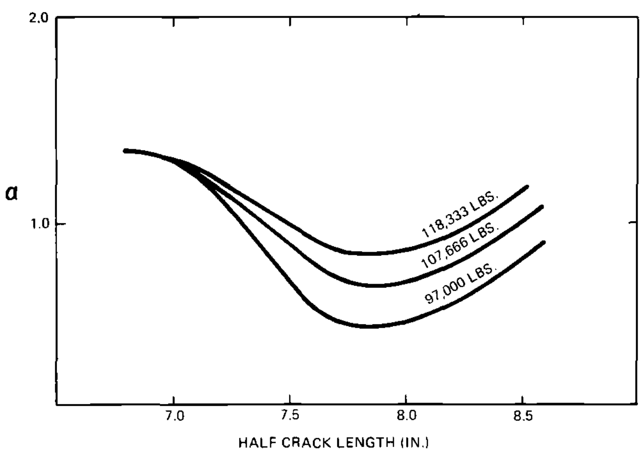

FIG. 6—*Stress intensity structural coefficient, reforced panel with reinforcement yielding.*

relation $K = P\,\alpha$, where P is the load (lb) on the structure. The stress intensity factors were found using analysis procedures similar to those described by Bloom and Sanders[3] and are fully described by Creager and Liu.[4]

In order to develop a failure prediction, the transparency may be used in the manner illustrated by Fig. 7 and described next. First note that for a given initial crack length, the K_r-curve may be set tangent to an α-curve corresponding to any applied load (P_1 or P_2 in Fig. 7). Each time this is done a load (P'_1 or P'_2) may be read from the ordinate of the K_r-curve at $\alpha = 1$. For the correct load P and P' will be equal. If P is too high then P' will be less than P. If P is too low then P' will be greater than P. If upper and lower bounds (say P_1 and P_2) are found, simultaneous linear interpolation on P_1 and P_2 and on P'_1 and P'_2 may be performed to arrive at a failure prediction. Using Fig. 7 as an example we may interpolate by setting

$$P_{\text{prediction}} = P'_1 + (P'_2 - P'_1)X = P_1 + (P_2 - P_1)X$$

Solving for X and substituting back results in

$$P_{\text{prediction}} = P'_1 + \frac{(P'_2 - P'_1)(P_1 - P'_1)}{(P'_2 - P'_1) - (P_2 - P_1)}$$

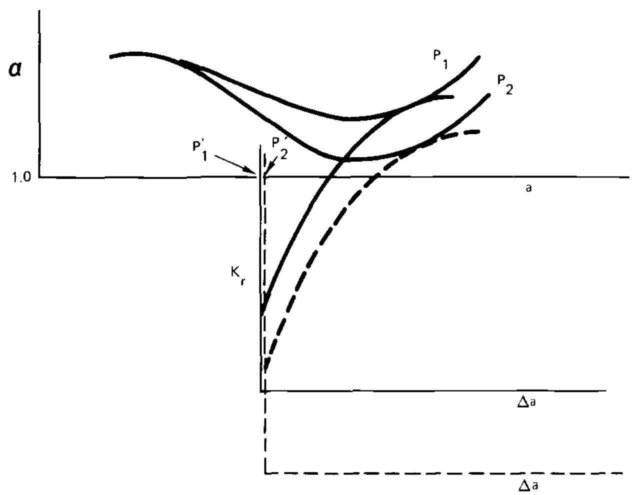

FIG. 7—*Schematic of prediction procedure.*

[3] Bloom, J. M. and Sanders, J. L., "The Effect of a Riveted Stringer on the Stress in a Cracked Sheet," *Journal of Applied Mechanics, Transactions,* American Society of Mechanical Engineers, Series E, Vol. 33, 1966.

[4] Creager, M. and Liu, A. F., "The Effect of Reinforcements on the Slow Stable Tear and Catastrophic Failure of Thin Metal Sheet," Paper No. 71-113, The American Institute of Aeronautics and Astronautics, 9th Aerospace Sciences Meeting, New York, N.Y., 1971.

Using the transparency and Fig. 6, one can find that for $a_0 = 7.0$

$$P'_1 = 109\,000 \quad \text{for } P_1 = 118\,333$$

$$P'_2 = 117\,000 \quad \text{for } P_2 = 107\,666$$

Therefore

$$P_{\text{prediction}} = 113\,000 \text{ lb}$$

It should be noted that the procedures just described can still be used when local crack tip yielding affects the effective crack length. Since the structural analysis curves are essentially stress intensity factor versus effective crack length, all that is necessary is that the abscissa of the resistance curve be effective change in crack length. Initial alignment offers no problem; since, at $\Delta a = 0$, effective length equals actual crack length.